1. Report No.	2. Government Accession No.	3. Recipient's Catalog No.
NASA CR-168191		

4. Title and Subtitle	5. Report Date
Research and Development Program for the Development of Advanced Time-Temperature Dependent Constitutive Relationships - Vol. 1 - Theoretical Discussion	July 1983
	6. Performing Organization Code
7. Author(s)	8. Performing Organization Report No
Dr. Brice N. Cassenti	R83-956077-1
	10. Work Unit No.
9. Performing Organization Name and Address	11. Contract or Grant No.
United Technologies Research Center 400 Main Street East Hartford, Conn. 06108	NAS3-23273
	13. Type of Report and Period Covered
12. Sponsoring Agency Name and Address	Contractor Final Report
NASA/Lewis Research Center 21000 Brookpark Road Cleveland, Ohio 44135	14. Sponsoring Agency Code

15. Supplementary Notes

Project Manager: R. L. Thompson, Mail Stop 49-6
National Aeronautics and Space Administration
Lewis Research Center, 21000 Brookpark Road,
Cleveland, Ohio 44135

16. Abstract

This report presents the results of a 10-month research and development program for the development of advanced time-temperature constitutive relationships. The program was conducted by the United Technologies Research Center for the NASA-Lewis Research Center under Contract NAS3-23273. The program included (1) the effect of rate of change of temperature, (2) the development of a term to include time independent effects, and (3) improvements in computational efficiency. It was shown that rate of change of temperature could have a substantial effect on the predicted material response. A modification to include time-independent effects, applicable to many viscoplastic constitutive theories, has been shown to reduce to classical plasticity. The computation time can be reduced by a factor of two if self-adaptive integration is used when compared to an integration using ordinary forward differences. During the course of the investigation, it was demonstrated that the most important single factor affecting the theoretical accuracy was the choice of material parameters.

17. Key Words (Suggested by Author(s))	18. Distribution Statement
Gas Turbine Engines, Creep, Plasticity, Visco-Plasticity, Constitutive Relationships, Thermovisco-Plasticity, Inelastic	Unlimited, Unclassified

19. Security Classif. (of this report)	20. Security Classif. (of this page)	21. No. of Pages	22 Price*
Unclassified	Unclassified		

* For sale by the National Technical Information Service, Springfield, Virginia 22151

R83-956077-1

Research and Development Program for the Development of Advanced Time-Temperature Dependent Constitutive Relationships

Volume I - Theoretical Discussion

TABLE OF CONTENTS

TABLE OF CONTENTS (Cont'd)

LIST OF SYMBOLS

C	inelastic strain
C^p	inelastic instantaneous strain
E	Young's modulus
G	shear modulus
J_2	second invariant of deviatoric stress, S_{ij}
K	bulk modulus or drag stress
K_1, K_2	drag stress material constants
k	material constant
$m_1, m_2, \ldots$	material constants
$n, n_1, n_2, \ldots$	material constants
$q_1, q_2, \ldots$	material constants
S	deviatoric stress
T	temperature
T_o	temperature at which thermal strain vanishes
t	time
w	work density
w^p	nonrecoverable work density
α	coefficient of thermal expansion
δ_{ij}	Kronecker delta
ε	total strain
$\varepsilon_1, \varepsilon_2$	maximum and minimum effective strain steps per subincrement
ν	Poisson's ratio
Ξ	instantaneous inelastic stress
σ	stress
σ_∞	material constant
Ω	back stress
ω	plastic "kinematic" back stress

FOREWORD

The work described in this report was performed by the United Technologies Research Center for the NASA-Lewis Research Center under Contract NAS3-23273. The program manager was Dr. Anthony J. Dennis and the principal investigator was Dr. Brice N. Cassenti. The NASA-Lewis technical project manager was Dr. Robert L. Thompson.

1.0 PROGRAM OUTLINE

This is the Final Report for the Research and Development Program for the development of Advanced Time-Temperature Dependent Constitutive Relationships. This program is being conducted by United Technologies Research Center for the NASA-Lewis Research Center under Contract No. NAS3-23273. Volume I contains the theoretical discussion and Volume II is the Programming Manual.

The objective is to improve the accuracy and efficiency of the nonlinear constitutive theories (computer models), developed and evaluated in Contract NAS3-22055. The program is divided into six tasks. The first task concerns development of a theoretical formulation to allow temperature dependence of the equilibrium stress state variable during elastic excursions in a thermomechanical hysteresis loop. In the second task, a new term is incorporated into three candidate theories to accommodate an inelastic instantaneous response. In the third task, the combined effects of Tasks I and II are investigated. In the fourth task, various techniques are incorporated into the subroutine HYPELA of the MARC* program to speed up computation. The fifth task involves the verification, documentation and delivery of the software program. The sixth task is reporting.

The Task I objective is to develop a theoretical formulation which allows for a change in the equilibrium stress state variable with temperature during elastic excursions in thermomechanical hysteresis loops. This formulation is incorporated into the three nonlinear constitutive theories evaluated in the previous contract NAS3-22055 and is encoded into the MARC* three-dimensional nonlinear finite element program. The comparison of these theories is completed by analyzing the response using three thermomechanical hysteresis loop tests performed on Hastelloy-X material.

The Task II objective is to incorporate into the candidate theory selected in Task I, a new term to accommodate an inelastic instantaneous response. For comparative purposes, the three thermomechanical "faithful cycle" hysteresis loops analyzed in Task I are repeated and analyzed in this task.

The Task III objective is to evaluate the theories developed to determine the combined improvement in predicting stresses and strains. The analytical results of this task are to be compared with those of Tasks I and II and Contract NAS3-22055 using the same thermomechanical hysteresis loops and geometry models used in Task I.

The Task IV objective is to improve the computational efficiency by:

---

*MARC is a three-dimensional nonlinear finite element program available from MARC Analysis Research Corporation, Palo Alto, California.

(1) incorporating an array containing the state variables in the viscoplastic theories into subroutine HYPELA of the MARC program to speed up computation time,

(2) further reducing computation time by modifying the MARC program so that the stiffness matrix is assembled once only during a calculation, with no further reassembly during succeeding increments. Furthermore, more efficient programming of the computer models developed in Tasks I and II and Contract NAS3-22055 is completed, and

(3) performing test cases of sufficient complexity to adequately demonstrate the improvements in computational efficiency.

Task V concerns verification, documentation and delivery of the software program.

Task VI consists of bimonthly technical and monthly financial reports together with a final technical report.

2.0 SUMMARY OF RESULTS

During the course of this investigation, several significant conclusions were drawn. They are:

1. The variation of material parameters with temperature must be carefully considered. This variation is best illustrated by examining the variation of the elastic moduli with temperature. If instantaneous, or tangent, moduli are used, a perfect elastic reaction where the material undergoes changes in temperature cannot be simulated. If secant moduli are used, then elastic nonisothermal reactions can be simulated. Similar considerations must be examined for other material parameters in any constitutive model. The use of secant material parameters in time dependent reactions introduces terms containing rate of change of temperature. For example, during nonisothermal elastic reactions the rate of change of stress will include strain times, the derivative of modulus with respect to temperature times the derivative of temperature with respect to time.

2. Including rate of change of temperature terms in the equilibrium stress formulation can have a significant effect on the predicted stress ratcheting during cyclic thermomechanical fatigue loading. The thermal ratcheting was also found to be sensitive to the material parameters used.

3. An instantaneous (i.e., plastic) response term has been introduced which can be shown to reduce to classical perfect plasticity. This term allows more accurate reproduction of low temperature material response.

4. The importance of accurately evaluating the material parameters is illustrated by comparing the poor comparisons at the end of Task I with the improved results at the end of Task III where more accurate material parameters were introduced.

5. A sixty percent reduction in CPU time can be attained by integrating the constitutive equations using a variable time step when compared to a fixed time step.

Conclusions 1 and 2 are discussed in the Task I description. Conclusion 3 is discussed in the Task II description. Conclusion 4 is illustrated by comparing the Task I and Task III results (in Task III, the material parameters were changed), and Task IV illustrates Conclusion 5.

3.0 TASK I - TECHNICAL DISCUSSION: RATE OF CHANGE OF TEMPERATURE EFFECTS

The Task I objective is to develop a theoretical formulation which allows for a change in the equilibrium stress state variable with temperature during elastic excursions in thermomechanical hysteresis loops. This formulation is incorporated into the three nonlinear constitutive theories evaluated in the previous contract NAS3-22055 and encoded into the MARC three-dimensional nonlinear finite element program. The three theories considered are discussed in detail in Ref. 1, along with several others, and include Walker's Theory, Miller's Theory and Kreig, Swearengen and Rhode's Theory. The predicted material response from each of the theories, using three thermomechanical hysteresis loop tests, is compared with results obtained on Hastelloy-X material.

This section consists of several subsections. Section 3.1 presents the three thermomechanical hysteresis loops modeled under this contract. The next section (3.2) discusses the variation in elastic moduli with temperature while the third section (3.3) introduces the three constitutive theories considered and the modifications that were made to include rate of change of temperature terms. The next three sections (3.4, 3.5 and 3.6) compare the predicted results for each of the three theories, with and without the rate of change of temperature terms.

3.1 Thermomechanical Fatigue Loops

Three thermomechanical fatigue (TMF) loops are used in the evaluation of the modified viscoplastic constitutive formulations to predict the response of Hastelloy-X combustor liners. These loops, with their imposed loadings, and their experimentally measured hysteresis loops are presented in Figs. 1-3. In the first and second loops, Figs. 1 and 2, the temperature varies sinusoidally with time, from 427 to 871 C, with a period of one minute. In the third loop, Fig. 3, the temperature again varies sinusoidally for one minute, going from 954 C to 504 C and back to 954 C. The temperature is then held for 40 seconds at 954 C which completes one cycle; the strain varies according to Fig. 3.

The thermomechanical loops used in this investigation represent a gradual increase in complexity. Figure 1 is a closed loop with equal maximum positive and negative strains. Figure 2 is an open loop but retains the equal maximum positive and negative strains while Fig. 3 is open with unequal maximum and minimum strains. These three cycles taken together will allow more accurate determinations of response of gas turbine engine hot section components.

3.2 Rate of Change of Temperature Effects in Thermoelasticity

The three TMF loops illustrated in Figs. 1-3 include not only changes in mechanical loading (i.e., imposed strain) but also large changes in temperature. To illustrate the effects of rate of change of temperature, consider an elastic response only. Three forms of the constitutive equations will be considered in one dimensional form. These three forms are compared to show that if perfect elasticity is to be represented then rate of change of temperature terms will appear. The three forms include:

(1) a tangent moduli formation

$$\dot{\sigma} = E(\dot{\epsilon} - \alpha\dot{T}) \tag{1}$$

(2) a secant moduli formation

$$\sigma = E\left[\epsilon - \alpha(T - T_0)\right] \tag{2}$$

and

(3) a mixed formulation

$$\sigma = E\left\{\epsilon - \int_0^t \alpha(\xi)\frac{dT}{d\xi}d\xi\right\} \tag{3}$$

where $E = E(\epsilon,T)$ is Young's Modulus

$\alpha = \alpha(\epsilon,T)$ is the coefficient of thermal expansion

$(\dot{}) = \frac{d(\ )}{dt}$ is the derivative with respect to time

σ is the stress

ϵ is the strain

T is the temperature, and

T_0 is the stress free temperature.

Equation (1) is the form presented for Miller's Theory and Krieg, Swearengen and Rhode's Theory in Ref. 1 for the elastic response, while Eq. (3) is the form presented in Ref. 1 for Walker's Theory. The MARC code assumes a form as in Eq. (3).

For an elastic response the material, by definition responds in a reversible manner, that is the stress is a unique function of strain and temperature, or

$$\sigma = \sigma(\epsilon, T) \tag{4}$$

Differentiating Eq. (4) with respect to time and comparing to Eq. (1) yields

$$\frac{\partial \sigma}{\partial \epsilon} = E \tag{5}$$

and

$$\frac{\partial \sigma}{\partial T} = -\alpha E \tag{6}$$

The mixed partials, Eqs. (5) and (6) must be equal. Thus,

$$\frac{\partial E}{\partial T} + \frac{\partial (\alpha E)}{\partial \epsilon} = 0 \tag{7}$$

If the material is linear in strain in the elastic region, E is not a function of strain and Eq. (7) becomes

$$\frac{1}{E}\frac{dE}{dT} + \frac{\partial \alpha}{\partial \epsilon} = 0 \tag{8}$$

This is a severe requirement for the coefficient of thermal expansion to satisfy and is based on a uniaxial stress state only. The more general case of a multiaxial stress state presents even more severe requirements. This case is examined in Appendix 1.

For the multiaxial stress states, Eq. (7) becomes, from Appendix 1,

$$\frac{\partial (\alpha K)}{\partial \epsilon_{ij}} + \frac{\delta_{ij}}{3}\frac{\partial K}{\partial T} = 0 \tag{9}$$

where $K = \frac{E}{3(1-2\nu)}$ is the bulk modulus, and

$$\delta_{ij} = \begin{cases} 1 & i = j \\ 0 & i \neq j \end{cases}$$

Equation (9) is equivalent to Eq. (7), but an even more severe requirement on the shear modulus, G, is shown to hold in Appendix 1.

$$\frac{\partial G}{\partial T} = 0 \tag{10}$$

Equation (10), requires that the shear modulus is not a function of temperature if the stress-strain law is elastic (i.e., if the stress-strain law is path independent). Therefore, it is not possible to represent an elastic response using temperature dependent elastic moduli defined as in Eq. (1).

The secant moduli formulation, Eq. (2), obviously satisfies the requirement represented in Eq. (4). Assuming the modulus and the coefficient of thermal expansion do not depend on strain

$$\begin{aligned} E &= E(T) \\ \alpha &= \alpha(T) \end{aligned} \quad \text{and}$$

The rate of change of stress in Eq. (2) becomes

$$\dot{\sigma} = E(\dot{\epsilon} - \alpha\dot{T}) + \left[\epsilon \frac{dE}{dT} - (T-T_0)\frac{d(\alpha E)}{dT}\right]\dot{T} \tag{11}$$

The first term is the same as that in Eq. (1). The second term is proportional to the rate of change of temperature and illustrates that rate of change of temperature terms can enter into a constitutive formulation in addition to the effects of thermal expansion.

The mixed formulation, Eq. (3), also places constraints on the material formulation. Taking the derivative of Eq. (3) with respect to time

$$\dot{\sigma} = E\dot{\epsilon} + \frac{\partial E}{\partial T}\epsilon\dot{T} + \frac{\partial E}{\partial \epsilon}\epsilon\dot{\epsilon} - \alpha E - \left\{\frac{\partial E}{\partial T}\dot{T} + \frac{\partial E}{\partial \epsilon}\dot{\epsilon}\right\}\int_0^1 \alpha(\xi)\frac{\partial T}{\partial \xi}\,d\xi \tag{12}$$

From Eq. (3),

$$\int_0^t \alpha(\xi)\frac{\partial \bar{\epsilon}}{\partial \xi}\,d\xi = \epsilon - \frac{\sigma}{E} \tag{13}$$

and substituting into Eq. (12)

$$\dot{\sigma} = \left[\epsilon + \frac{\sigma}{E}\frac{\partial E}{\partial \epsilon}\right]\dot{\epsilon} - \left[\alpha E - \frac{\sigma}{E}\frac{\partial E}{\partial T}\right]\dot{T} \tag{14}$$

For an elastic response, the stress is a single valued function of the strain and temperature, therefore,

$$\sigma = \sigma(\epsilon, T) \tag{15}$$

and

$$\dot{\sigma} = \frac{\partial \sigma}{\partial \epsilon}\dot{\epsilon} + \frac{\partial \sigma}{\partial T}\dot{T} \tag{16}$$

Comparing Eqs. (14) and (16)

$$\frac{\partial \sigma}{\partial \epsilon} = E + \frac{\sigma}{E}\frac{\partial \sigma}{\partial \epsilon} \tag{17}$$

and

$$\frac{\partial \sigma}{\partial T} = -\alpha E + \frac{\sigma}{E}\frac{\partial \epsilon}{\partial T} \tag{18}$$

The mixed second partial derivatives with respect to strain and temperature must be equal, which, from Eqs. (17) and (18) becomes,

$$\frac{\partial E}{\partial T} + \frac{1}{E}\frac{\partial \sigma}{\partial T}\frac{\partial E}{\partial \epsilon} = -\frac{\partial(\alpha E)}{\partial \epsilon} + \frac{1}{E}\frac{\partial \sigma}{\partial \epsilon}\frac{\partial E}{\partial T} \tag{19}$$

Substituting Eqs. (17) and (18) into Eq. (19) results in

$$\frac{\partial \alpha}{\partial \epsilon} = 0 \tag{20}$$

Appendix 2 shows that for the case of multiaxial loading, Eq. (20) becomes

$$\frac{\partial \alpha}{\partial \epsilon_{kl}} = 0 \tag{21}$$

and there are no other constraints on the material constants.

Equations (1) and (2) can be recast in integral form as

$$\sigma = \int_0^t E(\xi) \frac{d\epsilon}{d\xi} d\xi - \int_0^t \alpha(\xi) E(\xi) \frac{dT}{d\xi} d\xi \tag{22}$$

and

$$\sigma = E \int_0^t \frac{d\epsilon}{d\xi} d\xi - \alpha E \int_0^t \frac{dT}{d\xi} d\xi \tag{23}$$

respectively. Therefore, in the tangent moduli formulation, the material parameters appear inside the integrals while in the secant moduli formulation the material parameters are outside the integrals.

For an elastic response the formulation in Eqs. (2) or (23) is preferred but for an inelastic response the form has not been determined based on first principles. The material constants can appear either inside or outside the integrals. The correct choice can be determined by comparing analytical predictions for either choice with experimental results. This will be the subject of the following sections for the three specific constitutive models considered.

3.3 Discussion of the Three Constitutive Formulations

The three constitutive theories to be considered are: (1) Walker's, (2) Miller's and (3) Krieg, Swearengen, and Rhode's. Walker's Theory, from Ref. 1, is summarized in Appendix 3 in differential form and Appendix 4 in integral form. Equation (3.2) in Appendix 3 contains rate of change of temperature terms. These terms are a result of assuming the material constants n_1 and n_2 appear outside the integrals in Eq. (4.2) of Appendix 4. Miller's equations presented in Appendices 5 and 6 from Ref. 1 have an assumed temperature dependence based on activation energies.

Therefore, the material constants are not functions of temperature. An adjustment in the theory is then necessary to include rate of change of temperature terms. Krieg, Swearengen and Rhode's Theory from Ref. 1 is summarized in Appendices 7 and 8. Again, this theory contains no rate of change of temperature terms but the necessary modification can be made simply by moving the appropriate constants outside the integral. Tables 1, 2 and 3 present the material parameters for each of the three theories used in Ref. 1.

3.4 Rate of Change of Temperature Effects in Walker's Theory

Walker's Theory will produce results during nonisothermal loading that depend on rate of change of temperature terms, in addition to the effects during elastic loading. This is reflected by Eqs. (3.2) and (4.2) in Appendices 3 and 4. With respect to Walker's theory, as reported in Ref. 1, the differential form has been modified to more accurately reflect the integral form by the addition of the time derivative $\overset{\circ}{\Omega}_{ij}$. With respect to the elastic constants, Walker's theory requires the coefficient of thermal expansion not to be a function of the strain. In the remaining two theories, the coefficient of thermal expansion must be a function of the strain if the elastic moduli vary with temperature.

The constants in Walker's theory (taken from Ref. 1) are presented in Figs. 4-7 and in Table 1 as functions of temperature. Figures 4-7 are used as an aid in determining the proper interpolation functions and in determining derivatives with respect to temperature. These material constants exhibit rapid changes in the temperature range of 1000 F to 1400 F. The most important constant in the rate of change of temperature terms is n_2 (see Fig. 7 and Eq. (3.2) of Appendix 3). The parameter, n_2, displays a reversal in slope in the range from 1000 to 1400 F.

The user subroutine HYPELA of the MARC code, from Ref. 1, was modified to include rate of change of temperature terms. Figures 8-13 present the results from Walker's theory for the three TMF loops of Figs. 1-3, with and without the rate of change of temperature terms. Although the general shape of the loop remains the same, the steady state hysteresis loop is approached much more rapidly with the rate of change of temperature terms than without.

3.5 Rate of Change of Temperature Effects in Miller's Theory

Miller's theory, presented in Appendices 5 and 6 and taken from Ref. 1, was modified by making H_1 in Eq. (5.2) temperature dependent. The modified theory is summarized in Appendix 9. Figures 14-19 illustrate hysteresis loops at different temperatures for the values of H_1 listed in Table 4. These hysteresis loops should be compared to the corresponding experimental loops presented in Figs. 20-25 taken from Ref. 1. The remaining constants are taken from Ref. 1, and summarized in Table 2.

In Miller's theory, with the constant H_1 now assumed to be a function of temperature, the subroutine HYPELA in MARC was modified to include rate of change of temperature terms.

For the three TMF loops, Miller's Theory, with and without the rate of temperature terms, Figs. 26-31 show almost no change. This is partly due to fact that steady state is approached rapidly even without the rate of change of temperature terms and partly due to the fact that the material constant H_1 does not vary appreciably with temperature between 800 and 1200 F. It is difficult using Miller's theory to arrive at empirical values of H_1 at low temperatures that match the experimental results (for example, compare Figs. 14 and 20). Therefore, the lower temperature estimates for H_1 can vary appreciably from the chosen value.

3.6 Rate of Change of Temperature Effects in Krieg, Swearengen and Rhode's Theory

Krieg, Swearengen and Rhode's theory, Appendices 7 and 8, was modified by moving A_1 out of the integral in the integral form of the theory. Appendix 10 presents a summary of the modified theory, and Table 3 summarizes the constants which were taken from Ref. 1.

These modifications were included in a version of the MARC user subroutine HYPELA (see Ref. 1). The modified subroutine was tested using the three thermomechanical loops. Figures 32-37 present the resulting stress-strain hysteresis loops with and without the rate of change of temperature terms. For the two open thermomechanical loops, there was little change when the rate of change of temperature terms were included, compare Figs. 33 and 34 with Figs. 36 and 37, respectively. For the closed thermomechanical loop, Figs. 32 and 35, the steady state loop is approached more rapidly when the rate of change of temperature terms are included.

3.7 Summary

In all succeeding analyses only one viscoplastic theory is used. For these analyses Walker's theory was chosen becasue of its ability to represent more physical phenomena than Krieg, Swearengen and Rhode's theory. Miller's theory with its assumed variation of the material parameters with temperature made it more difficult to represent experimental hysteresis loops. A more recent version of Miller's theory Ref. 2 and Appendix 11, removes some of this difficulty but the number of material parameters has been substantially increased.

4.0 TASK II - TECHNICAL DISCUSSION: TIME INDEPENDENT RESPONSE

The Task II objective is to incorporate into one candidate theory from Task I, a new state variable to accommodate an inelastic instantaneous response. For comparative purposes, the three thermomechanical "faithful cycle" hysteresis loops analyzed in Task I are used in this task. Two forms for representing instantaneous response will be discussed. The first is based on an instantaneous stress state variable. The second uses an inelastic work rate. The last section will present results based on the inelastic work rate.

4.1 Instantaneous Stress State Variable

A particular formulation for the instantaneous stress state variable has been examined for uniaxial stress states. The formulation is summarized in Appendix 12. The particular case considered is summarized in Table 5, and includes all of the important features of Walker's formulation. The equations under these assumptions reduce to

$$\dot{\sigma} = \pm E \left(\frac{|\sigma - \Omega|}{K_1} \right)^n \operatorname{sgn}(\sigma - \Omega) \tag{24}$$

$$\dot{c} = \dot{\epsilon} - \frac{\dot{\sigma}}{E} \tag{25}$$

$$\dot{\Xi} = m_2 \dot{c} - m_3 |\dot{c}| \Xi \tag{26}$$

$$\dot{\Omega} = n_2 \dot{c} - n_3 |\dot{c}| \Omega \tag{27}$$

Consider the case of initially loading the material at a specified strain rate and take

$$\epsilon = C = 0, \Omega = \Xi = \sigma = 0, \dot{\epsilon} = \gamma \tag{28}$$

From Eqs. (24-27)

$$\dot{\sigma}\left(\frac{1}{E} + \frac{1}{m_2}\right) = \dot{\epsilon} \quad t = 0 \tag{29}$$

and the apparent Young's Modulus, E_0, during initial loading is

$$\frac{1}{E_0} = \frac{1}{E} + \frac{1}{m_2} \tag{30}$$

If the material is now loaded at constant strain rate, γ, until steady conditions result, and then suddenly the strain rate is changed to $-\gamma$, the material will now unload initially by

$$\dot{\sigma}\left(\frac{1}{E} + \frac{1}{2m_2}\right) = \dot{\epsilon} \tag{31}$$

which can be evaluated in a similar manner from Eqs. (24-27). Then the apparent Young's Modulus during fully reversed unloading, E_{rev}, is

$$\frac{1}{E_{rev}} = \frac{1}{E} + \frac{1}{2m_2} \tag{32}$$

therefore, the unloading slope is not equal to the initial loading slope in contradiction to experimental results. In order for the two slopes to be nearly equal, the constant m_2 must be large. A large value for m_2 should result in the instantaneous stress quickly saturating to its steady value and then having no subsequent effect on the response. This formulation is therefore not acceptable.

4.2 Inelastic Work Rate Formulation

A formulation based on the rate of work being done appears to be able to represent some of the time independent features appearing in the experimental data. The time independent terms can be developed based on a modification of the equations of Ref. 3. In Ref. 3, Walker used an expression of the form

$$\dot{c} = \dot{\epsilon} - \frac{\dot{\sigma}}{E} = \frac{\sigma}{\sigma_{max}} \left| \dot{\epsilon} - \frac{b}{a} \frac{\dot{\sigma}}{E} \right| \tag{33}$$

where σ_{max}, b and a are positive constants. As b/a approaches unity, the stress-strain curve on initial loading becomes identical to an elastic perfectly plastic response. There are limitations with this formulation, two of which are:

(1) the initial loading slope (i.e., Young's modulus) is not equal to an initial unloading slope if a is not equal to b, and

(2) the inelastic strain rate, $\dot{c}$, is opposite in sign to the total strain rate, $\dot{\epsilon}$, during initial unloading (i.e., if $\sigma > o$ then $\dot{c} > o$ even if $\dot{\epsilon} < o$).

Equation (33) does produce a time independent response similar to classical plasticity and therefore modifications of this formulation were developed. In order to incorporate a time independent formulation into viscoplastic theories, the inelastic strain rate, $\dot{c}_{ij}$, is decomposed into two parts as follows

$$\dot{c}_{ij} = \dot{c}_{ij}^{c} + \dot{c}_{ij}^{p} \tag{34}$$

where c_{ij}^{c} is the time dependent part, similar to classical creep strains, and c_{ij}^{p} is the time independent part, similar to classical plastic strains.

Such a decomposition is being developed by Haisler, Ref. 4, and Bradley, Ref. 5. Using Walker's theory, the time dependent inelastic strain is

$$\dot{c}_{ij}^{c} = \left\{ \frac{\sqrt{\frac{2}{3}\left(\frac{3}{2}s_{ij} - \Omega_{ij}\right)\left(\frac{3}{2}s_{ij} - \Omega_{ij}\right)}}{K} \right\}^{n} \frac{\left(\frac{3}{2}s_{ij} - \Omega_{ij}\right)}{\sqrt{\frac{2}{3}\left(\frac{3}{2}s_{ij} - \Omega_{ij}\right)\left(\frac{3}{2}s_{ij} - \Omega_{ij}\right)}} \tag{35}$$

The time independent inelastic strain rate can be taken as an expression similar to Eq. (33) but using work rates rather than strain rates. The total rate at which work is being done would replace the total strain rate. The elastic strain rate, $\dot{\sigma}/E$, would be replaced by a recoverable work rate. The total work rate, $\dot{W}$, is given by

$$\dot{w} = \sigma_{ij} \dot{\epsilon}_{ij} \tag{36}$$

and the nonrecoverable work, $\dot{W}^p$, will be taken as

$$\dot{w}^p = \langle (\sigma_{ij} - \frac{2}{3}\omega_{ij})\,\dot{C}^p_{ij} \rangle \tag{37}$$

where $\langle x \rangle = \begin{cases} x, x \geq o \\ o, x < o \end{cases}$ is the unit ramp function. ω_{ij} has a zero trace ($\omega_{kk} = o$) and can be used to represent kinematic hardening. The time independent inelastic strain can be taken to be

$$\dot{C}^p_{ij} = \frac{3(S_{ij} - \frac{2}{3}\omega_{ij})}{2\sigma_\infty^2} \langle \dot{w} - k\,(\dot{w} - \dot{w}^p) \rangle \tag{38}$$

where σ_∞ is the time independent yield stress and can be taken to be a function, for example, of temperature, nonrecoverable work (to simulate isotropic hardening), and if necessary total strain rate.

Substituting Eq. (38) into Eq. (37)

$$\dot{w}^p = \frac{3\,J_2'}{2\sigma_\infty^2} \langle (1-k)\,\dot{w} + k\dot{w}^p \rangle \tag{39}$$

where $3J_2' = \frac{2}{3}\,(\frac{3}{2}\,S_{ij} - \omega_{ij})(\frac{3}{2}\,S_{ij} - \omega_{ij})$. Equation (39) can be solved for $\dot{W}^p$.

$$\dot{w}^p = \frac{\frac{3(1-k)\,J_2'}{2\sigma_\infty^2} \langle \sigma_{ij}\dot{\epsilon}_{ij} \rangle}{1 - k\left(\frac{3J_2'}{2\sigma_\infty^2}\right)} \tag{40}$$

where use has been made of Eq. (37). Substituting Eqs. (36) and (40) into Eq. (38) gives the time independent inelastic strain

$$\dot{C}^p_{ij} = \frac{3(S_{ij} - \frac{2}{3}\omega_{ij})}{2\sigma_\infty^2} \; \frac{(1-k)\langle \sigma_{ij}\dot{\epsilon}_{ij} \rangle}{1 - k\left(\frac{3J_2'}{2\sigma_\infty^2}\right)} \tag{41}$$

For classical plasticity without hardening, k is unity and ω_{ij} vanishes. Equation (41) becomes indeterminate if

$$J_2' = \frac{1}{3}\sigma_\infty^2 \tag{42}$$

Therefore, σ_∞ can be identified with the classical uniaxial yield stress. Under these conditions, Eq. (38) becomes

$$\dot{c}_{ij}^p = \frac{3s_{ij}\langle \dot{w}^p \rangle}{2\sigma_\infty^2} \tag{43}$$

which is identical to classical plasticity theory as shown in Appendix 13. Appendix 14 presents Walker's theory modified to include these time independent strains with no associated hardening. There are two additional material constants, k and σ_∞, which are functions of temperature. Equation (41) in its most general form is capable of representing a wide range of stress-strain behavior. For example, taking

$$\omega_{ij} = Hc_{ij}^p \tag{44}$$

to represent kinematic hardening, and

$$\sigma_\infty = \left\{\sigma_0 + \sigma_1\left[\frac{q_2 w^p/\sigma_1}{1+q_2 w^p/\sigma_1}\right]\right\}\left\{1 + q_1 \ln\left(\frac{\dot{\epsilon}}{\dot{\epsilon}_0}\right)\right\} \tag{45}$$

where H is the kinematic hardening slope,

σ_0 is the initial "yield" stress,

σ_1 and σ_2 can be used to represent isotropic hardening,

q_1 can be used to represent strain rate effects, and

$\dot{\epsilon}_0$ is the strain rate appropriate to σ_0.

A uniaxial loading simulation was performed using the equations in Appendix 14, but with Eqs. (44 and 45) together with the data in Table 6. Figure 38 presents the resulting stress strain hysteresis loop which is similar to the experimental loops at 800 deg F presented in Fig. 22, and Fig. 39 presents the inelastic strain as a function of total strain hysteresis loop.

4.3 Time Independent Hysteresis Loops

The time independent response equations can be simplified by using the rest stress, Ω (equilibrium stress), to represent kinematic work hardening in the time dependent response and proportionally varying the equivalent yield stress, σ_∞, in the same manner as the drag stress, K. Appendix 13 summarizes the governing equations. This then leaves two additional constants to be evaluated for the theory σ_∞ (at R equal to zero) and k. The constant k has been taken to be zero for all temperatures while σ_∞ was set to infinity for 1200 F to 1800 F. At 1000 F and 800 F, the constant σ_∞ was determined and the constants n_2 and n_3 were changed to more closely match the experimental results. In addition, the constants K_1 and 1/n at 1400 F were changed to more closely match the experimental results. The 1400 F change only effects strain rate results higher than those presented. Table 7 summarizes the new values for each of the constants. Figures 40-47 show the resulting hysteresis loops. At 1000 F, the loops are significantly more accurate with the new values of n_2 and n_3, compare Figs. 20-25 with Figs. 40-47, than the predictions of Ref. 1. The effect on the predicted stress when the time independent terms are included will be discussed in the next section.

The time dependent and time independent inelastic strains can be separated experimentally by performing creep and relaxation tests beginning at various points on the steady state stress strain hysteresis loops.

5.0 TASK III - TECHNICAL DISCUSSION: COMBINED TASK I AND TASK II EFFECTS

The Task III objective is to evaluate the theories developed to determine the combined improvement in predicting stresses and strains. The analytical results of this task are compared with those of Tasks I and II and Contract NAS3-22055 using the same thermomechanical hysteresis loops and geometry models used in Task I.

The subroutine HYPELA was modified to include the time independent terms as a part of Task II. The material constants in their final form appear in Table 7, the initial form of the constants appear in Table 1. Figures 48-53 show the effect of changing constants and including time independent terms and rate of change of temperature terms for the closed symmetric TMF cycle. The other two TMF cycles were only minimally effected (see Figs. 54 and 55). Figures 48-53 show a definite improvement in accuracy primarily due to the change in the low temperature material properties. Adding the time independent terms and the nonisothermal terms has only a minimal effect.

A slight improvement in the predicted response of the open nonsymmetric TMF cycle was attained by setting the material constant σ_∞ at 1200 F to 60 ksi with no appreciable change in the other two TMF loops, as illustrated in Figs. 56 to 58. Figure 59, taken from Ref. 1, shows the predicted stress strain response for the open nonsymmetric TMF cycle using the material parameters from Table 1. Comparing Figs. 58 and 59, there is a considerable improvement in the predicted response when compared to the experimental response (Fig. 3). This is primarily due to the change in low temperature material constants.

Summarizing the combined effects of Tasks I and II showed that accurately modeling the low temperature hysteresis loops had the most effect, followed by the instantaneous inelastic response. The rate of change of temperature terms studied under Task I produced changes in the thermal ratcheting. Thermal ratcheting seemed to occur more often when there were sudden changes in the slope of the stress strain curves.

6.0 TASK IV - TECHNICAL DISCUSSION: IMPROVEMENTS IN COMPUTATIONAL EFFICIENCY

The Task IV objective is to improve the computational efficiency by:

(1) incorporating an array containing the state variables into subroutine HYPELA of the MARC program to speed up computation time,

(2) further reducing computation time by modifying the MARC program so that the stiffness matrix is assembled once only during a calculation, with no further reassembly during succeeding increments. Further, more efficient programming of the computer models developed in Tasks I and II and Contract NAS3-22055 (Ref. 1) is completed, and

(3) performing test cases of sufficient complexity to adequately demonstrate the improvements in computational efficiency.

The first part of this section presents various numerical techniques for integrating the differential equations for the modified Walker theory summarized in Appendix 14. The second part summarizes the computational savings that results when various modifications were made to the MARC finite element code and the user subroutine HYPELA of the MARC code. Reference 6 presents a complete discussion for the modifications to the MARC code necessary to incorporate the equations of Appendix 14 in an efficient manner.

6.1 Numerical Integration of the Modified Walker's Theory

Three methods for integrating the constitutive equations were examined: (1) a forward difference with error estimates for revising the time step, (2) a backward difference, and (3) integrating an integral form of the equations.

The forward difference integration, similar to Ref. 7, is based on an error estimate, E, given by

$$E = \Delta R + \frac{\sqrt{3\Delta J_2}}{2\mu} \tag{46}$$

where

$$\Delta R = \sqrt{\frac{2}{3}\Delta C_{ij}\Delta C_{ij}}$$

and

$$\Delta J_2 = \frac{3}{2} \Delta S_{ij} \Delta S_{ij}$$

Δ of a quantity is the change in the quantity over time step Δt.

If the error estimate is too large

$$\epsilon > \epsilon_1 \tag{47}$$

then the time step is halved and the step is repeated. If the error estimate is too small

$$\epsilon < \epsilon_2 \tag{48}$$

then the time step is doubled for the next integration step.

Figure 60 shows the resulting stress-strain loop for the symmetric closed TMF cycle using a 200 step per cycle forward difference without the error estimate. This should be compared with Fig. 61 where

$$\epsilon_1 = 10^{-4}$$

and

$$\epsilon_2 = 10^{-5}$$

For this case, 195 steps per cycle resulted with an increase in computation time of 0.4 percent. In Fig. 62, the allowable "errors" have been increased ten times and although the response demonstrates some instability, the stress-strain loop is still approximately correct. In Fig. 62, only 38 steps per cycle were required and a decrease in computation time of 75 percent resulted. This is obviously a viable method for determining the time step magnitude automatically.

A backward difference algorithm was developed which is summarized in Appendix 15. Figures 63-66 display the resulting stress-strain loop for the closed symmetric cycle for various numbers of increments per cycle. At 16 increments per cycle, Fig. 65, the loop is marginally accurate when compared to Fig. 60. This represents a savings of approximately 75 percent since about 2.5 iterations to solve the resulting nonlinear simultaneous equations per loading increment were required.

Although the forward difference worked adequately for all test cases considered, the backward difference convergence was slow in cases where the term n_6 was not equal to zero and the strain rate was small (i.e., on the order of 10^{-6}/sec). A quadratic Newton's method was also used to solve for ΔG and Ω_{ij}^{k+1} but there was no benefit over a linear Newton's method. Therefore, in these cases, a sufficiently small step size was required.

The equations for the modified Walker's theory were recast in integral form, see Appendix 16. This form was also tested and the results were similar to the results for the backward difference.

Summarizing, three methods for integrating the equations were examined. They included: (1) forward differences using error estimates to revise the time step, (2) backward differences, and (3) recasting the equations in integral form and then numerically integrating. Tests of these methods were performed on the one dimensional form of the equations. The forward differences with error estimates saved up to 75 percent of the computational time. The backward difference integration was stable for large time steps and converged rapidly for typical thermal cycle problems, resulting in a savings of computational times of about 75 percent. Unfortunately, at low strain rates and high temperatures, where thermal recovery can be important, convergence was sometimes unacceptably slow. Results for the integral form indicated that the savings and problems are similar to the backward differences. The convergence problems make the backward difference and integral form integration methods unreliable and therefore only the forward difference integration with error estimates was used in the MARC code modifications.

6.2 Computational Efficiency Improvements

Three approaches were investigated to improve the computational efficiency. One of these is the numerical integration discussed above. The second included the approach of storing the state variables in an array in HYPELA. This proves to be advantageous only if all of the 16 state variables for each integration point of each element can be stored in core. Therefore, there is a savings only on relatively small models. In the third approach, the MARC code was modified to save the inverted stiffness matrix (i.e., use back-substitution), thereby saving the CPU time necessary to solve the simultaneous equations.

In the subrouinte HYPELA of the MARC code, the constitutive equations were integrated using a forward difference for the time derivative. Each increment in the MARC code is divided into a number of subincrements. The number of subincrements is stored as the variable NSPLIT. For an ordinary forward difference NSPLIT is a constant. For a forward difference integration with error checking, a self-adaptive scheme, the variable NSPLIT is changed according to whether the estimated error is larger or smaller than the allowable bounds (Eqs. (46-48)).

The MARC code could then be run in four modes depending on whether NSPLIT is constant (ordinary forward difference) or variable (self-adaptive forward difference) and whether matrix inversion is performed or back substitution is used. Two different test cases were used in the tests. The first was a two element by two element uniaxial axisymmetric mesh, with the loading given by the open non-symmetric loop in Fig. 3. The second test case was identical except a seven by seven element mesh was used. The first case was run for 48 loading increments and the second for 10 increments. Table 8 summarizes the resulting UNIVAC 1110 CPU time for five different combinations. Most of the savings resulted when a variable time step was used. Using matrix inversion produced a negligible increase in the CPU time when compared to back substitution. In the test runs using a constant time step the value of NSPLIT was taken to be the maximum value attained in the equivalent self-adaptive run. Figure 67 shows NSPLIT at the end of each MARC increment using the 2x2 finite element mesh and self adaptive integration, for the first complete cycle of the open nonsymmetric loop. A total of 219 subincrements were required. If NSPLIT was set at 16 subincrements per increment then a variable time step would produce a 72 percent savings.

In Fig. 67, at increments 10 to 15 and increments 38 to 45, NSPLIT is large. At these increments the larger changes in mechanical and thermal loading occurred. In increments 20 to 36 NSPLIT is equal to one which occurs during the hold time for the temperature and strain (i.e., the time during which temperature and strain are constant).

Summarizing, most of the CPU savings was attained by using variable step integration while utilizing back substitution produced a relatively small savings. Indications are that large problems would have to be run (1000 degrees of freedom) before the equation solution time becomes large.

7.0 CONCLUSIONS

During the course of this investigation several significant conclusions were drawn. They are:

1. The variation of material parameters with temperature must be carefully considered. This variation is best illustrated by examining the variation of the elastic moduli with temperature. If instantaneous, or tangent, moduli are used, a perfect elastic reaction where the material undergoes changes in temperature cannot be simulated. If secant moduli are used, then elastic nonisothermal reactions can be simulated. Similar considerations must be examined for other material parameters in any constitutive model. The use of secant material parameters in time dependent reactions introduces terms containing rate of change of temperature.

2. Including rate of change of temperature terms in the equilibrium stress formulation can have a significant effect on the stress or strain, ratcheting during cyclic thermomechanical fatigue loading. The thermal ratchetting was also found to be sensitive to the material parameters used.

3. An instantaneous (i.e., plastic) response term has been introduced which can be shown to reduce to classical perfect plasticity. This term allows more accurate reproduction of low temperature material response.

4. The importance of accurately evaluating the material parameters is illustrated by comparing the poor comparisons of the end of Task I, Fig. 9, with the improved results at the end of Task III, Fig. 50.

5. A sixty percent reduction, Table 8, in CPU time can be attained by integrating the constitutive equations using a variable time step when compared to a fixed time step.

REFERENCES

1. Walker, K. P.: Research and Development Program for Nonlinear Structural Modeling with Advanced Time-Temperature Dependent Constitutive Relationships. Final Report NASA CR-165533, November 1981.

2. Miller, A. K.: Some Improvements in the MATMOD-Z Constitutive Equations for Non-Elastic Deformation of Zircaloy. Department of Materials Science and Engineering. Stanford University, SU-DMS-82-T-1, 1982.

3. Walker, K. P. and E. Krempl: An Implicit Functional Representation of Stress-Strain Behavior. Mech. Res. Comm., Vol. 5, No. 4, pp. 185-190, 1978.

4. Haisler, W.: Application of an Uncoupled Elastic-Plastic Creep Constitutive Model to Metals at High Temperatures. Presented at the Symposium on Nonlinear Constitutive Relations for High Temperature Applications, May 19-20, 1982. The University of Akron, Akron, Ohio.

5. Bradley, W. L.: A New Uncoupled Viscoplastic Constitutive Model. Presented At the Symposium on Nonlinear Constitutive Relations for High Temperature Applications, May 19-20, 1982, The University of Akron, Akron, Ohio.

6. Cassenti, B. N.: Research and Development Program for the Development of Advanced Time-Temperature Dependent Constitutive Relationships - Vol. 2 - Computer Code Documentation.

7. Kumar, V. M. Morjaria, and S. Mukherjee: Numerical Integration of Some Stiff Constitutive Models of Inelastic Deformation. Transactions of the ASME, Journal of Engineering Materials and Technology, Vol. 102, pp. 92-96, January 1980.

TABLE 1

Material Constants for Walker's Theory (Ref. 1)

Material Constant	982°C 1800°F	871°C 1600°F	760°C 1400°F	648°C 1200°F	537°C 1000°F	427°C 800°F
λ	11.5E6	15.4E6	17.8E6	18.1E6	17.2E6	17.8E6
μ	4.9E6	6.9E6	8.4E6	9.0E6	9.0E6	9.8E6
K_1	59292	91505	251886	95631	75631	50931
K_2	0	0	0	0	0	0
n^{-1}	.233	.195	.244	.079	.059	.059
m	1.16	1.16	1.16	1.16	1.16	1.16
n_1	0	0	0	0	0	0
n_2	1.0E6	5.0E6	2.0E7	1.5E7	6.0E7	30.0E7
n_3	312	673	1179	781	1000	8000
n_4	0	0	0	0	0	0
n_5	0	0	0	0	0	0
n_6	2.73E-3	8.98E-4	0	0	0	0
n_7	0	0	0	0	0	0
Ω	-1200	-1434	-2000	-2000	0	0

TABLE 2

Material Constants for Miller's Theory (Ref. 1)

$K_o = 8000$

$n = 1.598$

$B = 1.0293E14$

$H_1 = 1.0E7$

$A_1 = 9.305E-4$

$H_2 = 100$

$C_2 = 50000$

$A_2 = 5.9425E-12$

$Q^* = 104600$

$T_m = 1588°K$

$k = 1.9859$

$$\theta' = \exp\left\{- Q^*/kT\right\} \quad \text{for } T \geq .6T_m$$

$$\theta' = \exp\left\{\frac{-Q^*}{.6kT_m}\left(1 + \ln\frac{.6T_m}{T}\right)\right\} \text{ for } T < .6T_m$$

where T is the temperature in degrees Kelvin. The Lame constants λ and μ are as given in Table 1.

TABLE 3

Material Constants for Krieg, Swearengen and Rhode's Theory (Ref. 1)

Material Constant	982°C 1800°F	871°C 1600°F	760°C 1400°F	648°C 1200°F	537°C 1000°F	427°C 800°F
λ	11.5E6	15.4E6	17.8E6	18.1E6	17.2E6	17.8E6
μ	4.9E6	6.9E6	8.4E6	9.0E6	9.0E6	9.8E6
K_o	59292	91505	251886	95631	75631	50931
n^{-1}	.223	.195	.244	.079	.059	.059
A_1	1.0E6	5.0E6	2.0E7	1.5E7	6.0E7	30.0E7
A_2	243	14.96	1.54	.66	1.79E-3	.59
A_3	1.0E-12	1.0E-12	1.0E-12	1.0E-12	1.0E-12	1.0E-12
A_4	0	0	0	0	0	0
A_5	0	0	0	0	0	0

TABLE 4

Constant H_1 in Miller's Theory

Temperature deg F	H_1 psi
800	10×10^6
1000	10×10^6
1200	8×10^6
1400	10×10^6
1600	6×10^6
1800	3×10^6

TABLE 5

Parameters for Instantaneous Stress State Examination

Parameter	Value
E	nonzero constant
n	nonzero constant
K_1	nonzero constant
K_2	0
n_1, m_1	0
n_2, m_2	nonzero constant
n_3, m_3	nonzero constants
n_{4-6}, m_{4-6}	0

TABLE 6

Constants in Time Independent Simulations

$k = 0.3$

$K = \infty$

$\varepsilon_{max} = 0.006$

$q_1 = .004$

$q_2 = 0$

$\dot{\varepsilon}_o = .001$

$\sigma_o = 70$ ksi

$\sigma_1 = 30$ ksi

$H = 7.5 \times 10^6$ psi

TABLE 7

Material Constants for Modified Walker's Theory

Material Constant	982°C 1800°F	871°C 1600°F	760°C 1400°F	648°C 1200°F	537°C 1000°F	427°C 800°F
λ	11.5E6	15.4E6	17.8E6	18.1E6	17.2E6	17.8E6
μ	4.9E6	6.9E6	8.4E6	9.0E6	9.0E6	9.8E6
K_1	59292	91505	110696	95631	75631	50931
K_2	0	0	0	0	0	0
n^{-1}	.233	.195	.1497	.079	.059	.059
m	1.16	1.16	1.16	1.16	1.16	1.16
n_1	0	0	0	0	0	0
n_2	1.0E6	5.0E6	2.0E7	1.5E7	1.9E7	1.0E7
n_3	312	673	1179	781	320	250
n_4	0	0	0	0	0	0
n_5	0	0	0	0	0	0
n_6	2.73E-3	8.98E-4	0	0	0	0
n_7	0	0	0	0	0	0
$\overset{o}{\Omega}$	-1200	-1434	-2000	-2000	0	0
σ_∞ at R = 0	∞	∞	∞	∞	48000	48000
k	0	0	0	0	0	0

TABLE 8

UNIVAC CPU Times

TMF1 - MARC Increments 0-10

7X7 Elements

Matrix Inversion	NSPLIT	CPU Time (Sec)	Percent Savings
Yes	Constant	335	0
Yes	Variable	141	58
No	Variable	131	61

TMF1 - MARC Increments 0-48

2X2 Elements

Matrix Inversion	NSPLIT	CPU Time (Sec)	Percent Savings
Yes	Constant	233	0
No	Variable	90	61

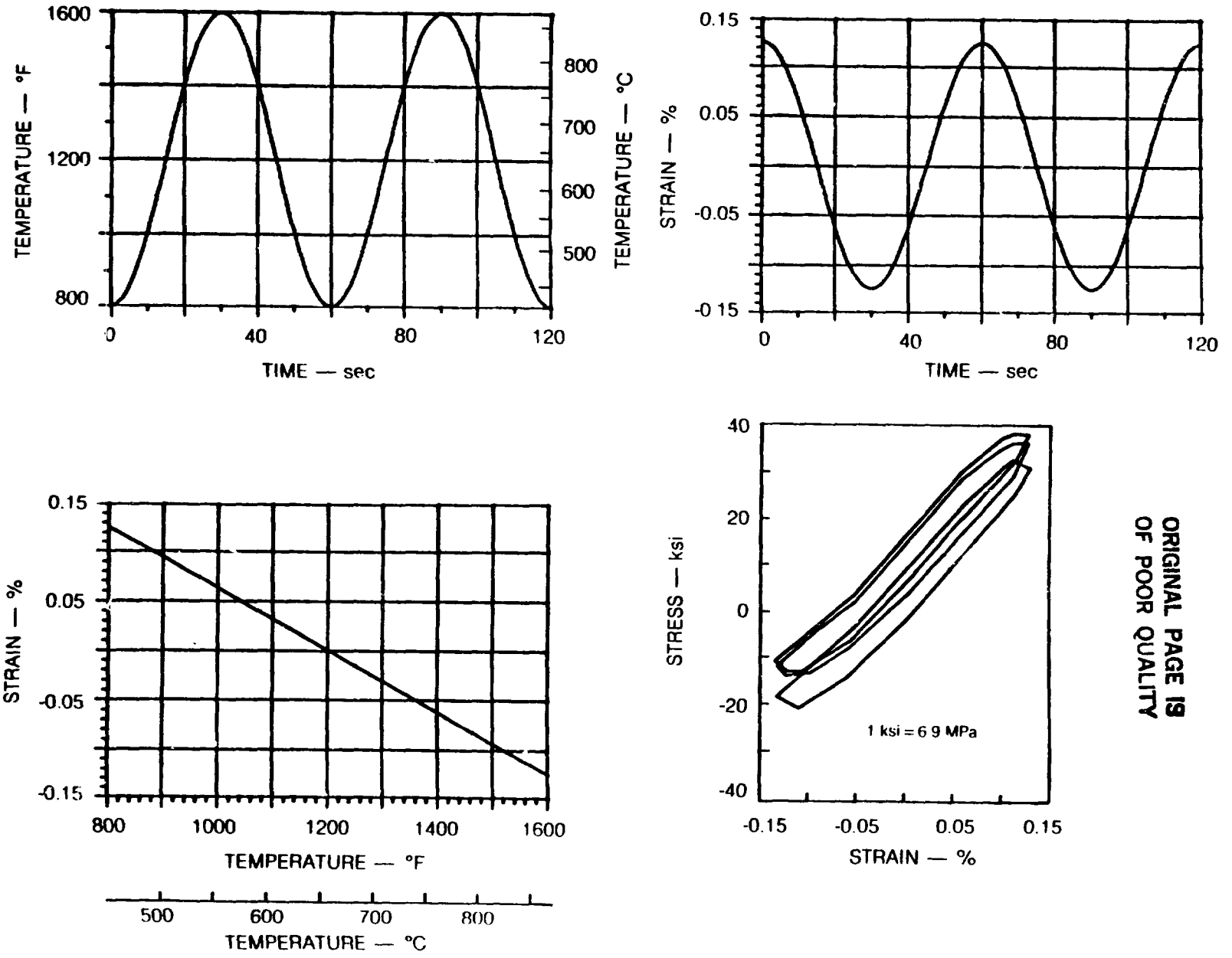

ORIGINAL PAGE IS
OF POOR QUALITY

Figure 1. TMF Cycle No. 1: Closed Symmetric Cycle

83-4-18-2

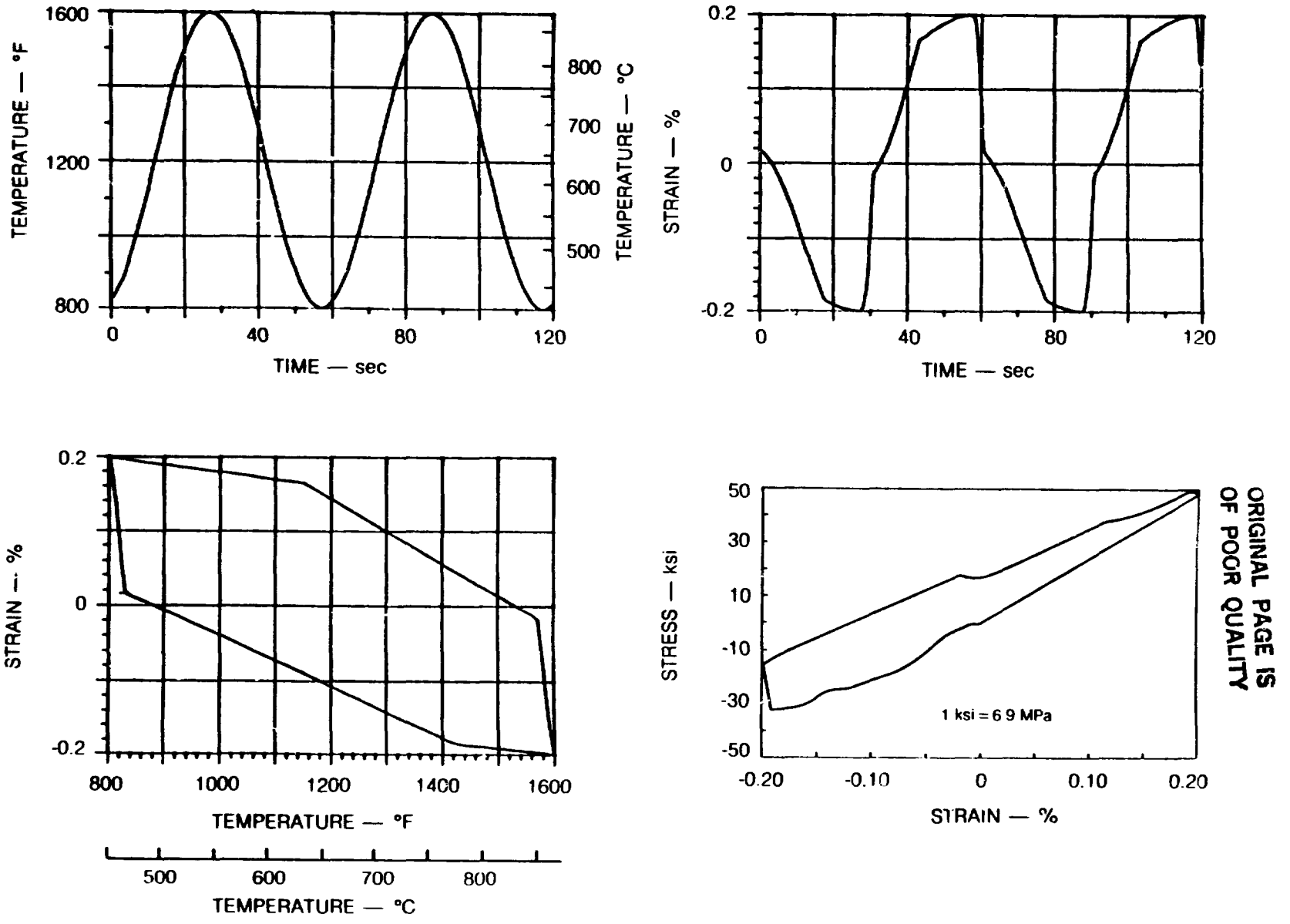

Figure 2. TMF Cycle No. 2: Open Symmetric Cycle

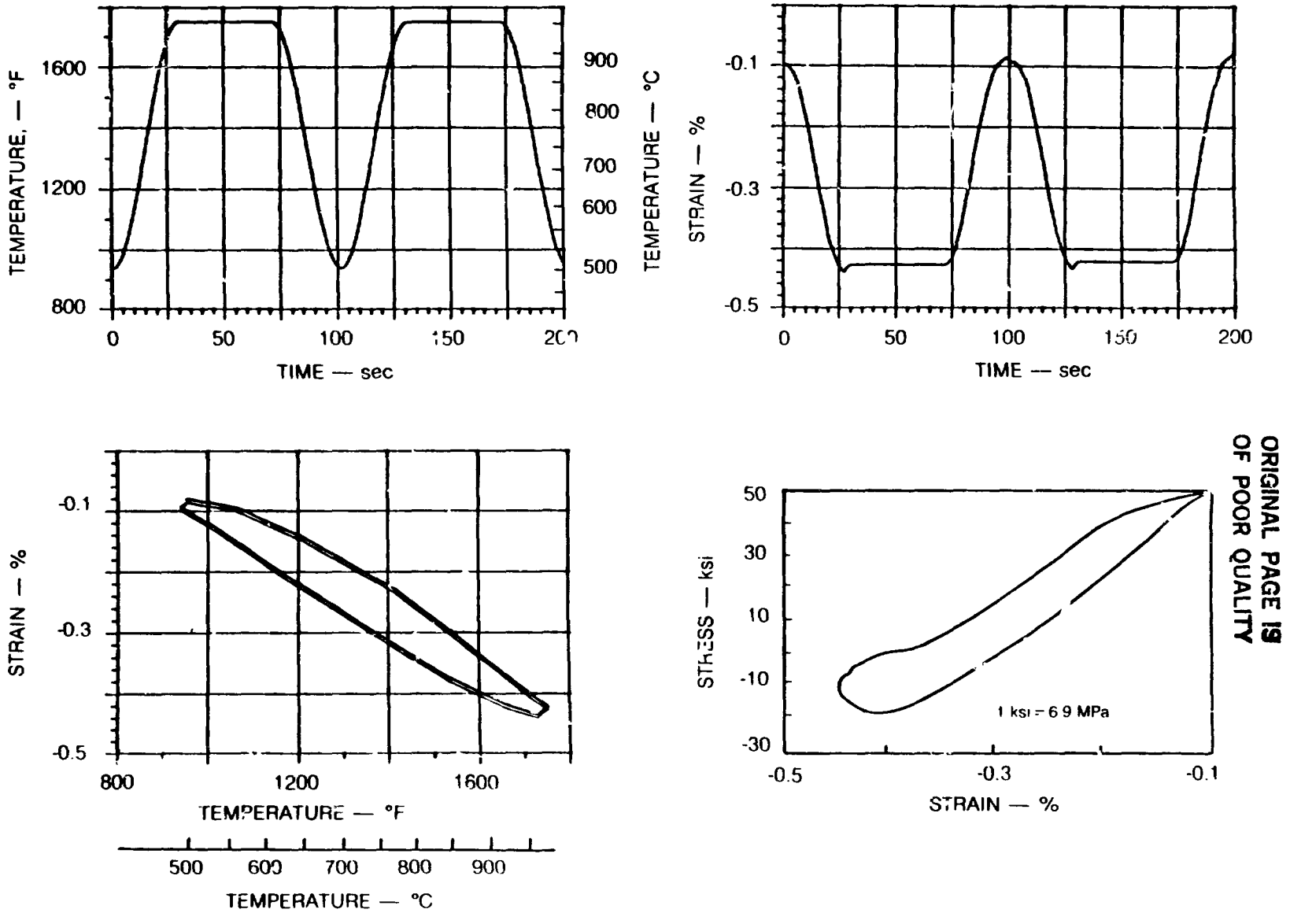

ORIGINAL PAGE IS
OF POOR QUALITY

83-4-18-1

Figure 3. TMF Cycle No. 3: Open Nonsymmetric Cycle

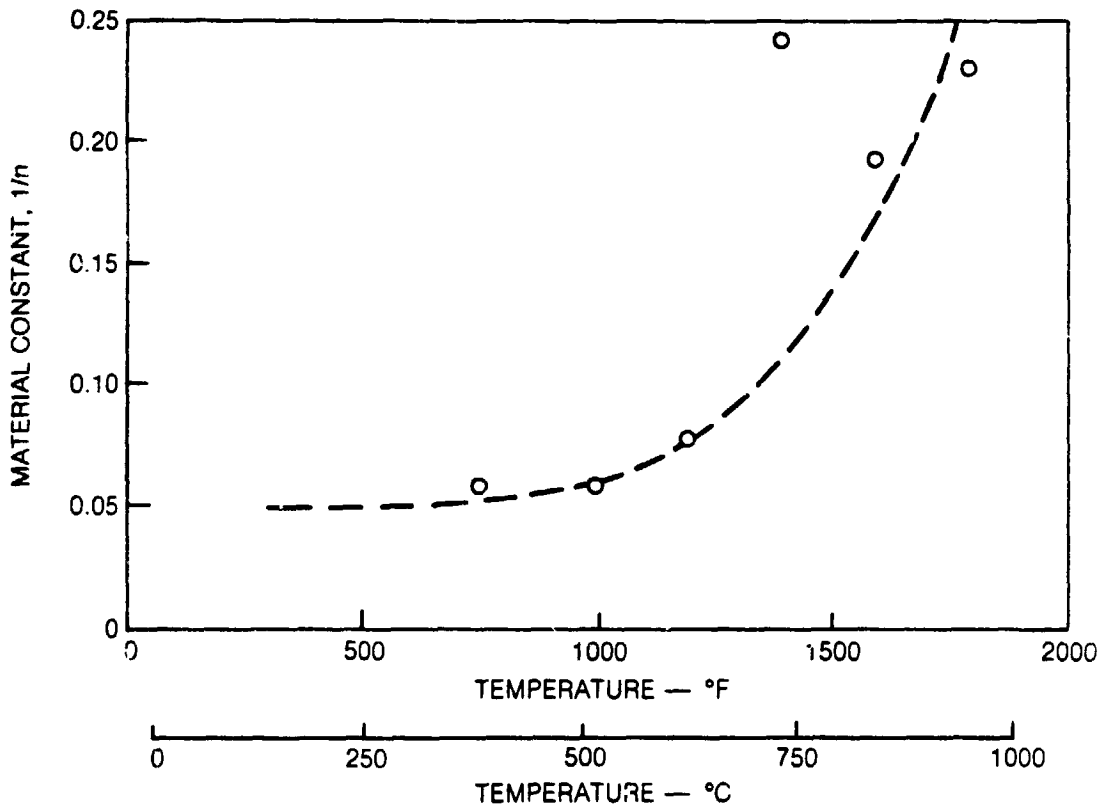

Figure 4. Evaluated Power Law Exponent, n, has a Step Change Occuring Between 1400 F and 1200 F

82-4-57-15

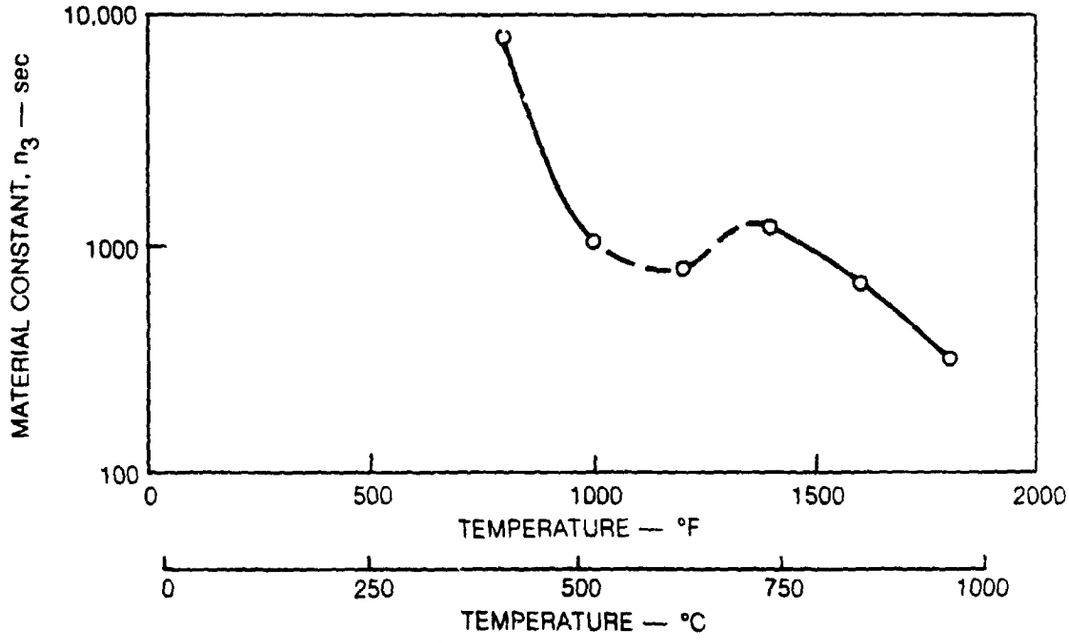

Figure 5. Evaluated Thermal Recovery Equilibrium Stress Parameter, n_3, has a Reversal in Slope Occurring Between 1000 F and 1400 F

82-4-57-14

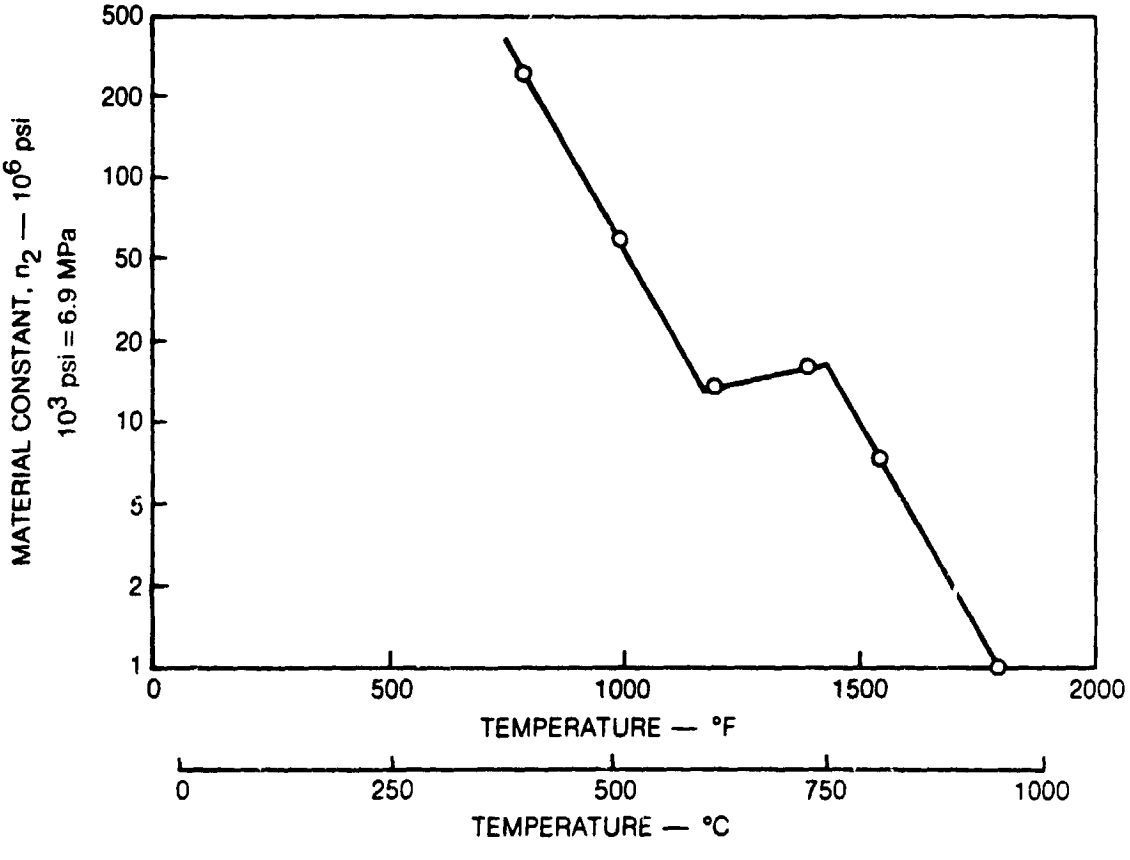

Figure 6. Evaluated Dynamic Recovery Equilibrium Stress Parameters, n_2, has a Reversal in Slope Occurring Between 1200 F and 1400 F

82-4-57-13

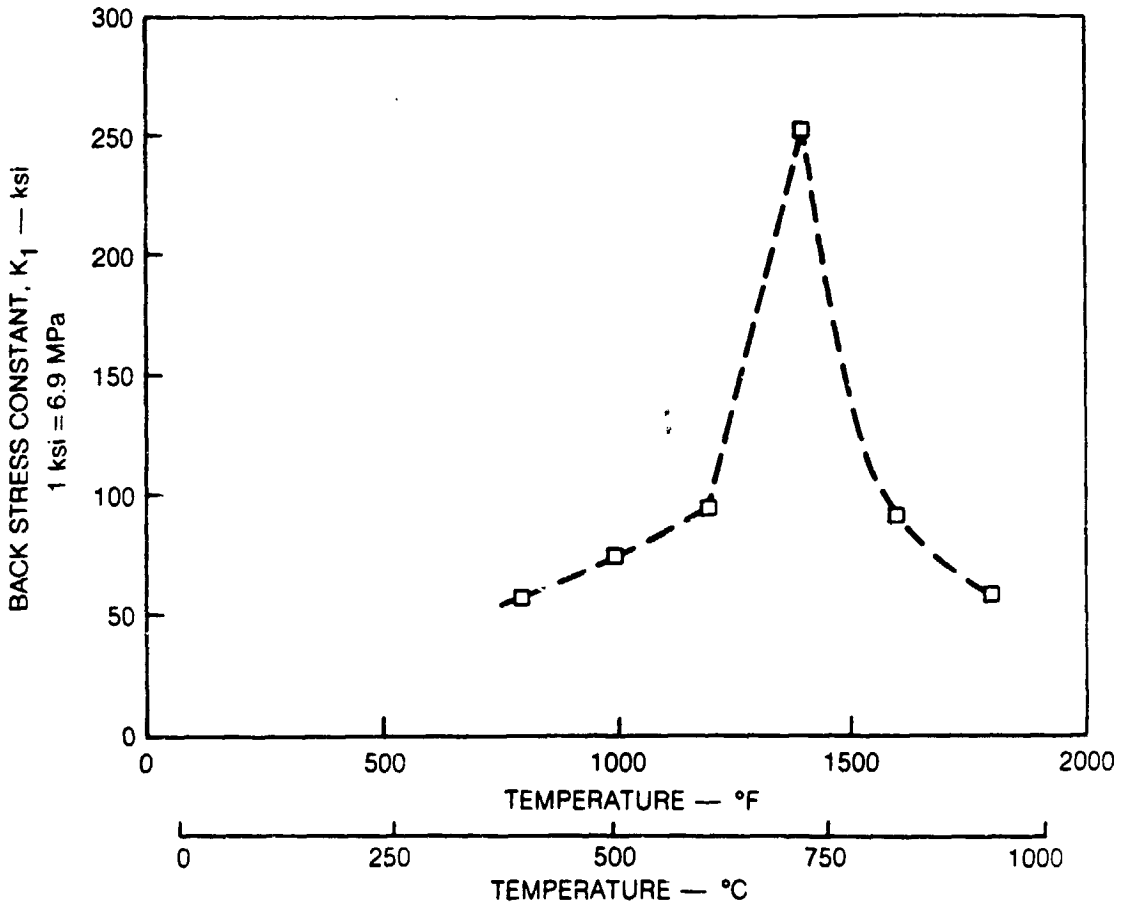

Figure 7. Constant Back Stress Parameter, K_1, has a Major Discontinuity Occurring Between 1200F and 1600F

82-4-57-12

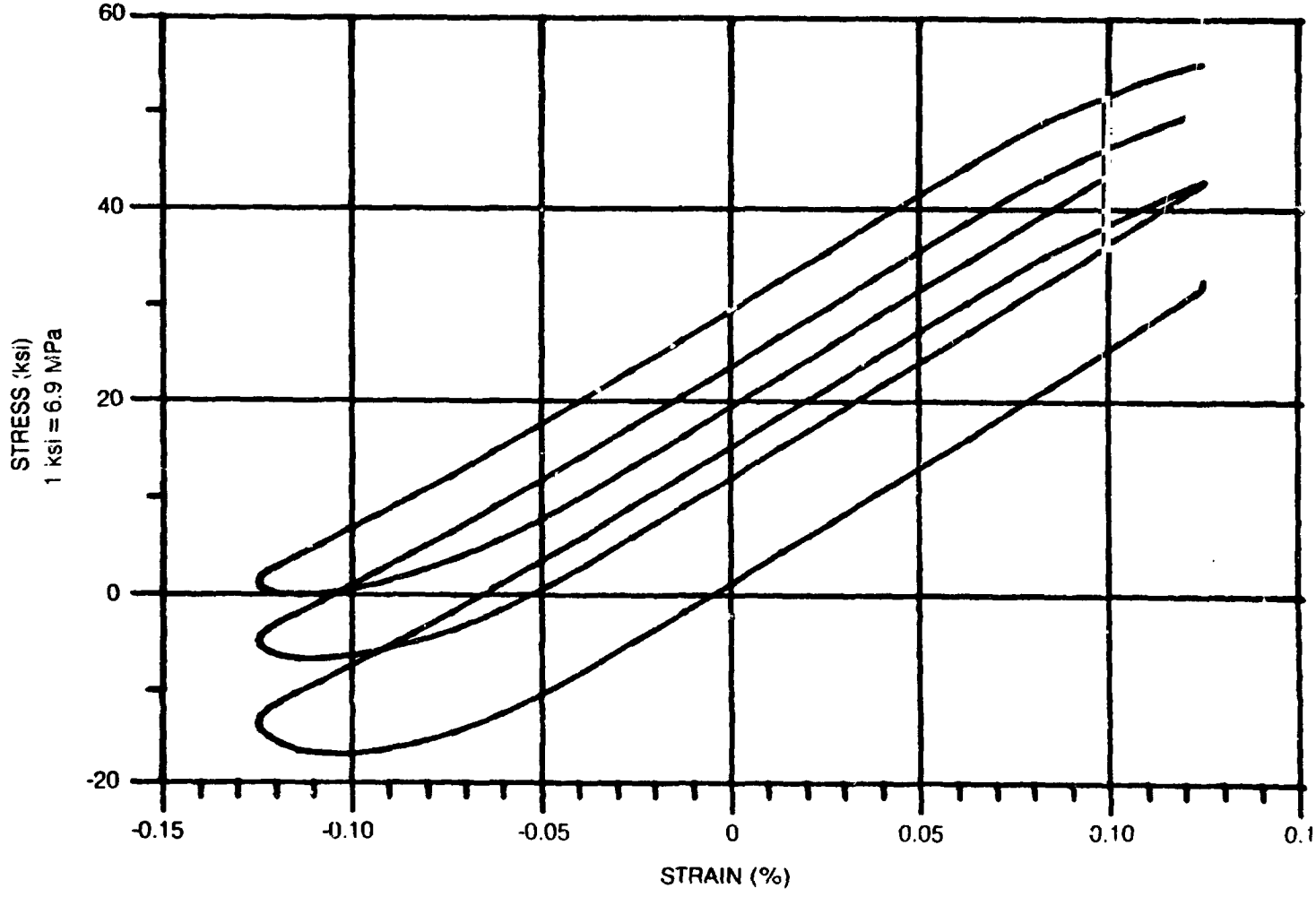

Figure 8. Predicted Response Using Walker's Theory for Closed Symmetric TMF Cycle Without Rate of Change of Temperature Terms

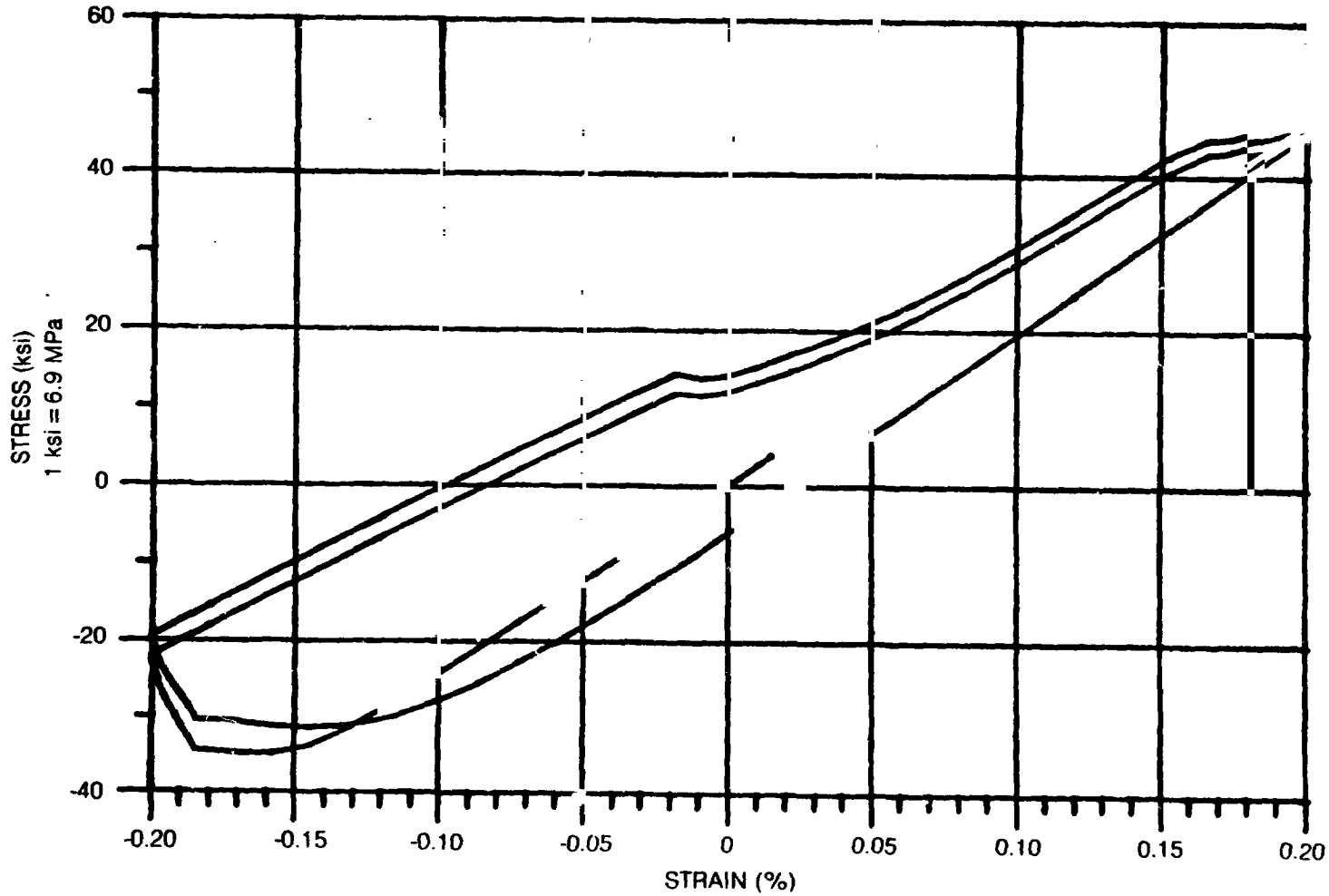

Figure 9. Predicted Response Using Walker's Theory for Open Symmetric TMF Cycle Without Rate of Change of Temperature Terms

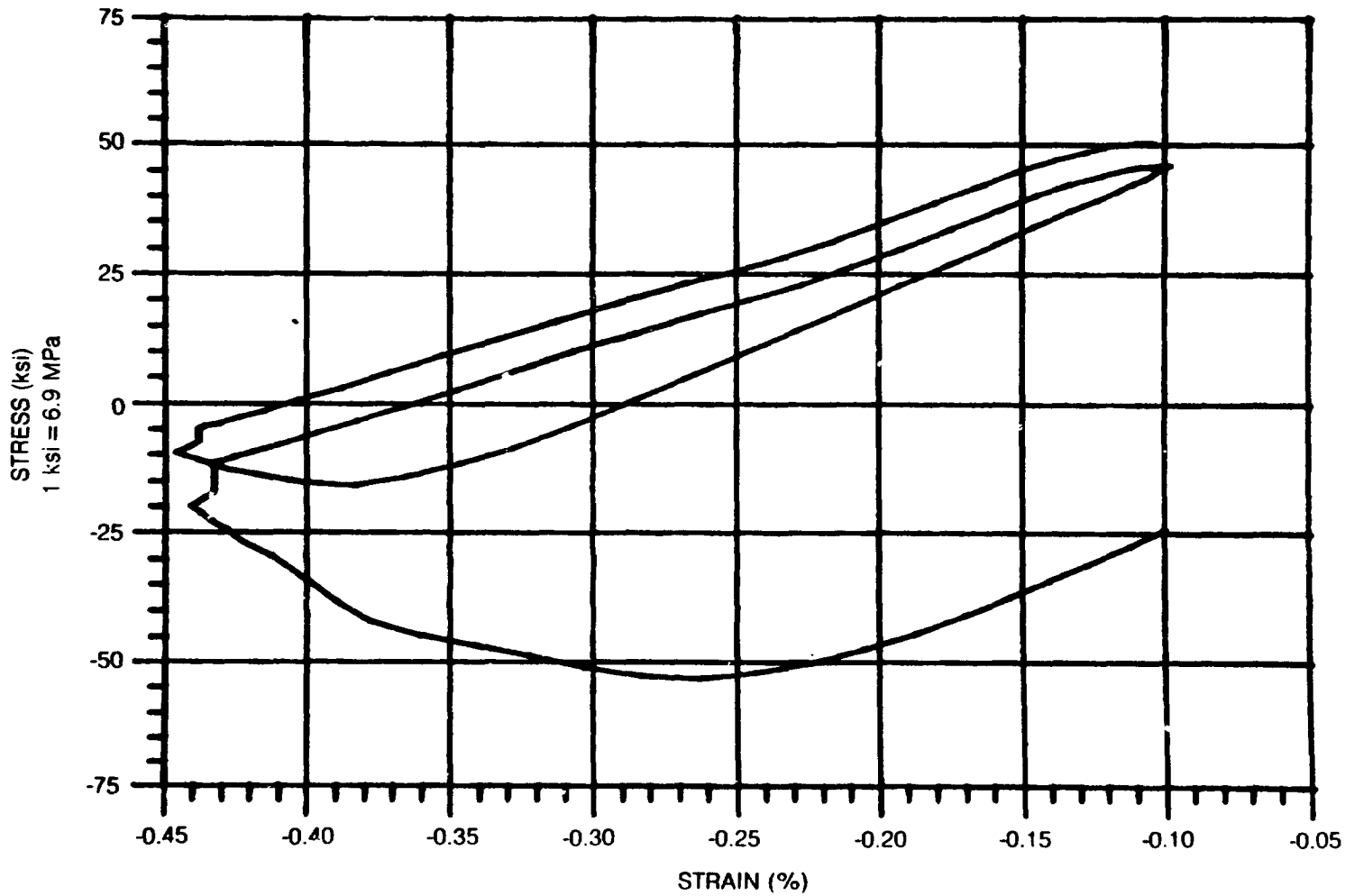

Figure 10. Predicted Response Using Walker's Theory for Open Nonsymmetric TMF Cycle Without Rate of Change of Temperature Terms

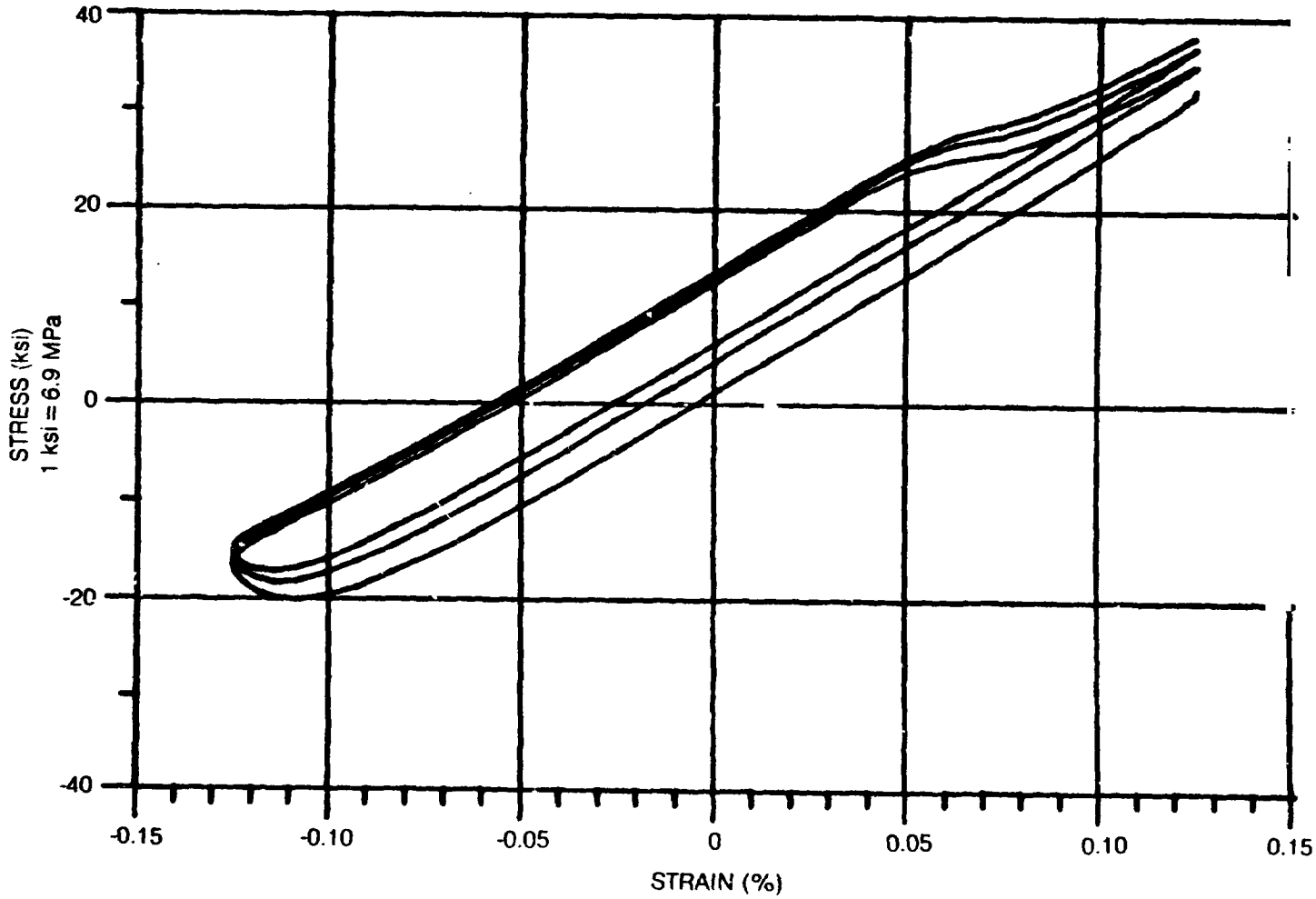

Figure 11. Predicted Response Using Walker's Theory for Closed Symmetric TMF Cycle With Rate of Change of Temperature Terms

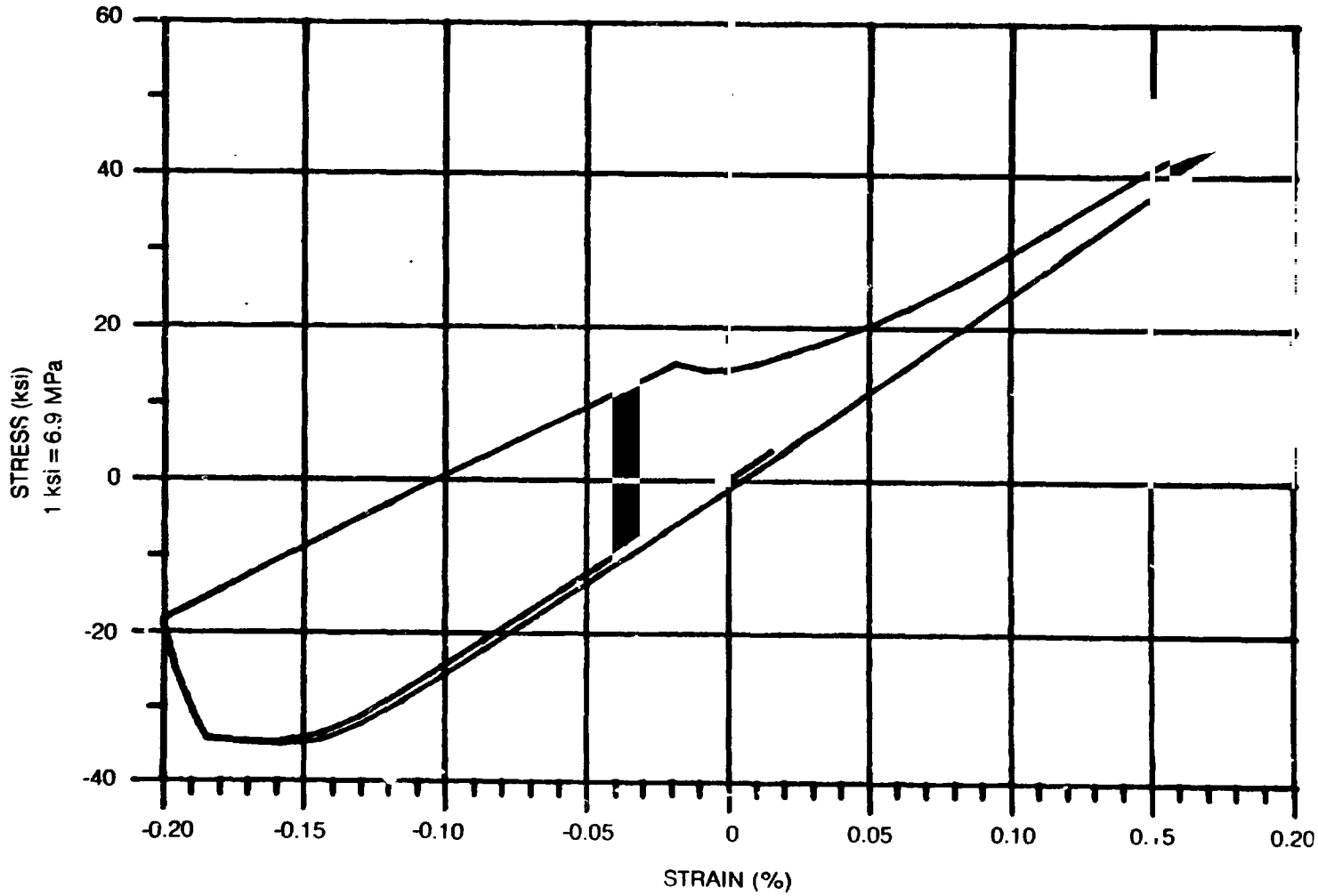

Figure 12. Predicted Response Using Walker's Theory for Open Symmetric TMF Cycle With Rate of Change of Temperature Terms

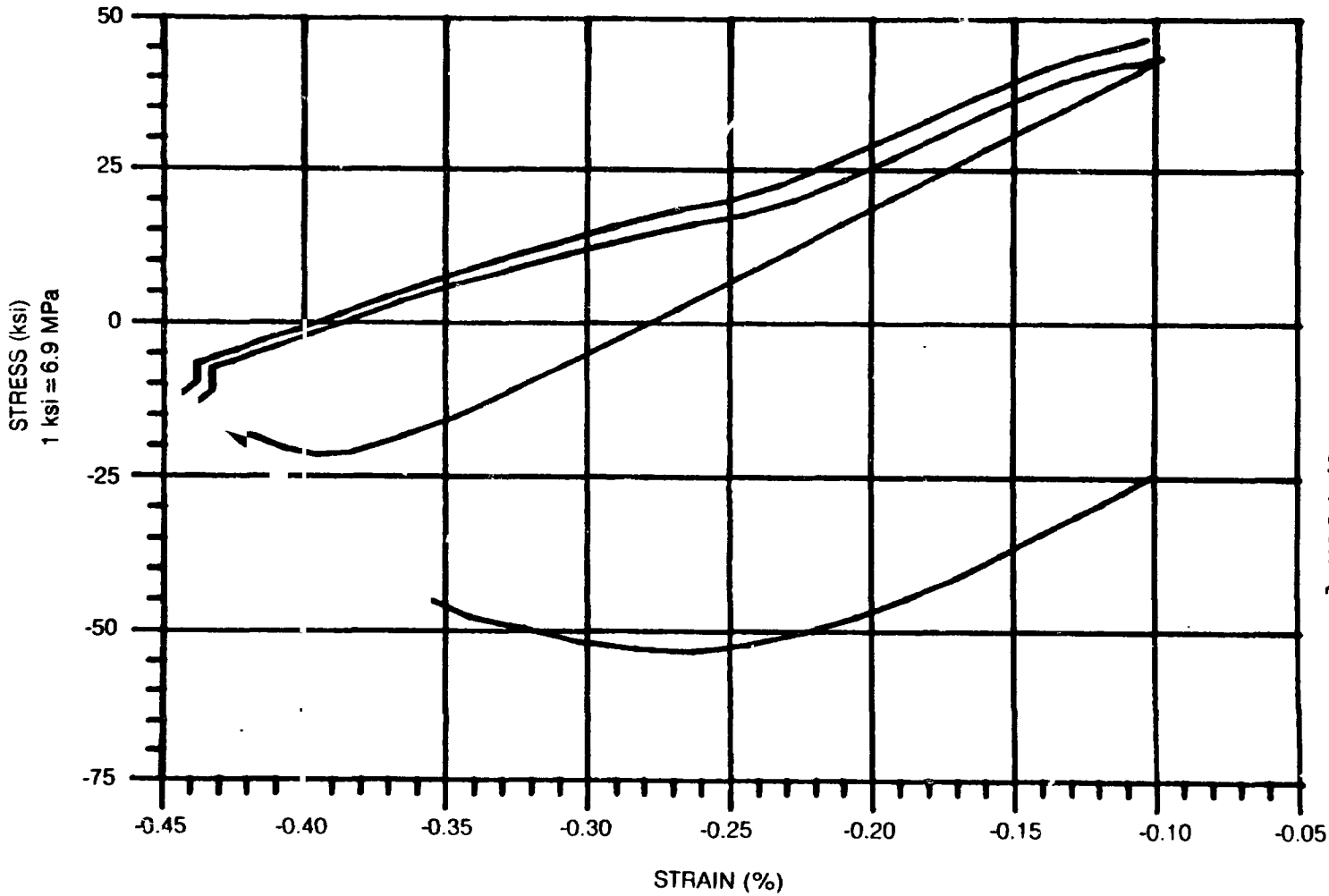

Figure 13. Predicted Response Using Walker's Theory for Open Nonsymmetric TMF Cycle With Rate of Change of Temperature Terms

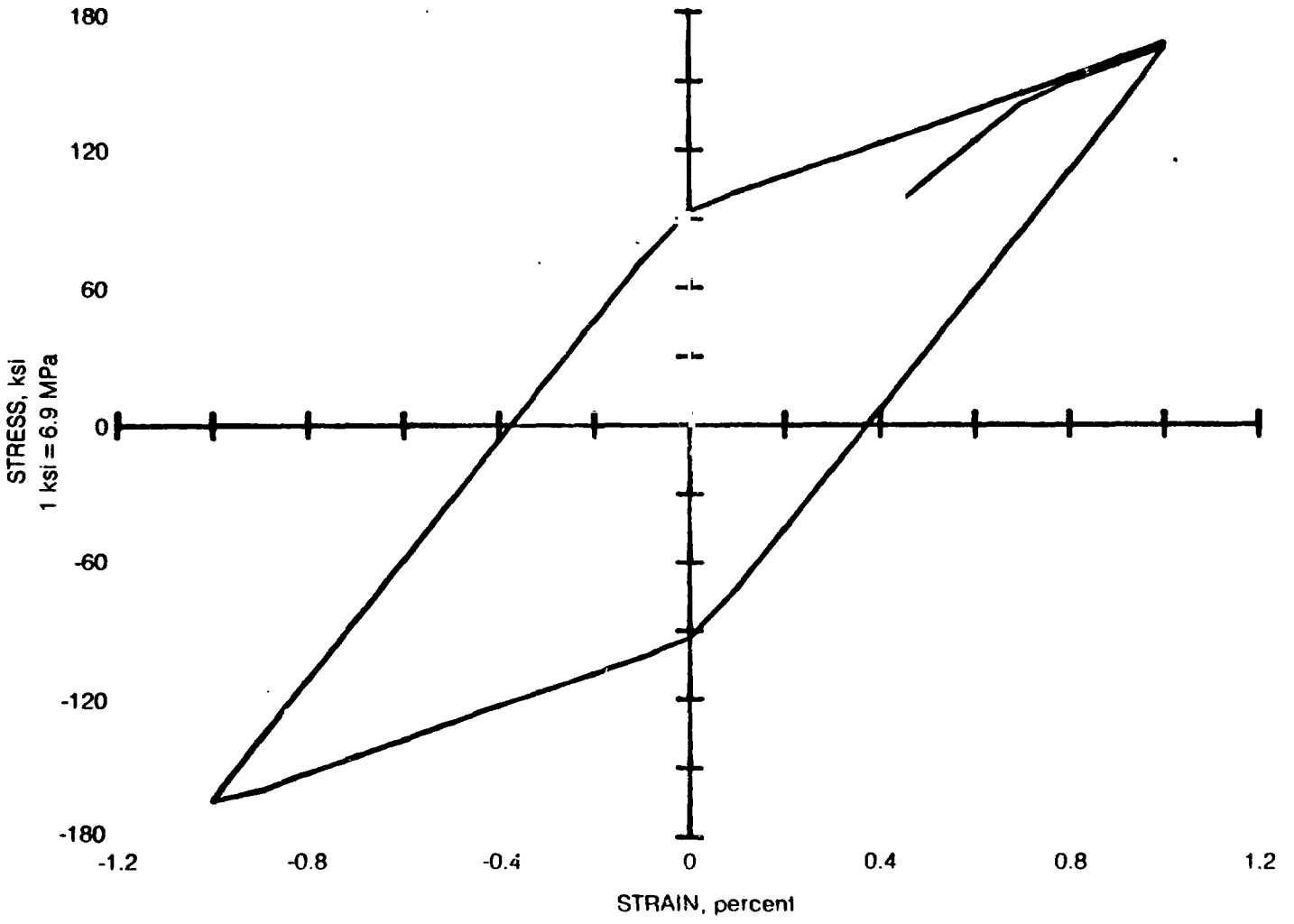

Figure 14. Hysteresis Loop for Hastelloy-X Using Miller's Theory at 427 C for a Strain Rate of 2.00×10^{-2}

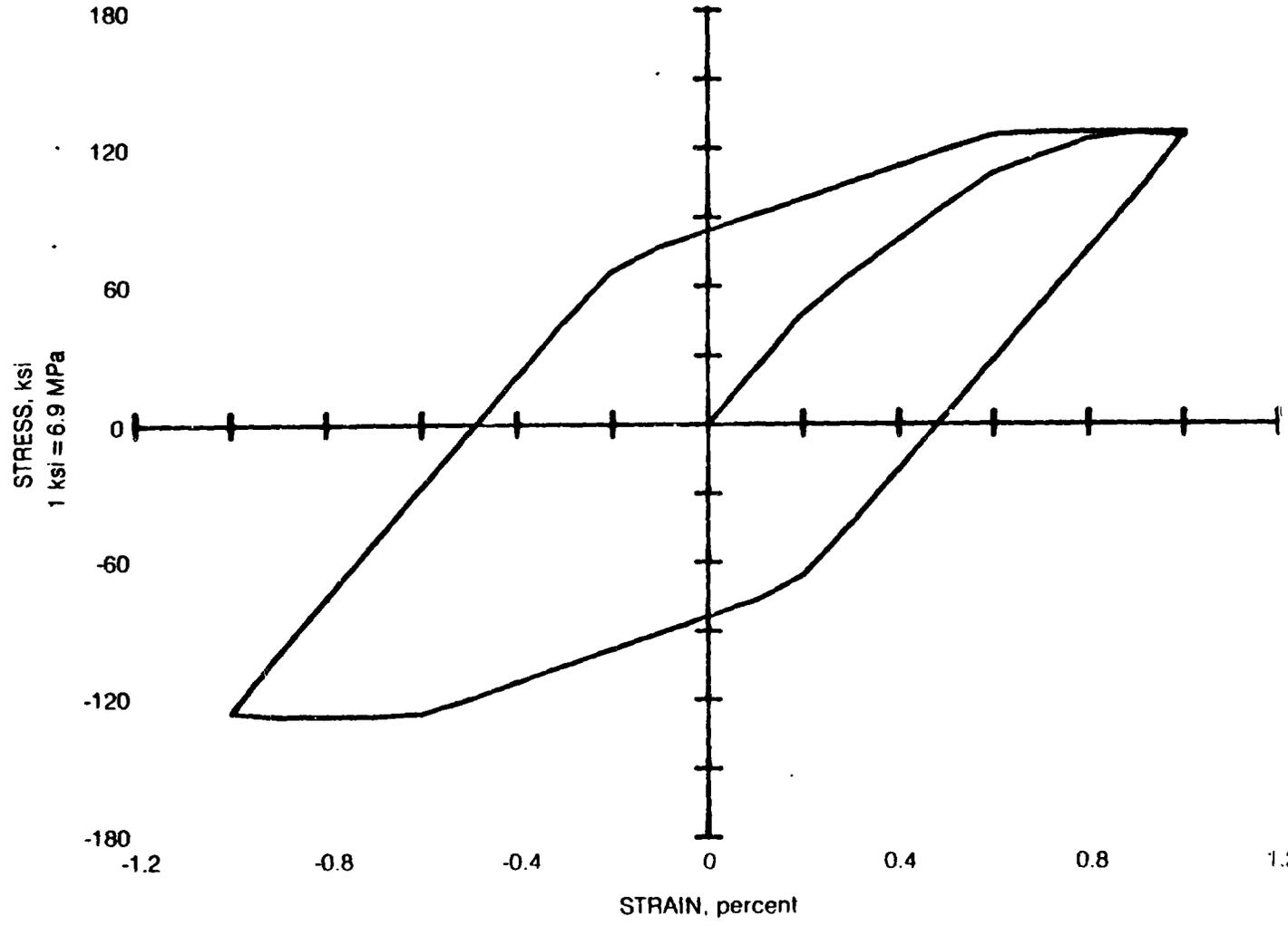

Figure 15. Hysteresis Loop for Hastelloy-X Using Miller's Theory at 538 C for a Strain Rate of 6.67×10^{-3}

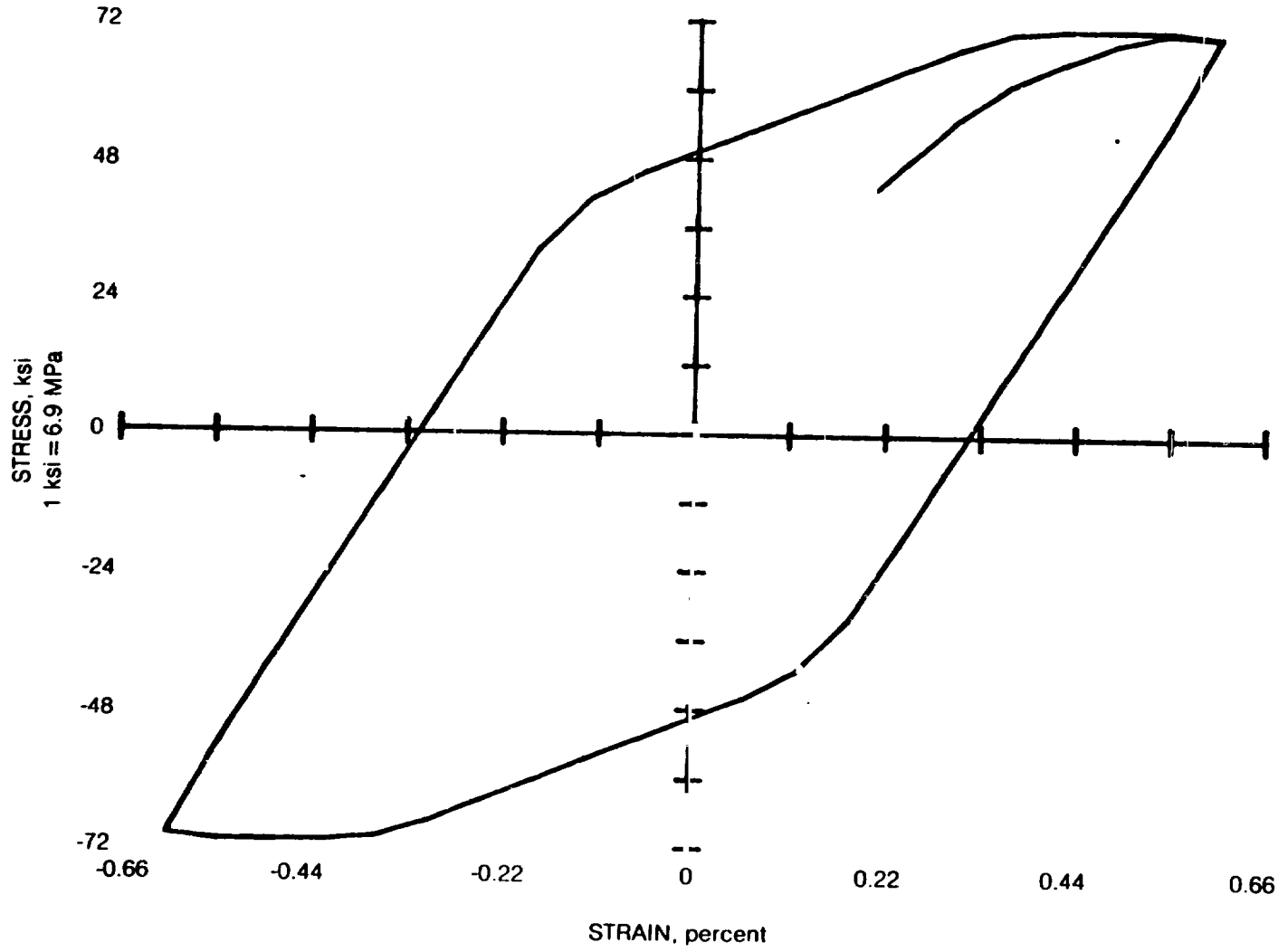

Figure 16. Hysteresis Loop for Hastelloy-X Using Miller's Theory at 649 C for a Strain Rate of 3.70×10^{-5}/sec

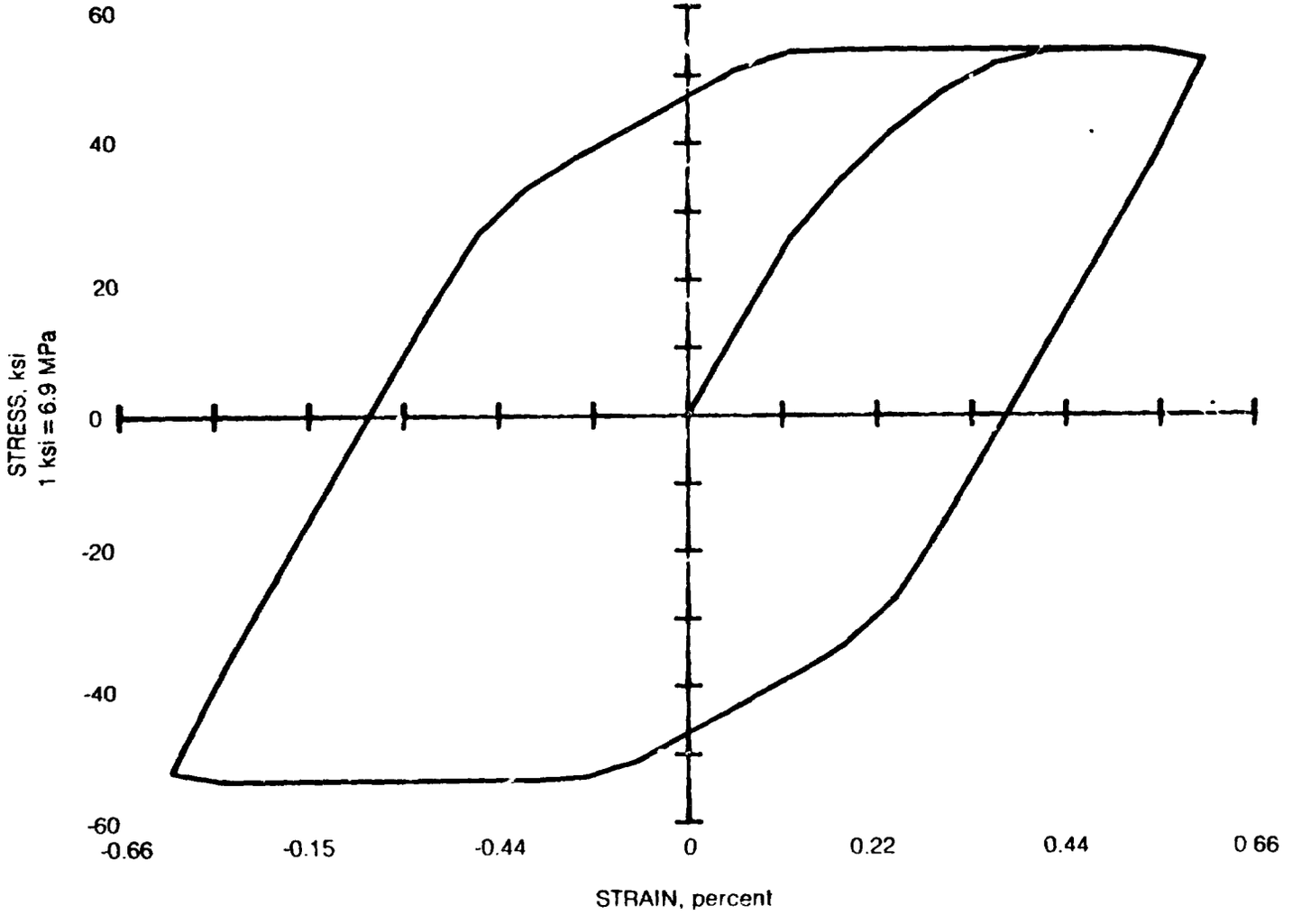

Figure 17. Hysteresis Loop for Hastelloy-X Using Miller's Theory at 760 C for a Strain Rate of 3.70×10^{-4}/ sec

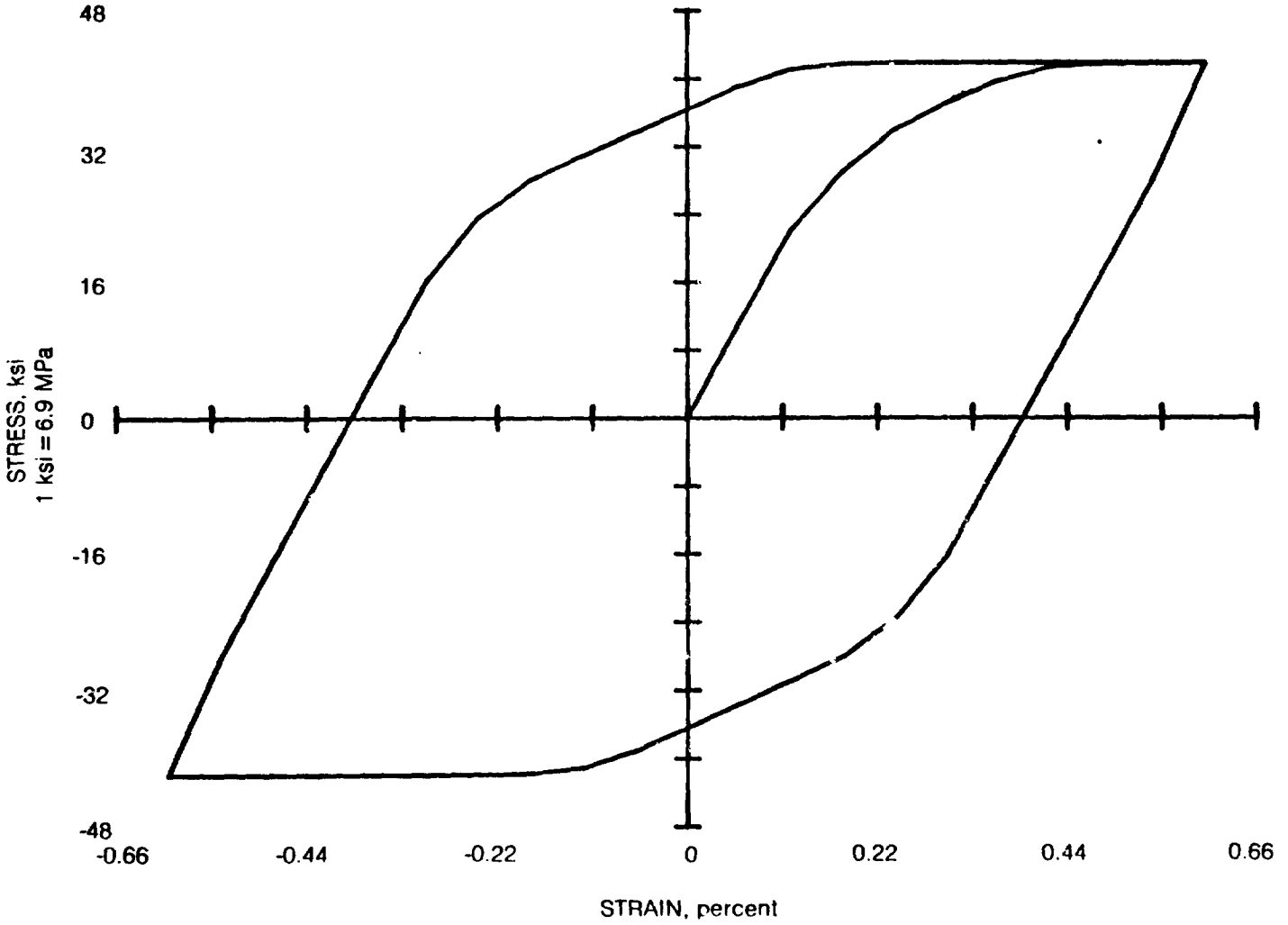

Figure 18. Hysteresis Loop for Hastelloy-X Using Miller's Theory at 871 C for a Strain Rate of 3.90×10^{-3}/sec

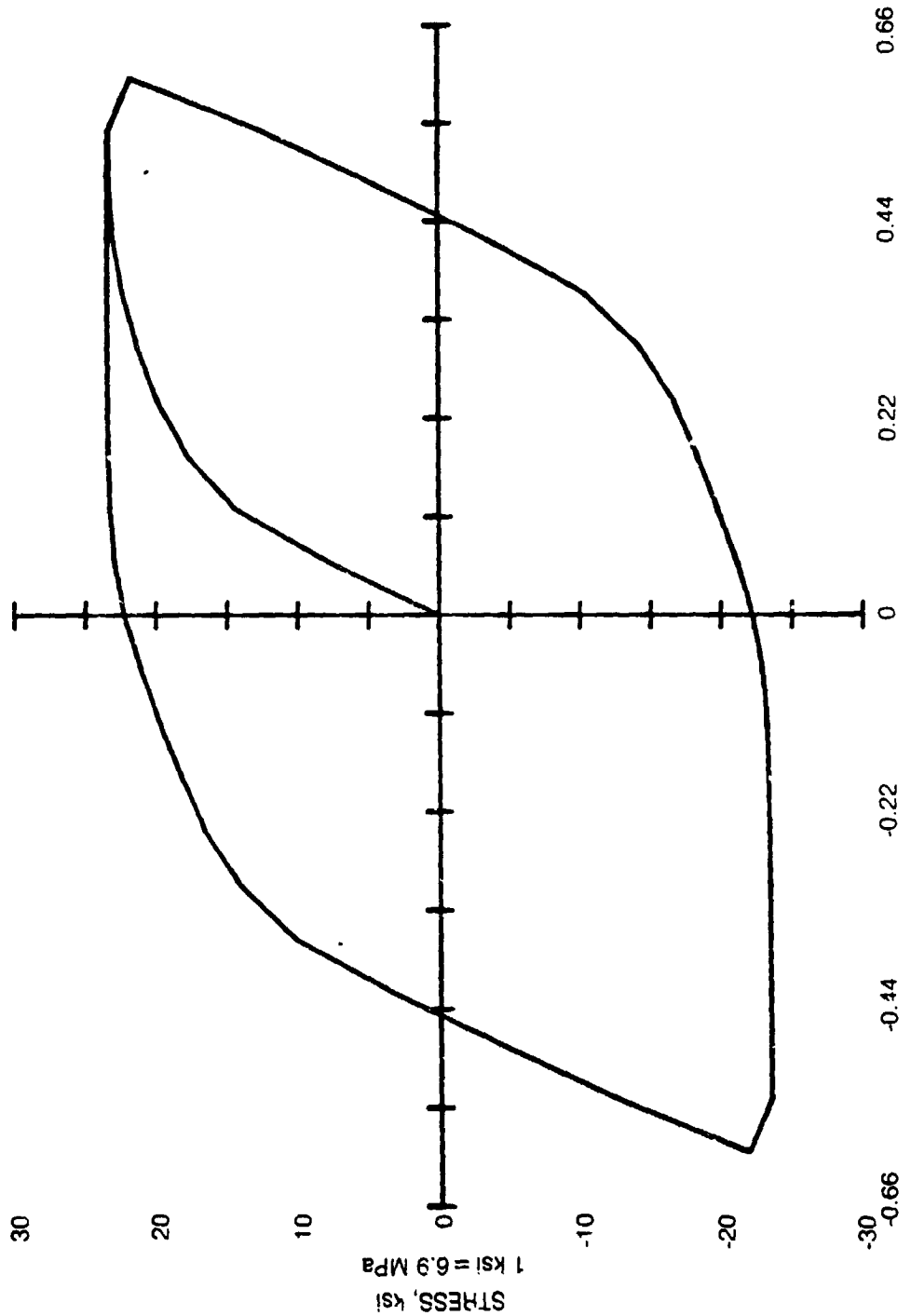

Figure 19. Hysteresis Loop for Hastelloy-X Using Miller's Theory at 982 C for a Strain Rate of 3.87×10^{-3}/sec

83-2-87-6

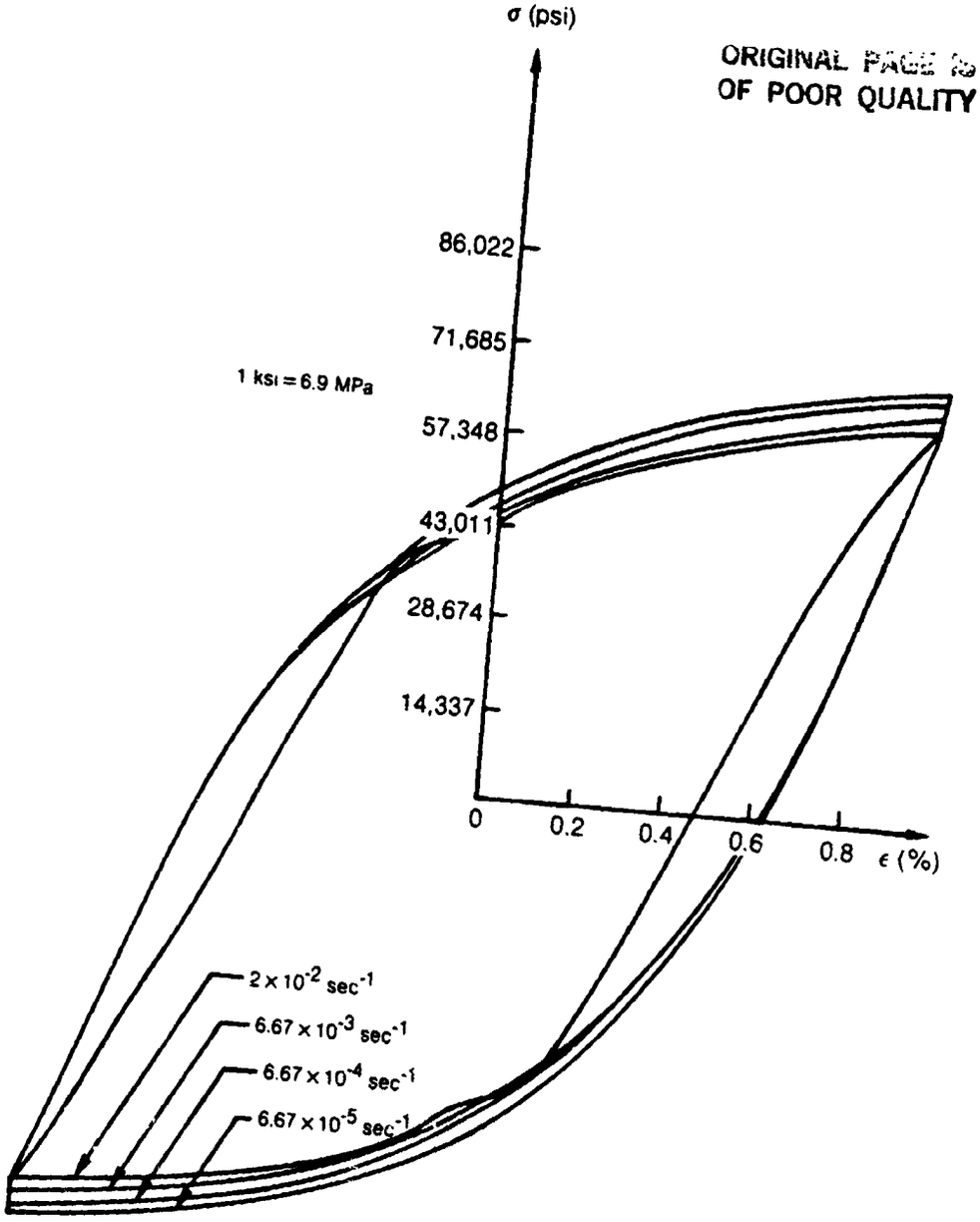

Figure 20. Experimental Steady State Hysteresis Loops for Hastelloy-X Showing Inverse Strain Rate Sensitivity at 427°C (800°F)

STRAIN AMPLITUDE IS ± 1 PERCENT

82-4-57-11

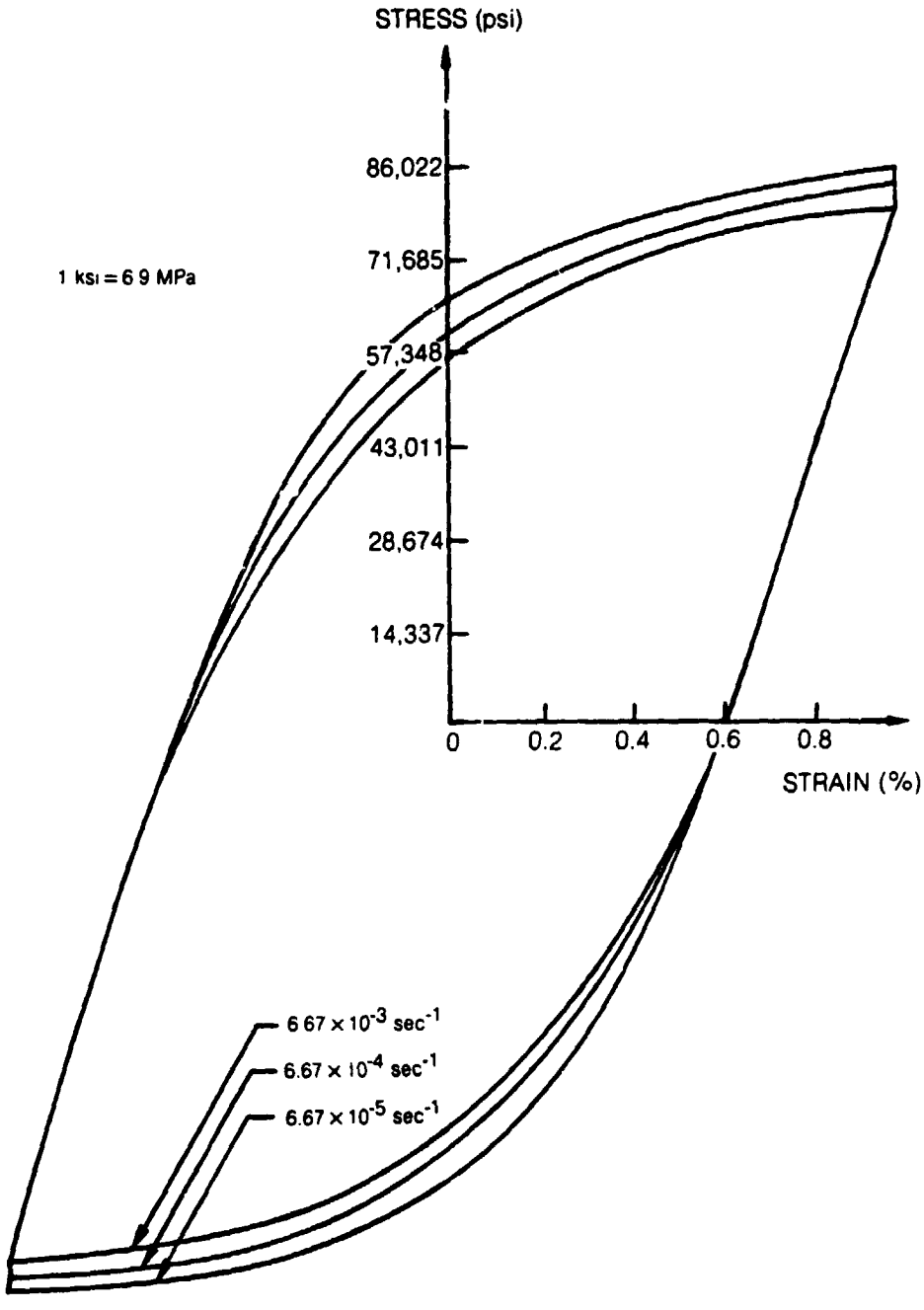

Figure 21. Experimental Steady State Hysteresis Loops for Hastelloy-X Showing Inverse Strain Rate Sensitivity at 538°C (1000°F)

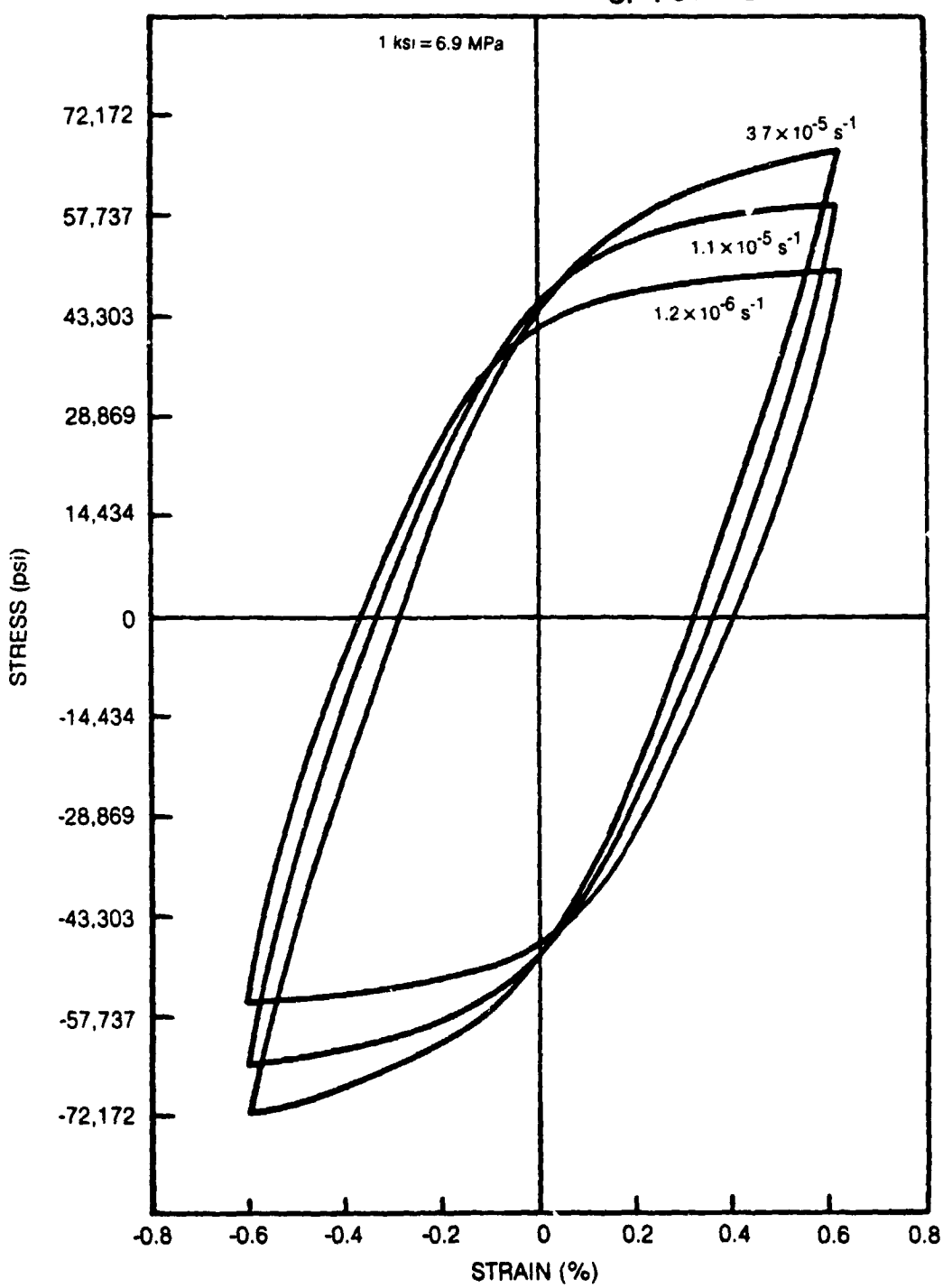

Figure 22. Experimental Steady State Hysteresis Loops for Hastelloy-X at 649°C (1200°F)

82-4-57-9

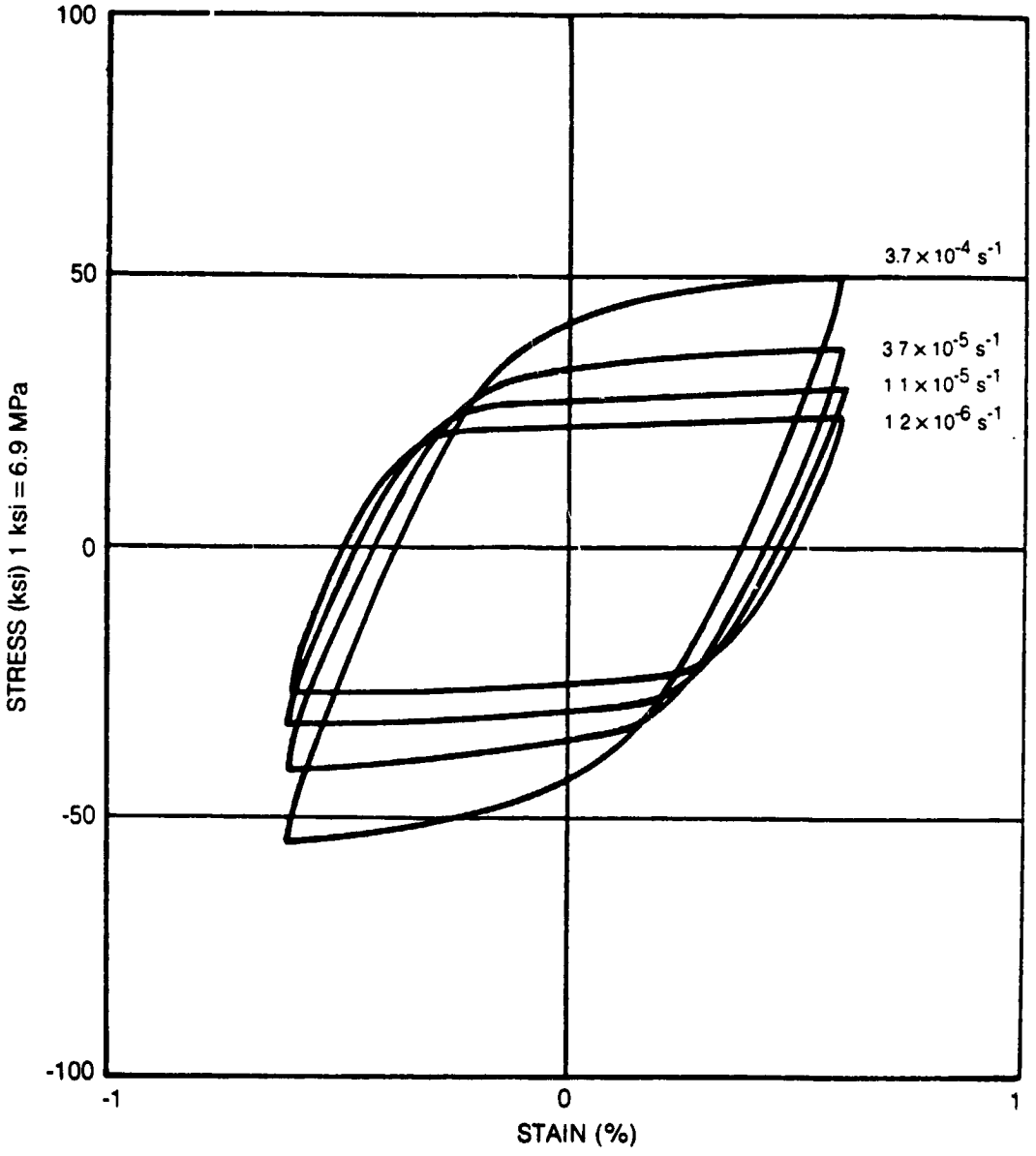

Figure 23. Experimental Steady State Hysteresis Loops for Hastelloy-X at 760°C (1400°F)

82-4-57-8

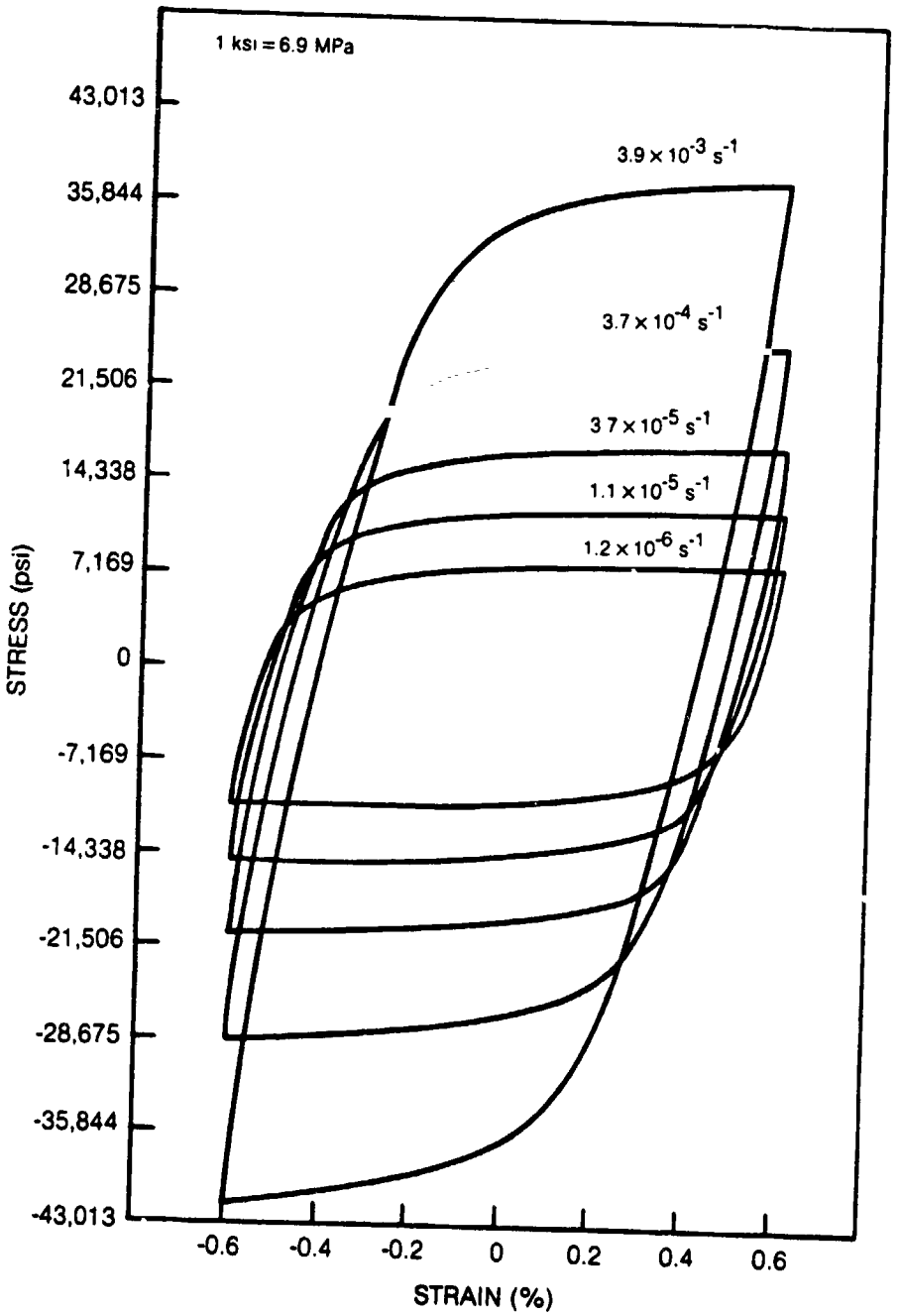

Figure 24. Experimental Hysteresis Loops for Hastelloy-X at 871 °C (1600 °F)

82-4-57-7

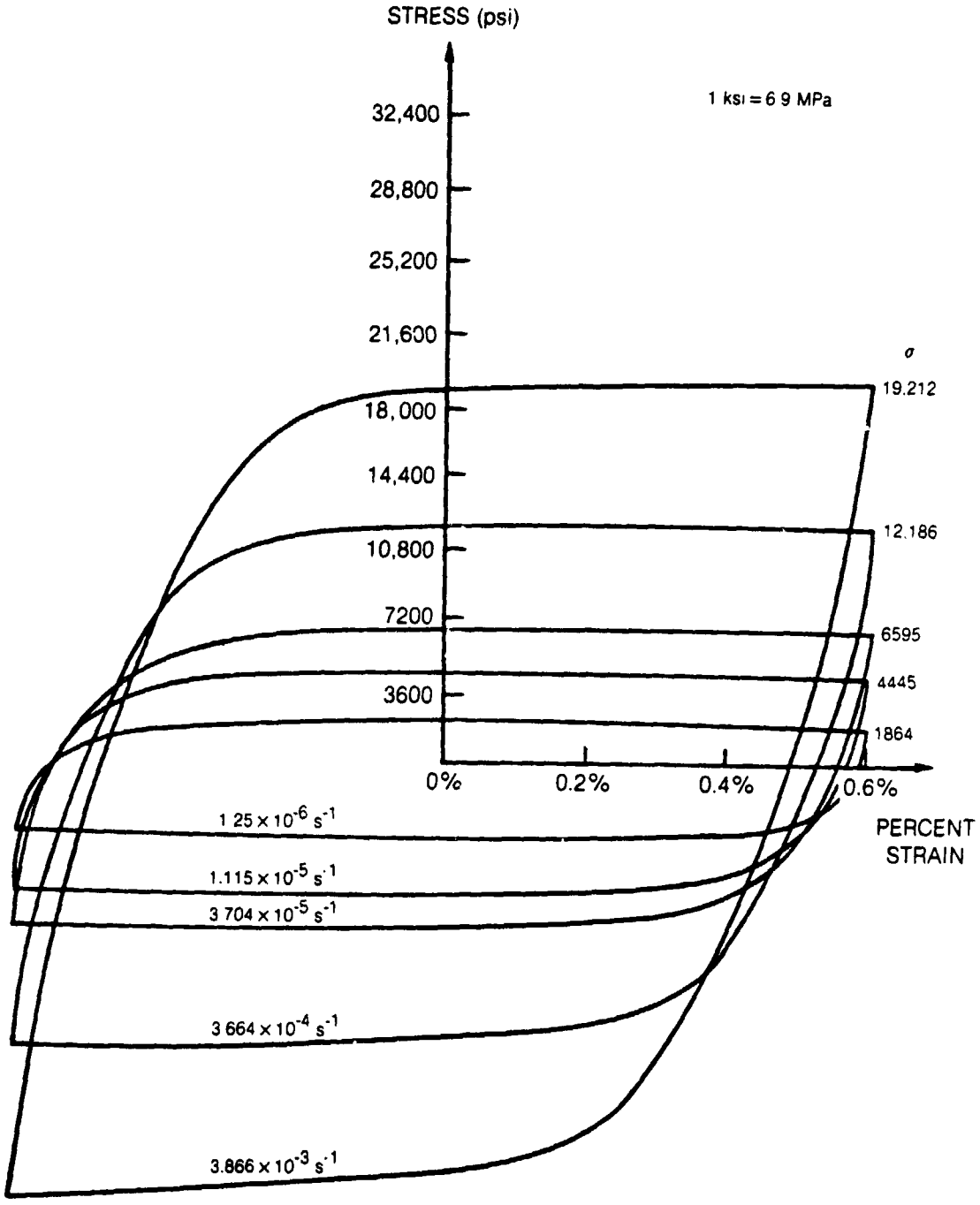

Figure 25. Experimental Hysteresis Loops for Hastelloy-X at 982°C (1800°F)

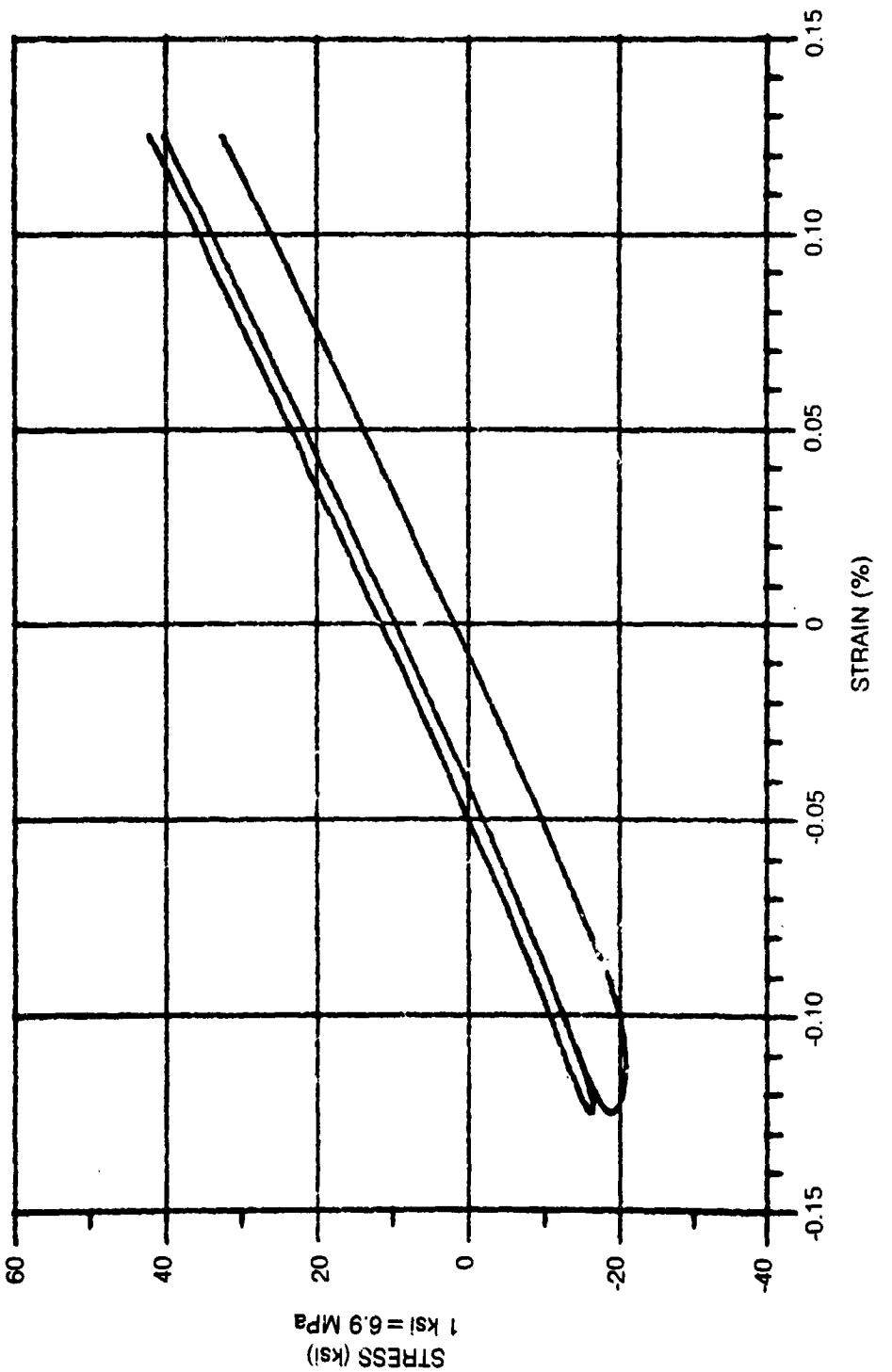

Figure 26. Predicted Response Using Miller's Theory for Closed Symmetric TMF Cycle Without Rate of Change of Temperature Terms

82-4-57-28

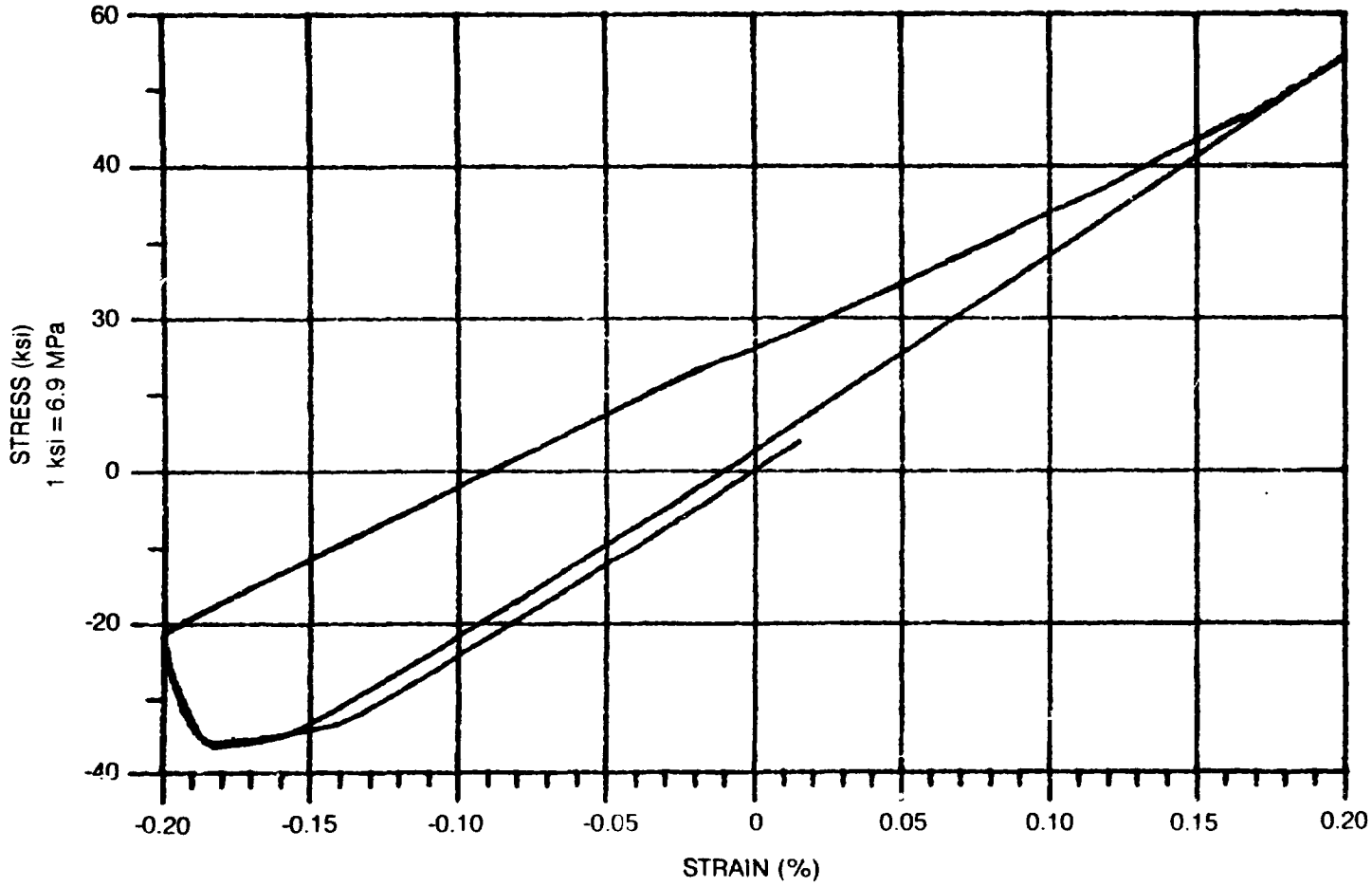

Figure 27. Predicted Response Using Miller's Theory for Open Symmetric TMF Cycle Without Rate of Change of Temperature Terms

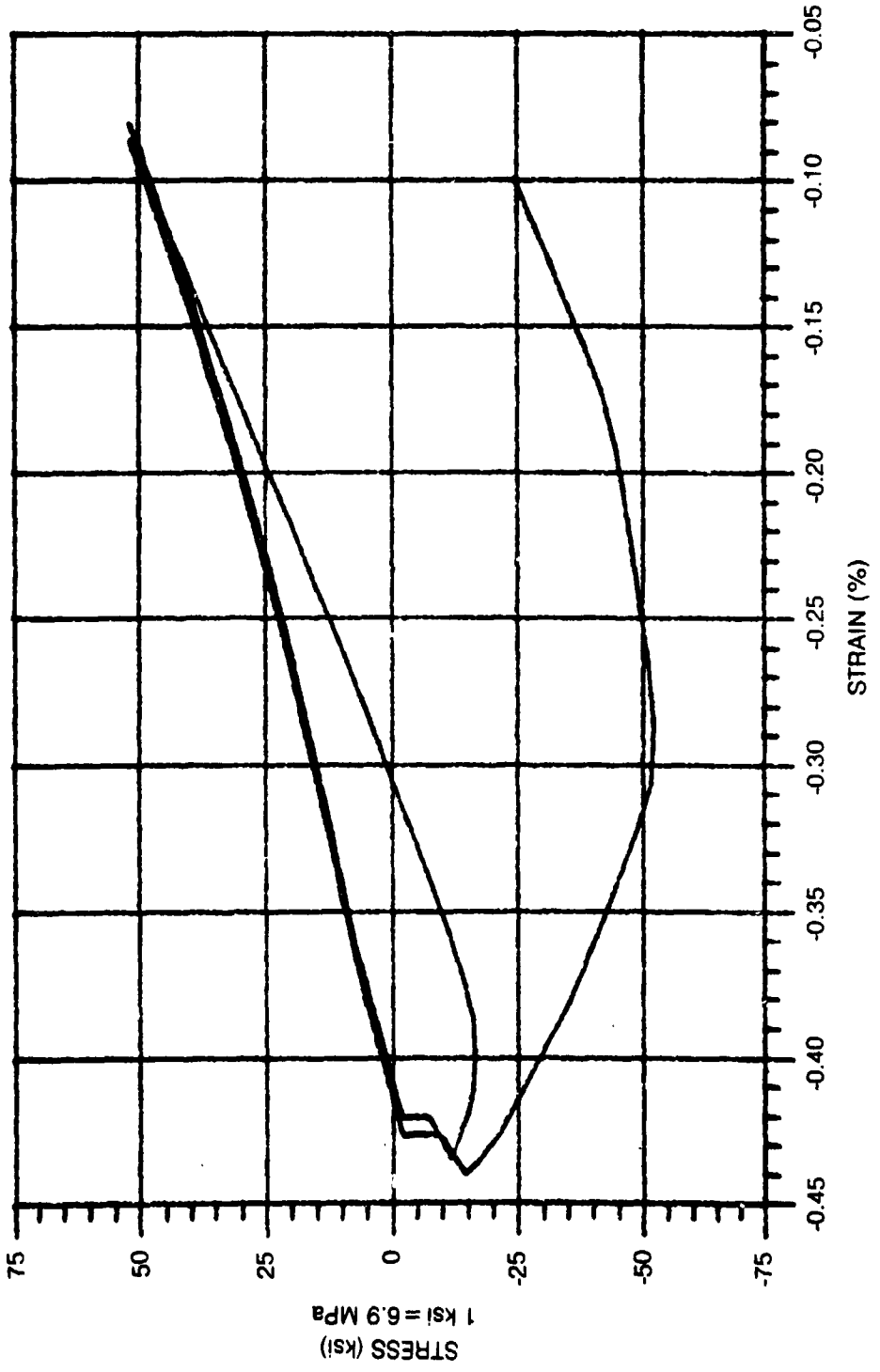

Figure 28. Predicted Response Using Miller's Theory for Open Nonsymmetric TMF Cycle Without Rate of Change of Temperature Terms

82-4-57-30

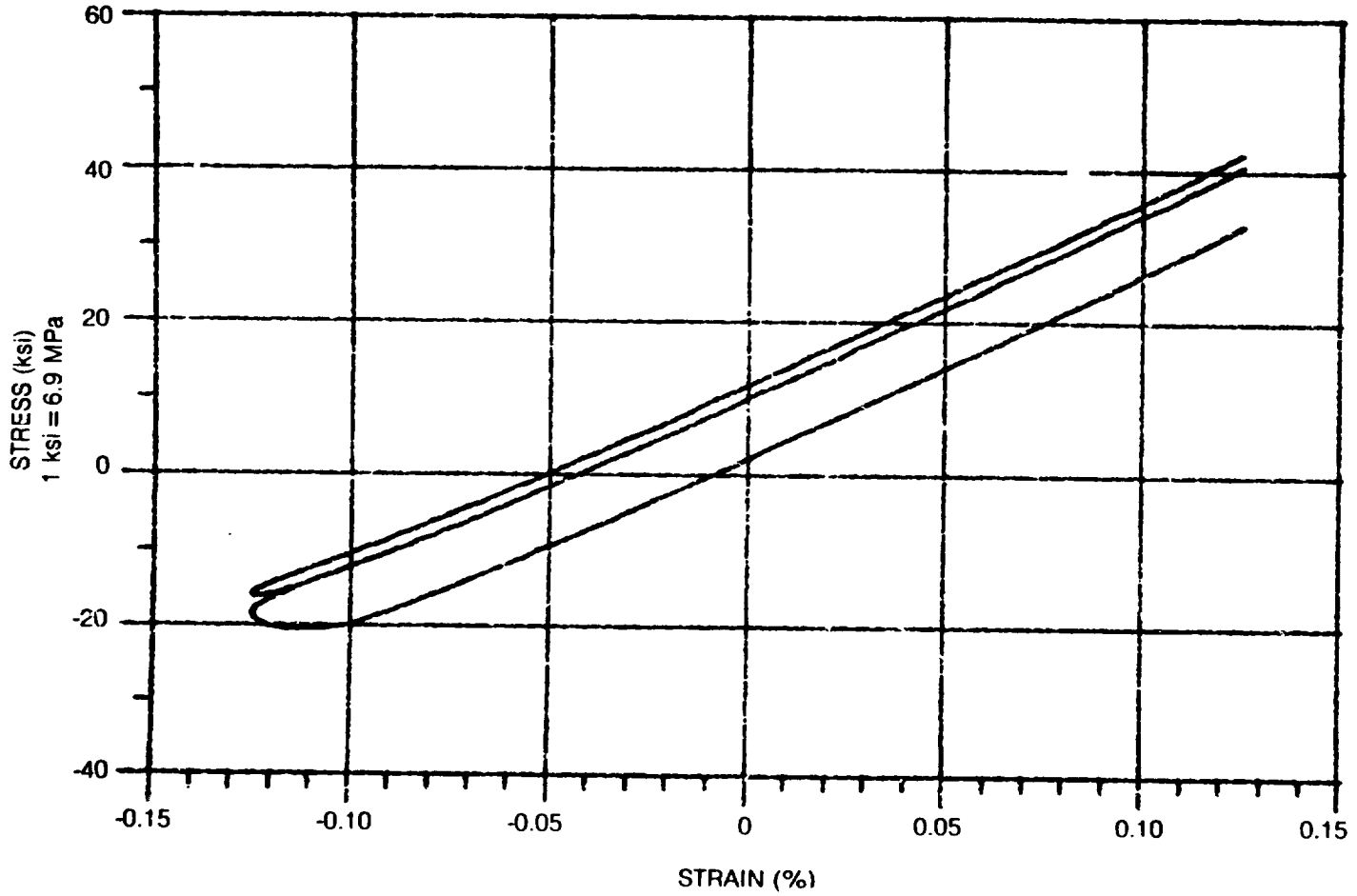

Figure 29. Predicted Response Using Miller's Theory for Closed Symmetric TMF Cycle With Rate of Change of Temperature Terms

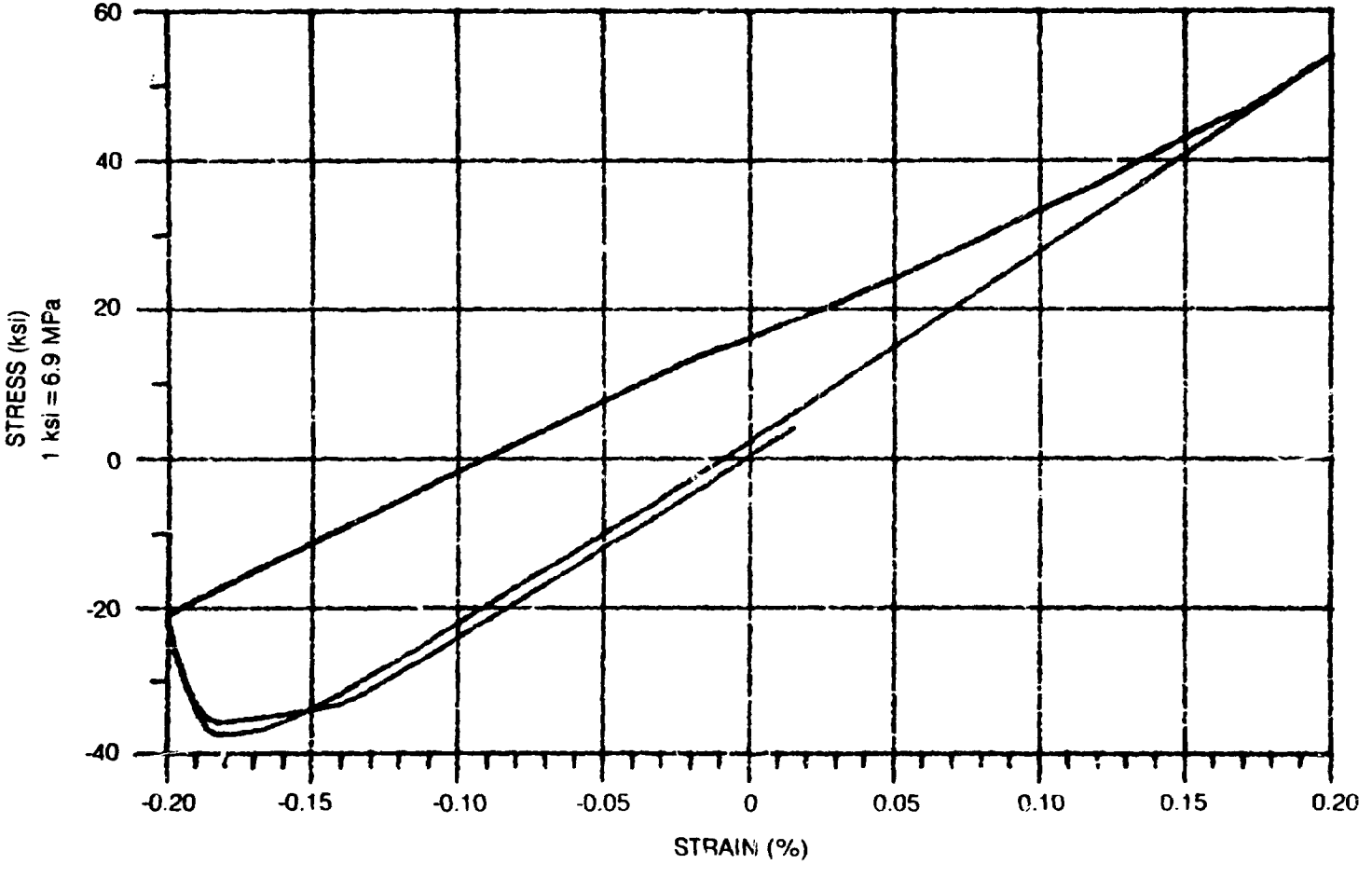

Figure 30. Predicted Response Using Miller's Theory for Open Symmetric TMF Cycle With Rate of Change of Temperature Terms

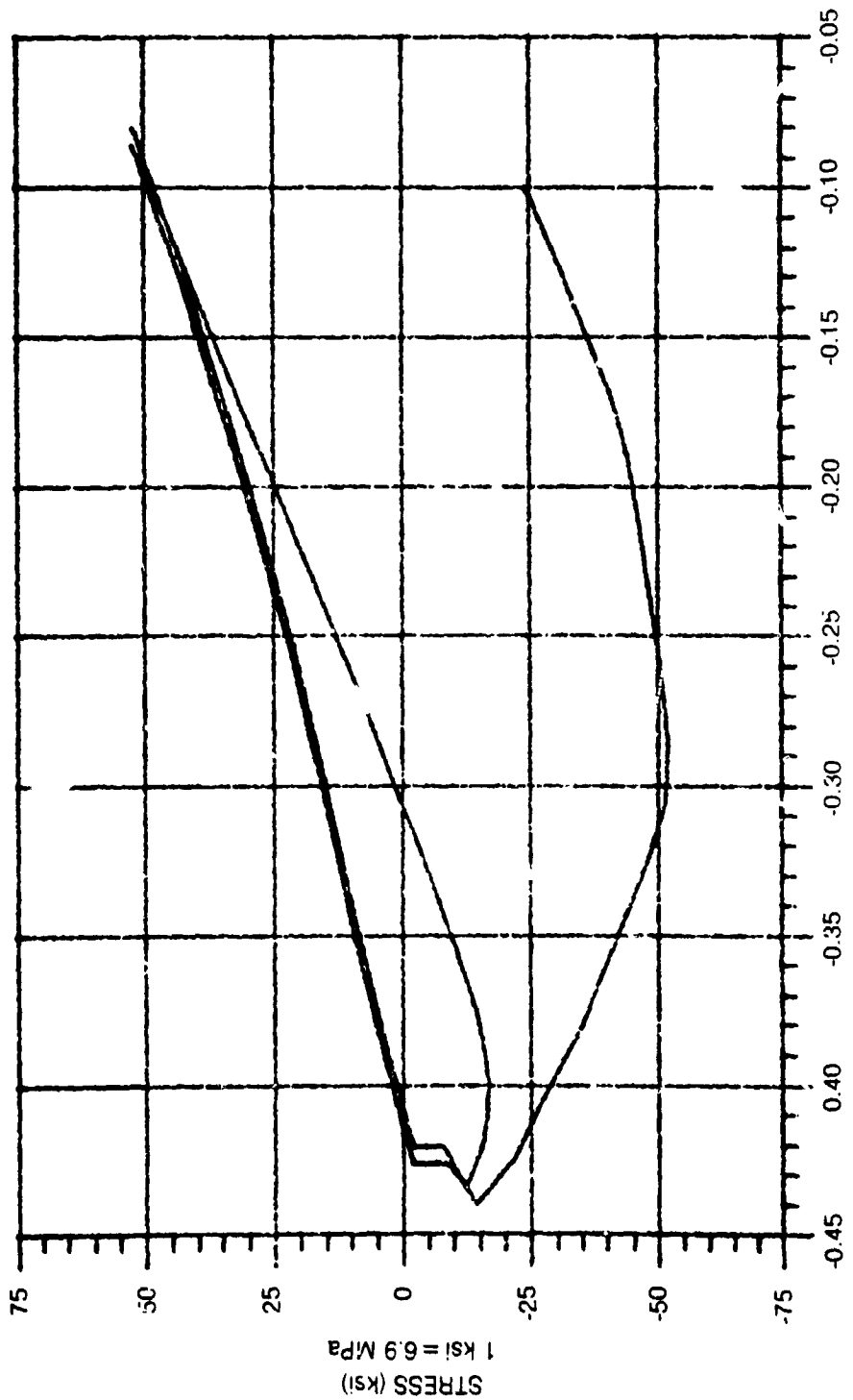

Figure 31. Predicted Response Using Miller's Theory for Open Nonsymmetric TMF Cycle With Rate of Change of Temperature Terms

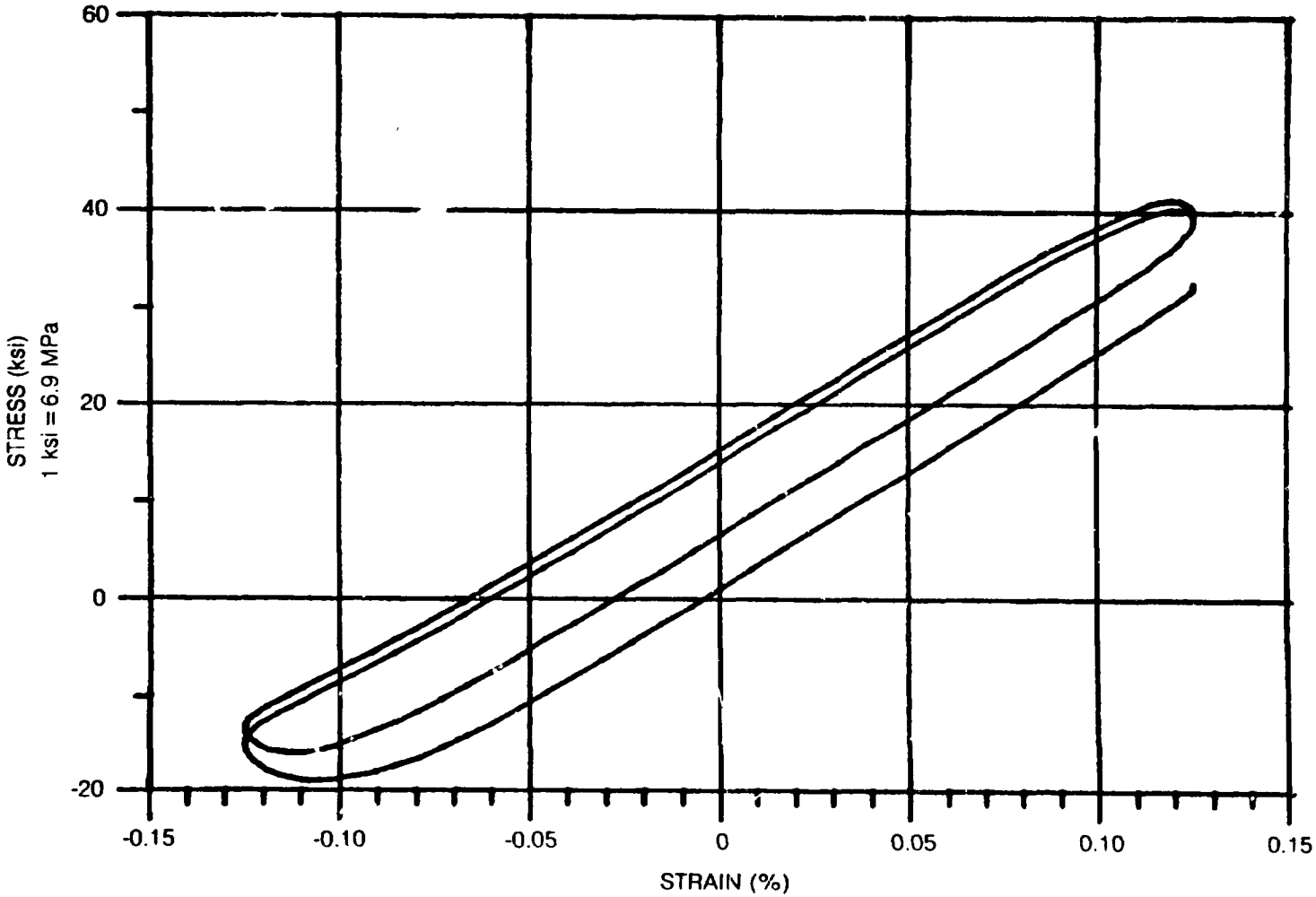

Figure 32. Predicted Response using Krieg, Swearengen and Rohde's Theory for Closed Symmetric TMF Cycle Without Rate of Change of Temperature Terms

82-6-76-1

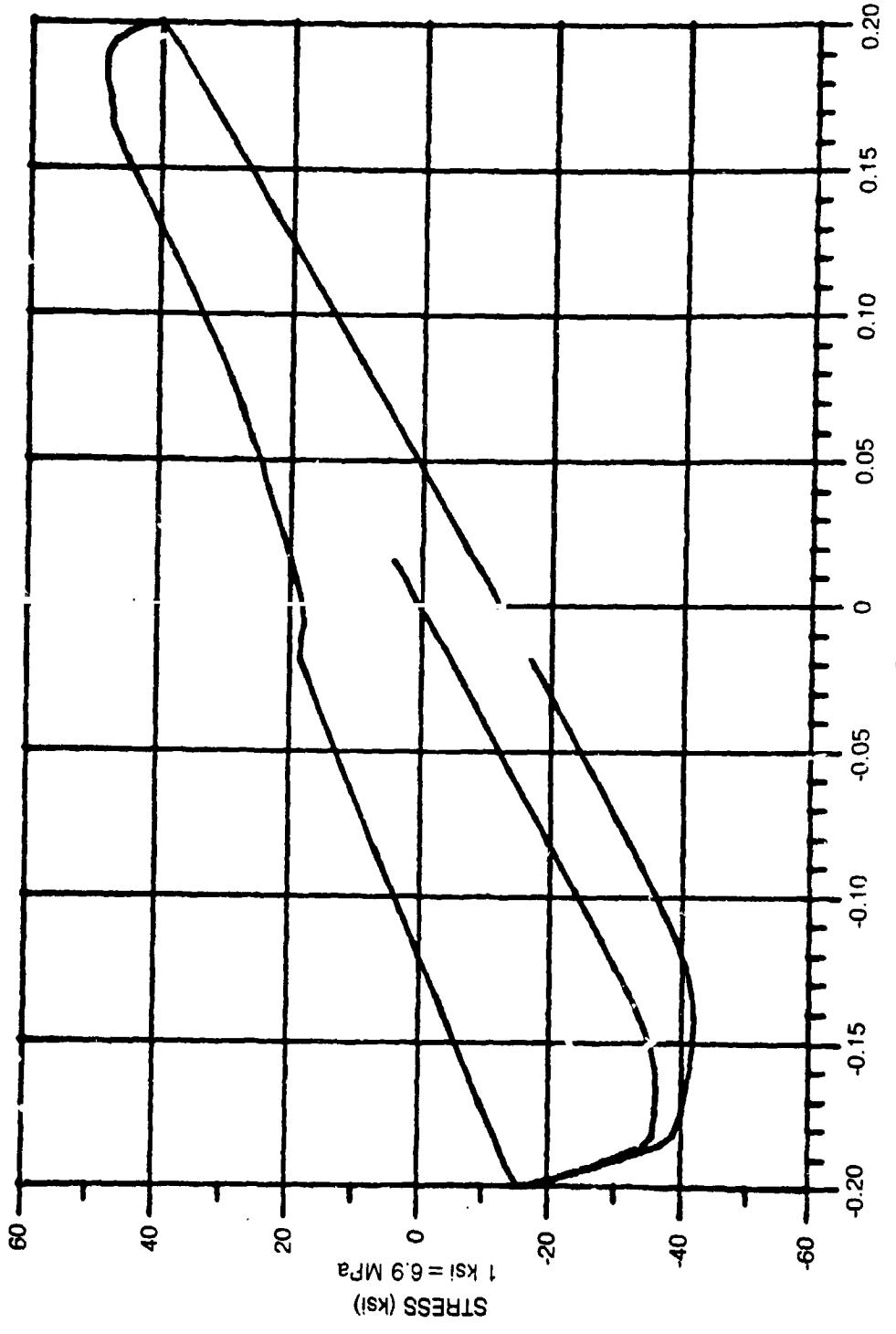

Figure 33. Predicted Response Using Krieg, Swearengen and Rohde's Theory for Open Symmetric TMF Cycle Without Rate of Change of Temperature Terms

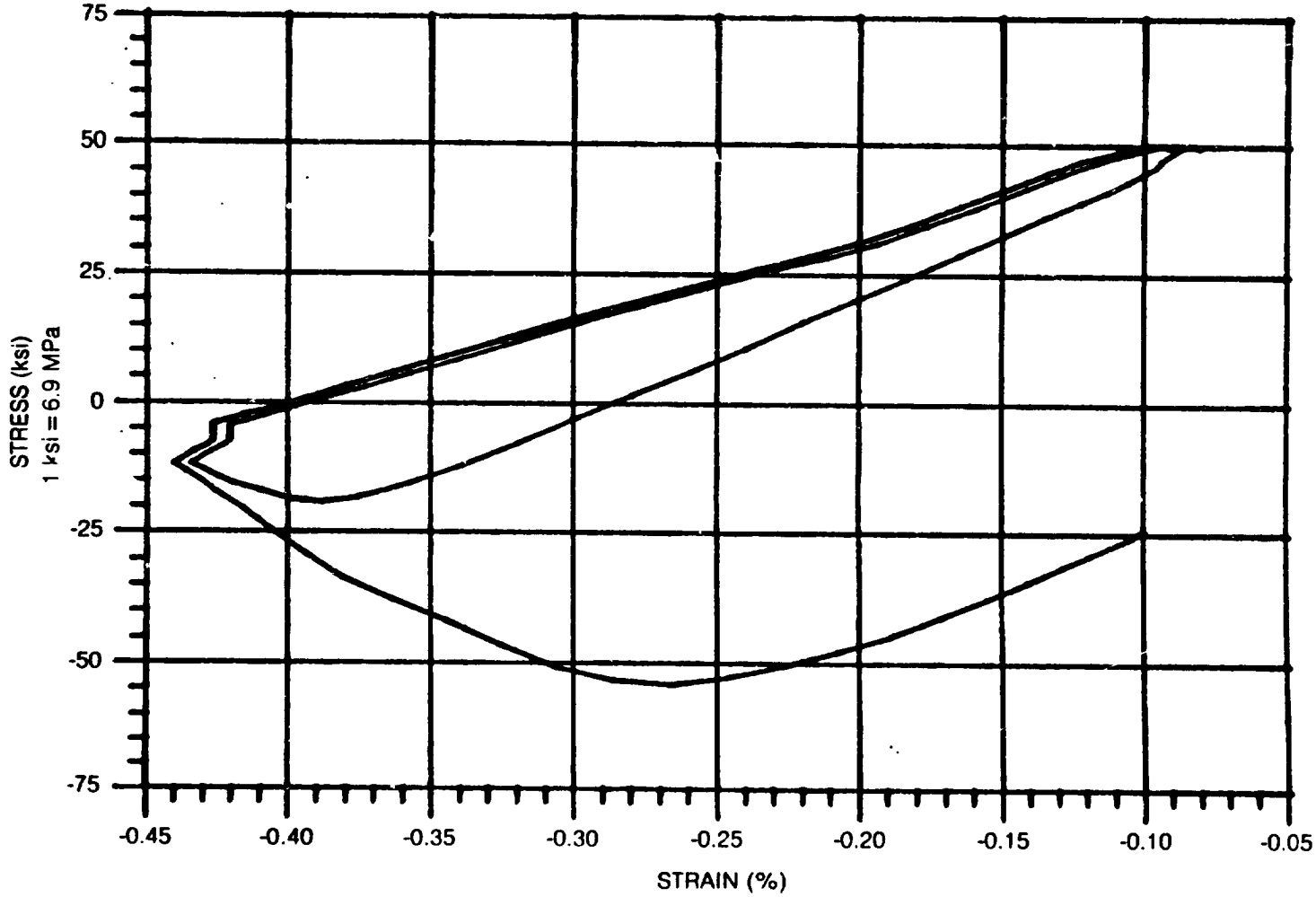

Figure 34. Predicted Response Using Krieg, Swearengen and Rohde's Theory for Open Nonsymmetric TMF Cycle Without Rate of Change of Temperature Terms

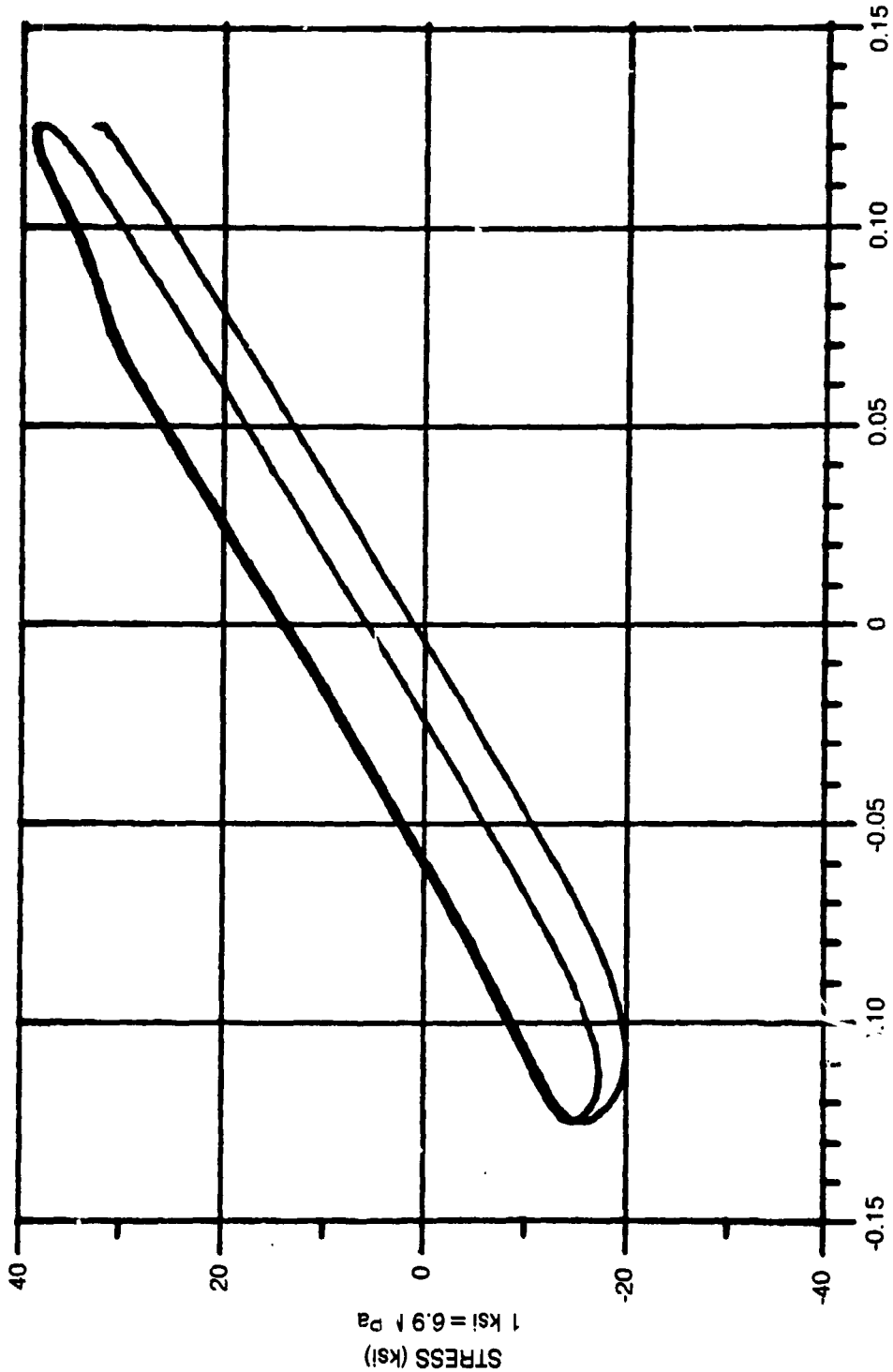

Figure 35. Predicted Response Using Krieg, Swearengen and Rohde's Theory for Closed Symmetric TMF Cycle With Rate of Change of Temperature Terms

82-6-76-4

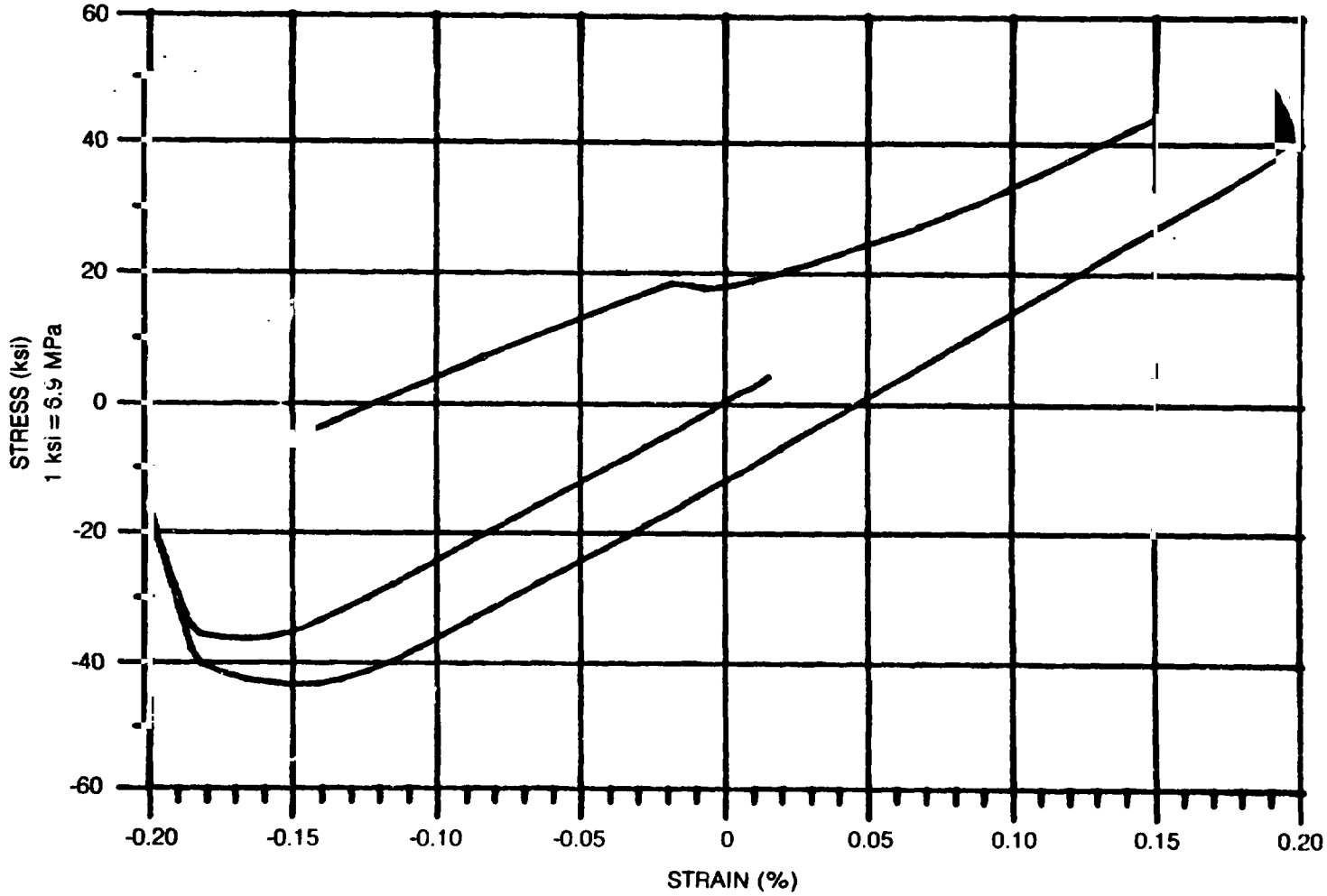

Figure 36. Predicted Response Using Krieg, Swearengen and Rohde's Theory for Open Symmetric TMF Cycle With Rate of Change of Temperature Terms

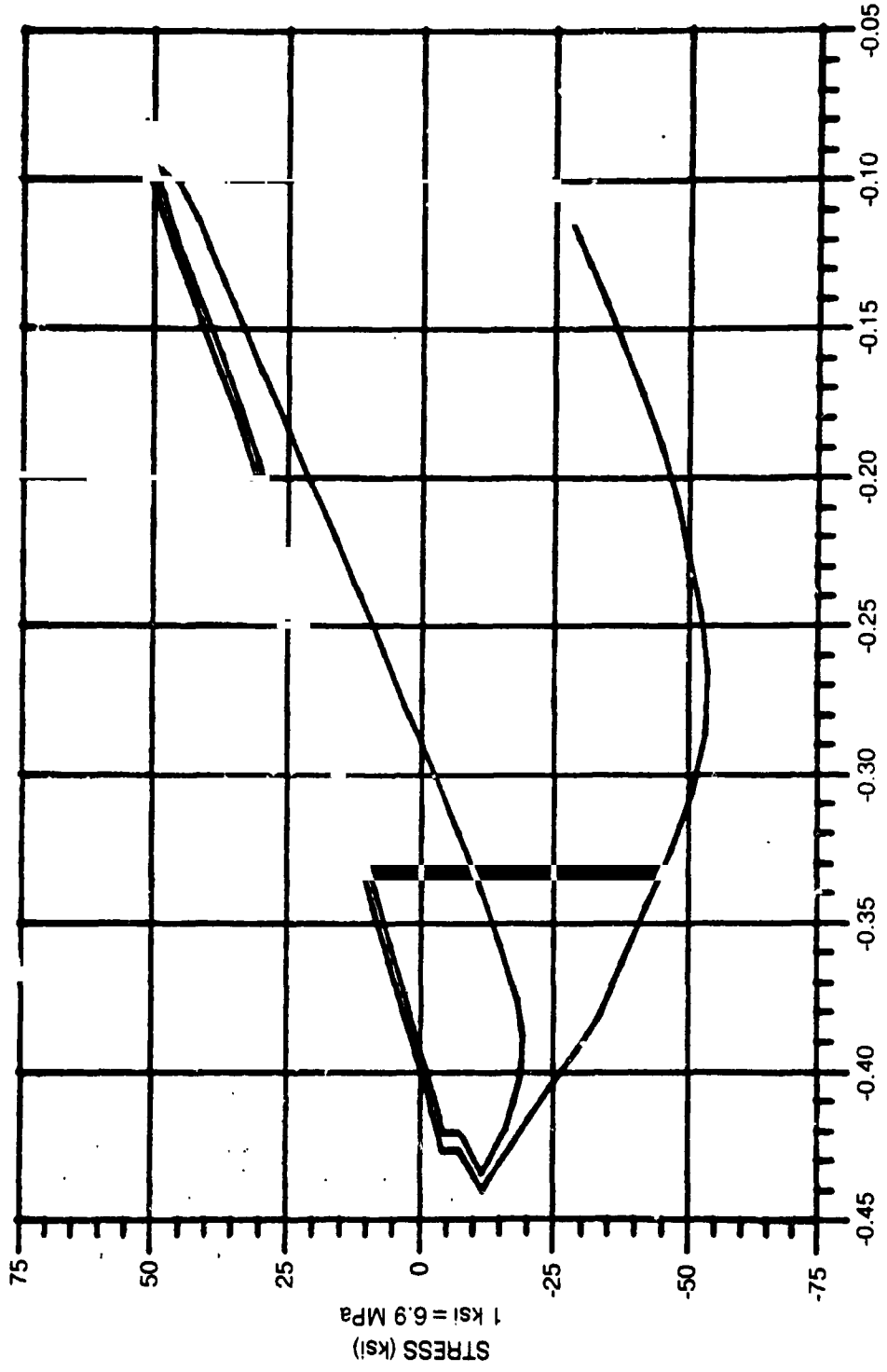

Figure 37. Predicted Response Using Krieg, Swearengen and Rohde's Theory for Open Nonsymmetric TMF Cycle With Rate of Change of Temperature Terms

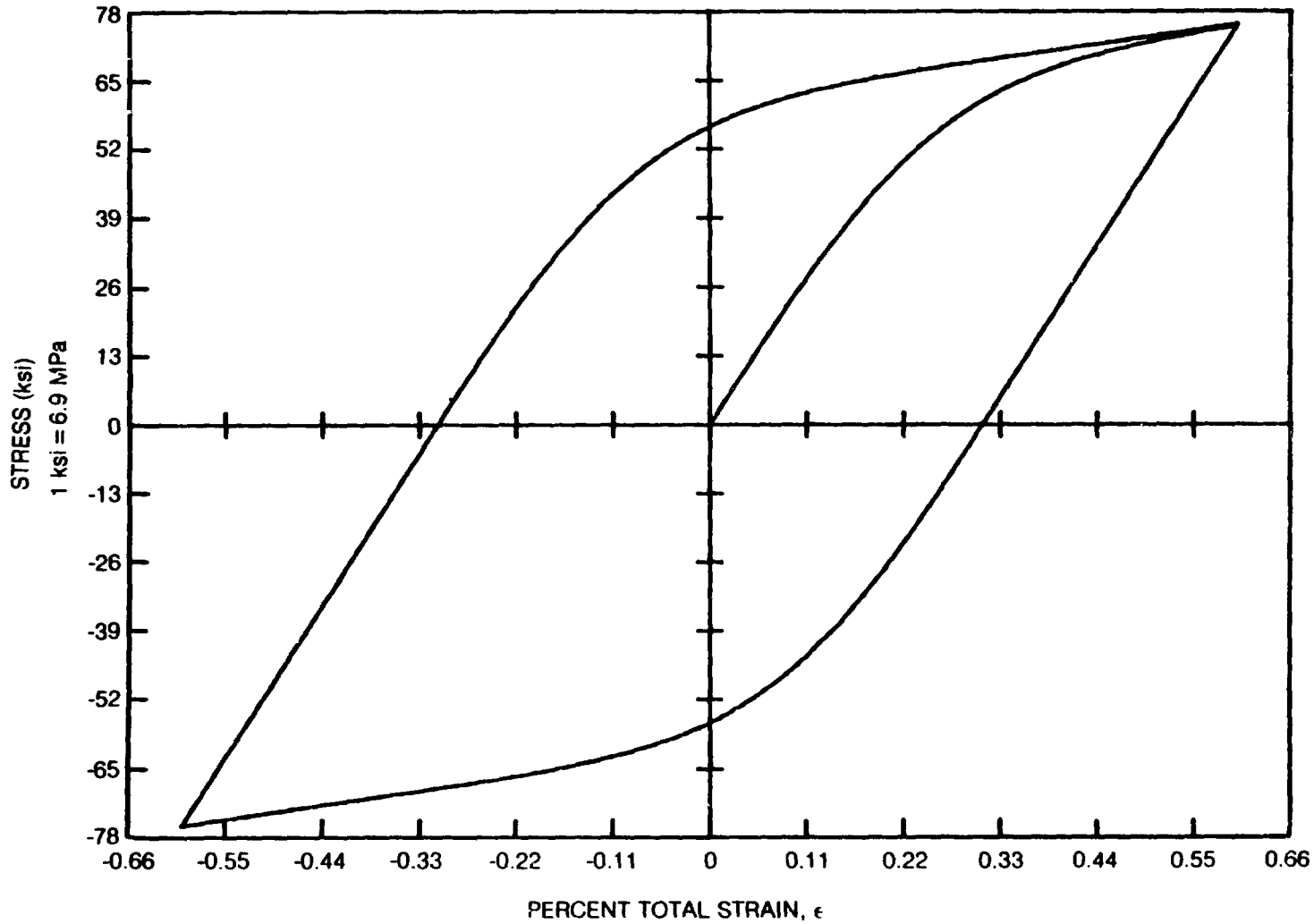

Figure 38. Typical Stress-Strain Hysteresis Loop Using Time Independent Formulation

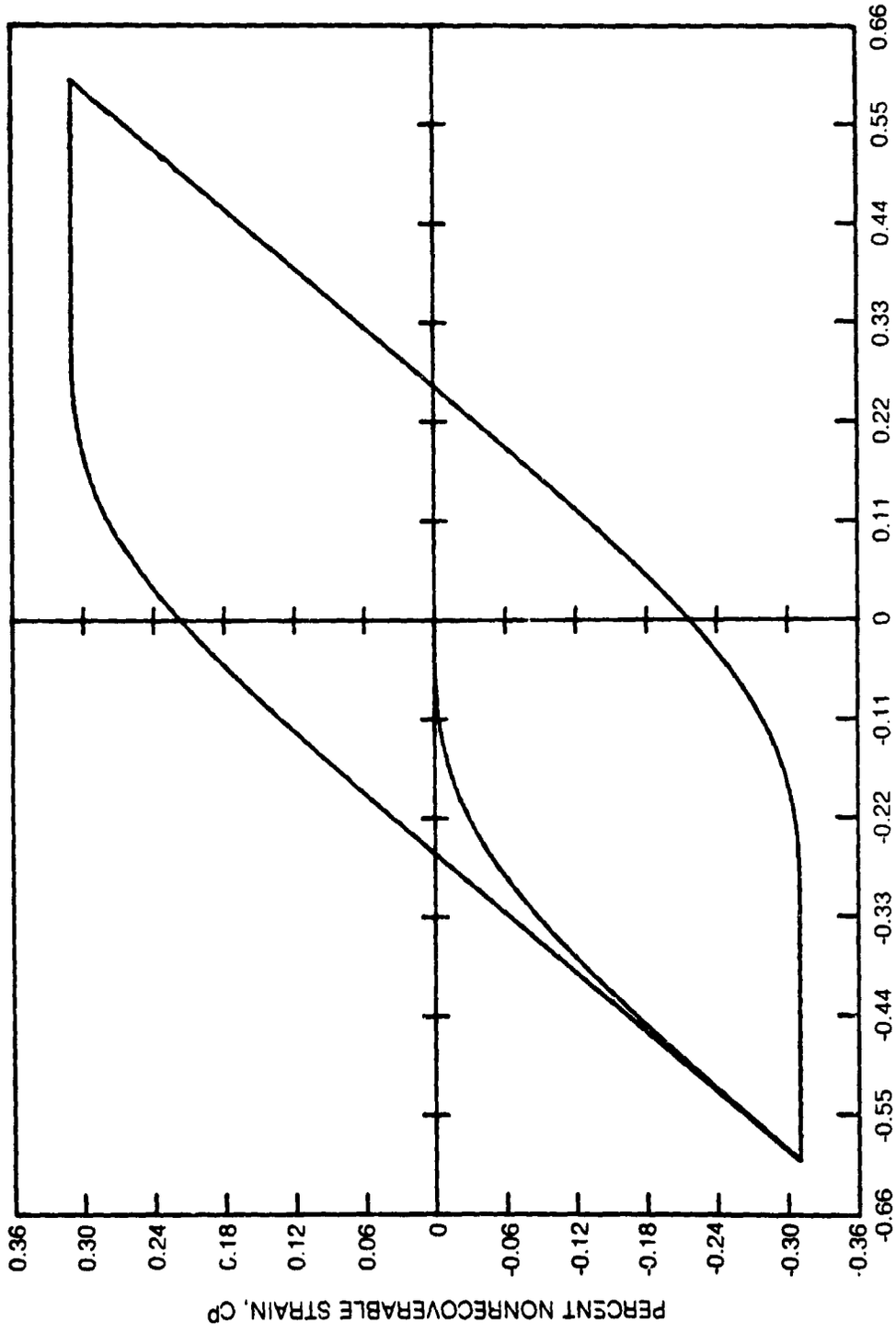

Figure 39. Typical Inelastic Strain Response Using Time Independent Formulation

82-6-76-8

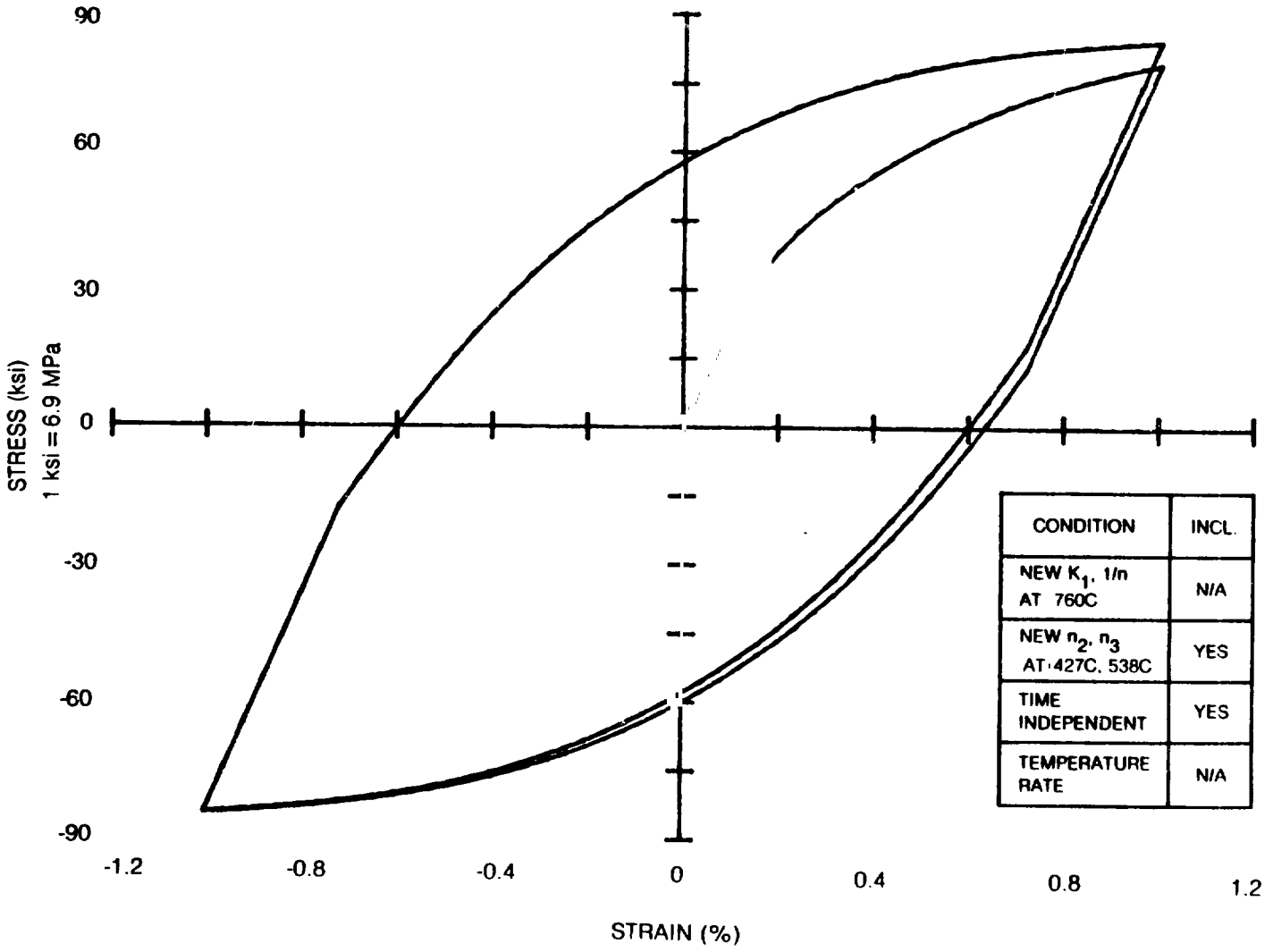

Figure 40. Modified Walker's Theory at 538 C and 0.0000667/sec Strain Rate

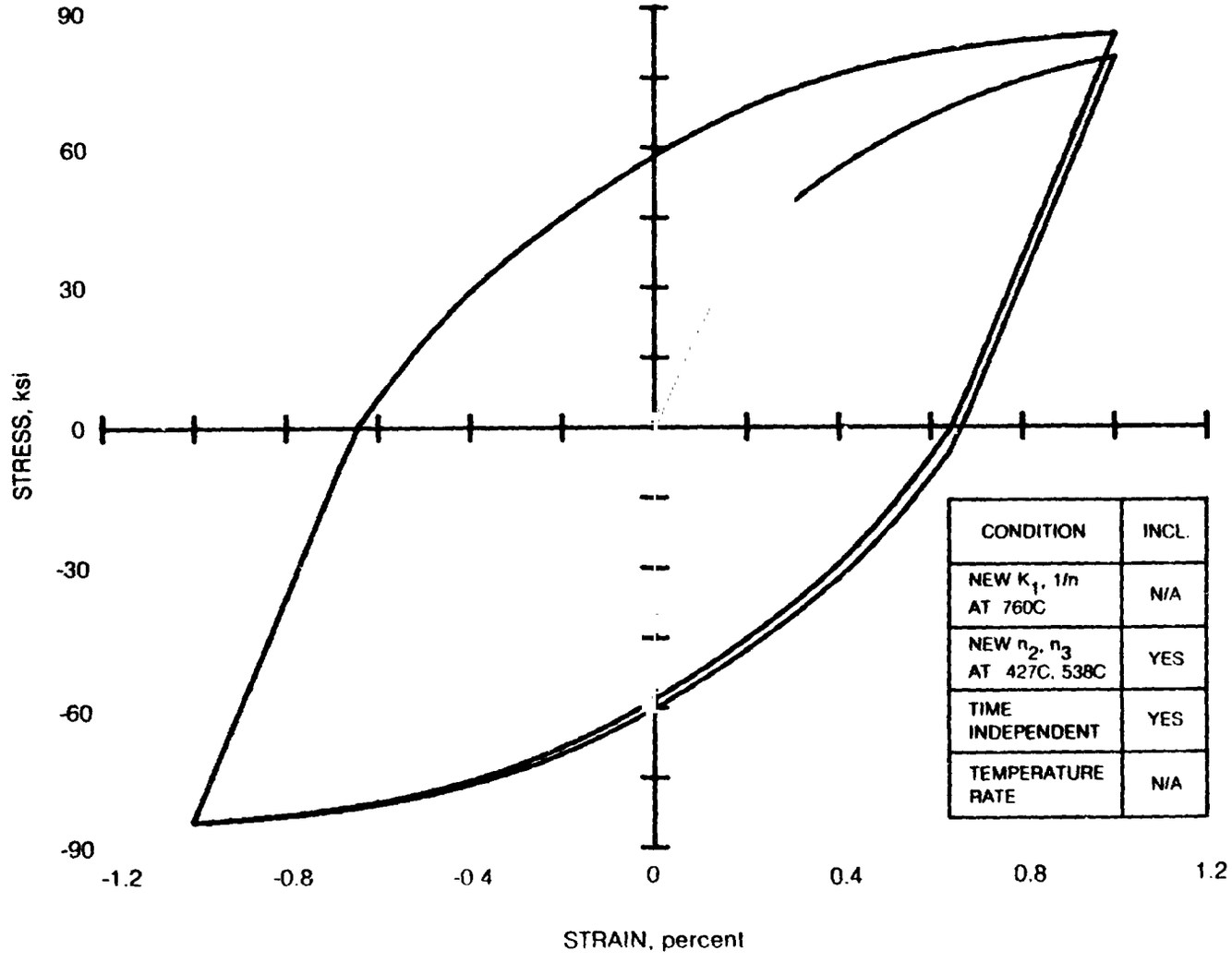

Figure 41. Modified Walker's Theory at 538 C and 0.02/sec Strain Rate

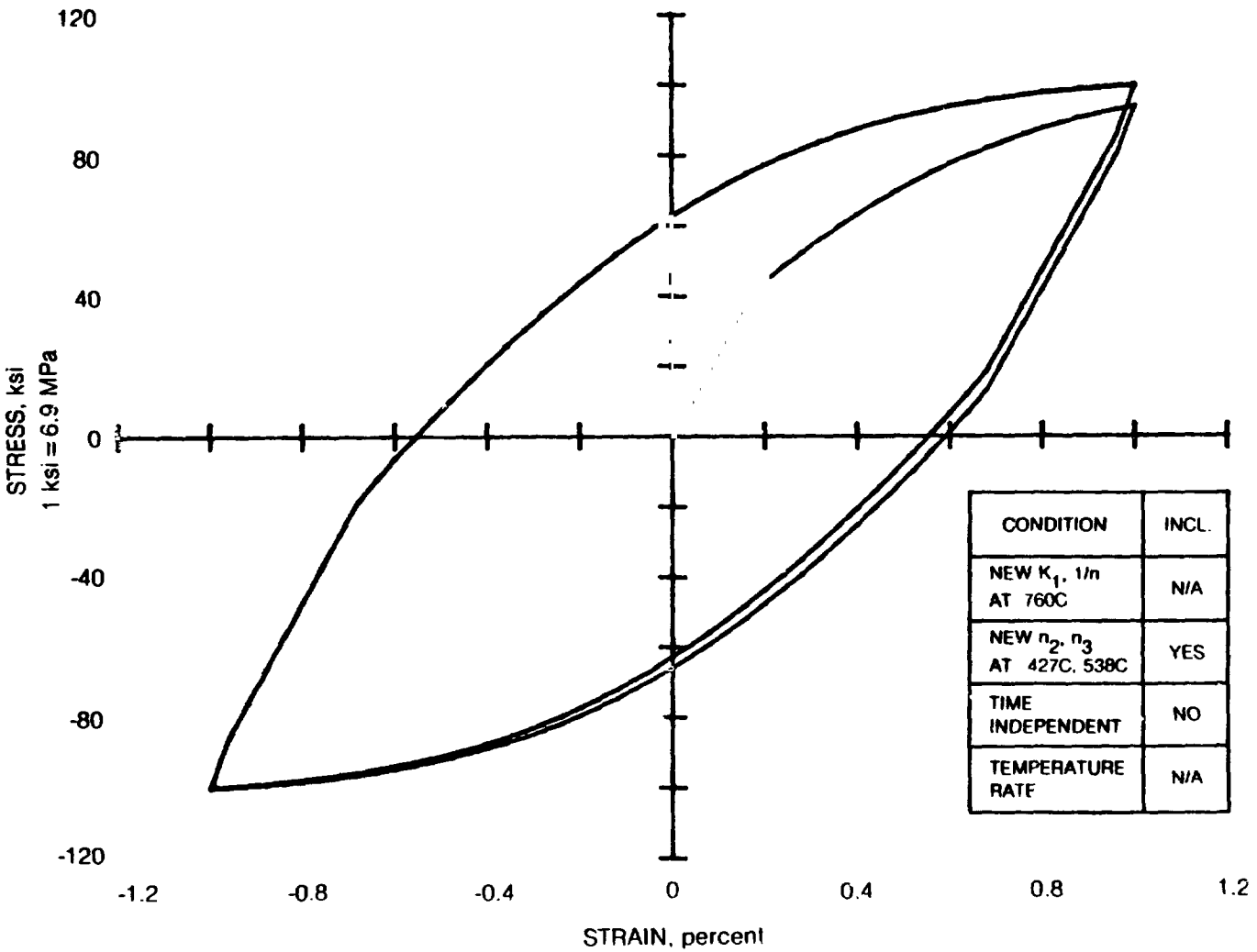

Figure 42. Original Walker's Theory at 538 C and 0.000667/sec Strain Rate

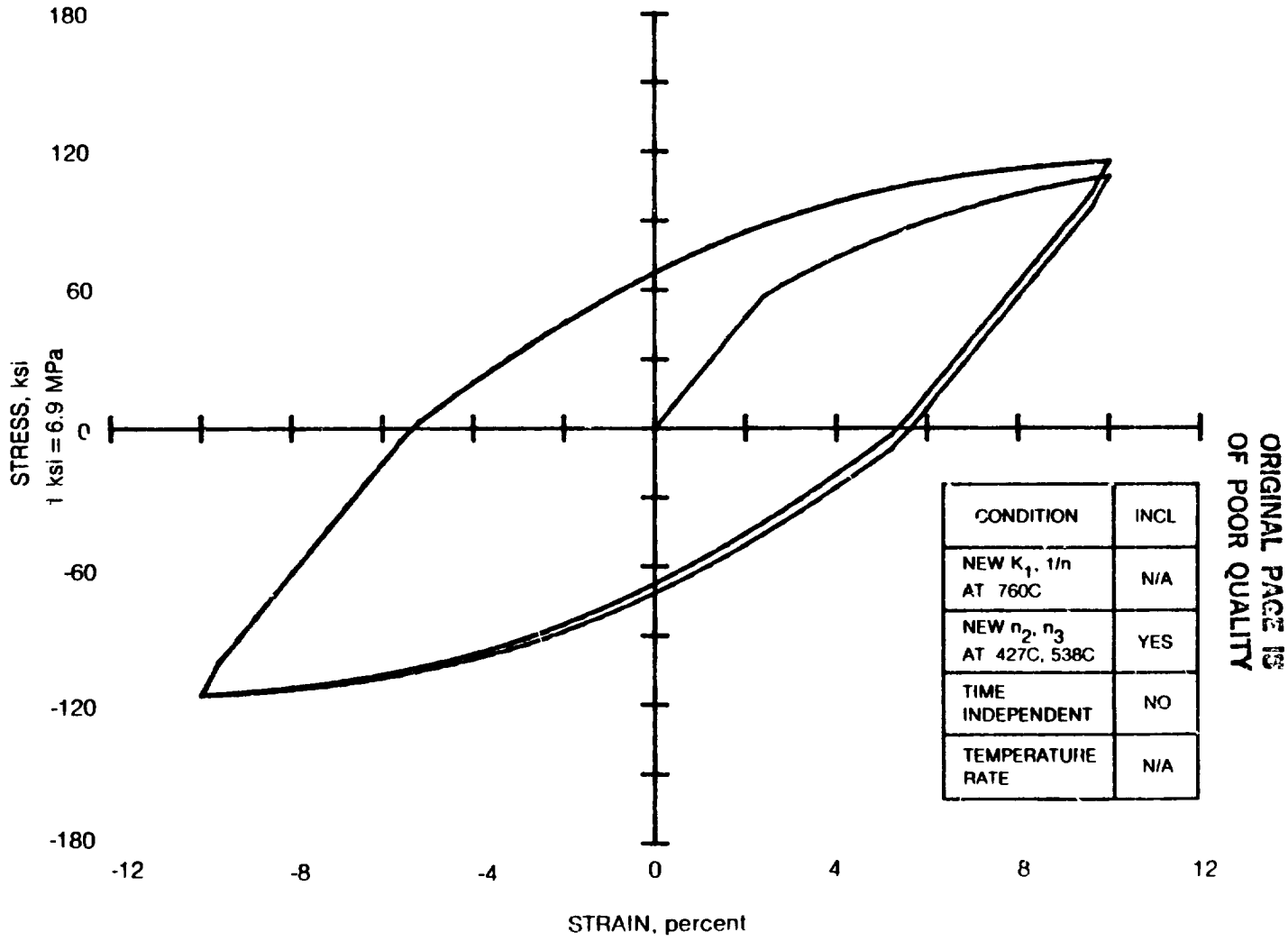

Figure 43. Original Walker's Theory at 538 C and 0.02/sec Strain Rate

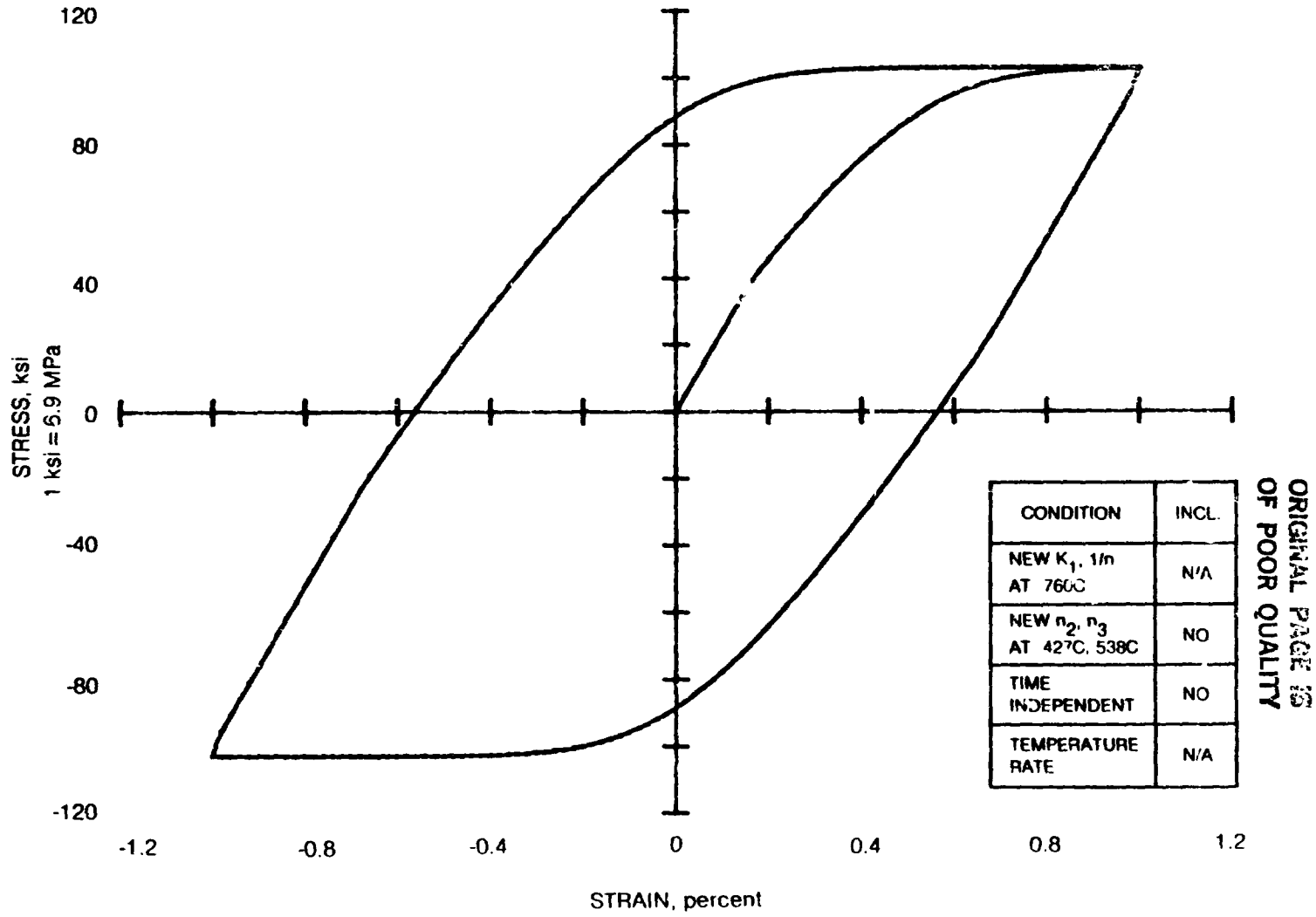

Figure 44. Original Walker's Theory at 538 C and 0.000066/sec Strain Rate

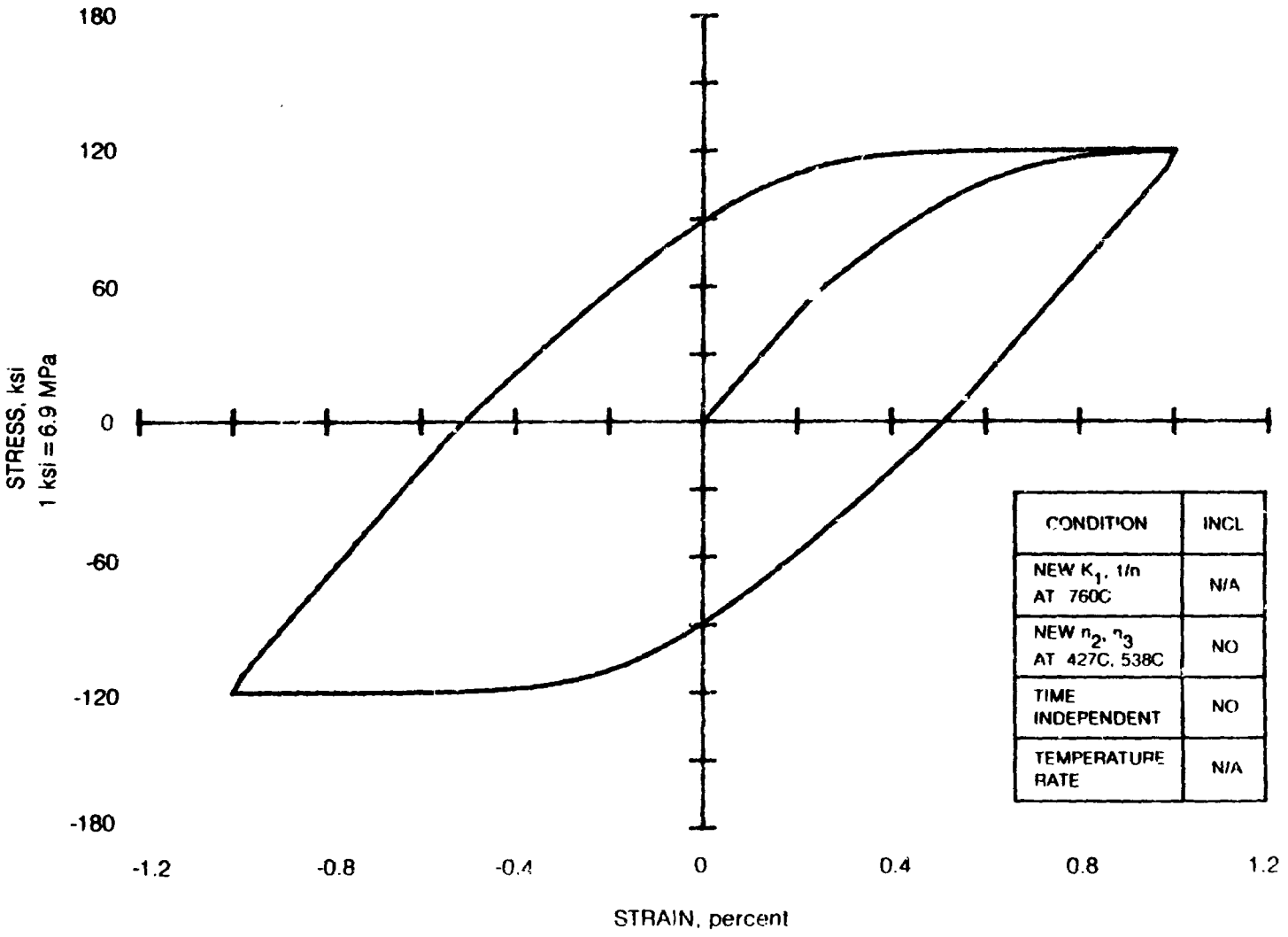

Figure 45. Original Walker's Theory at 538 C and 0.02/sec Strain Rate

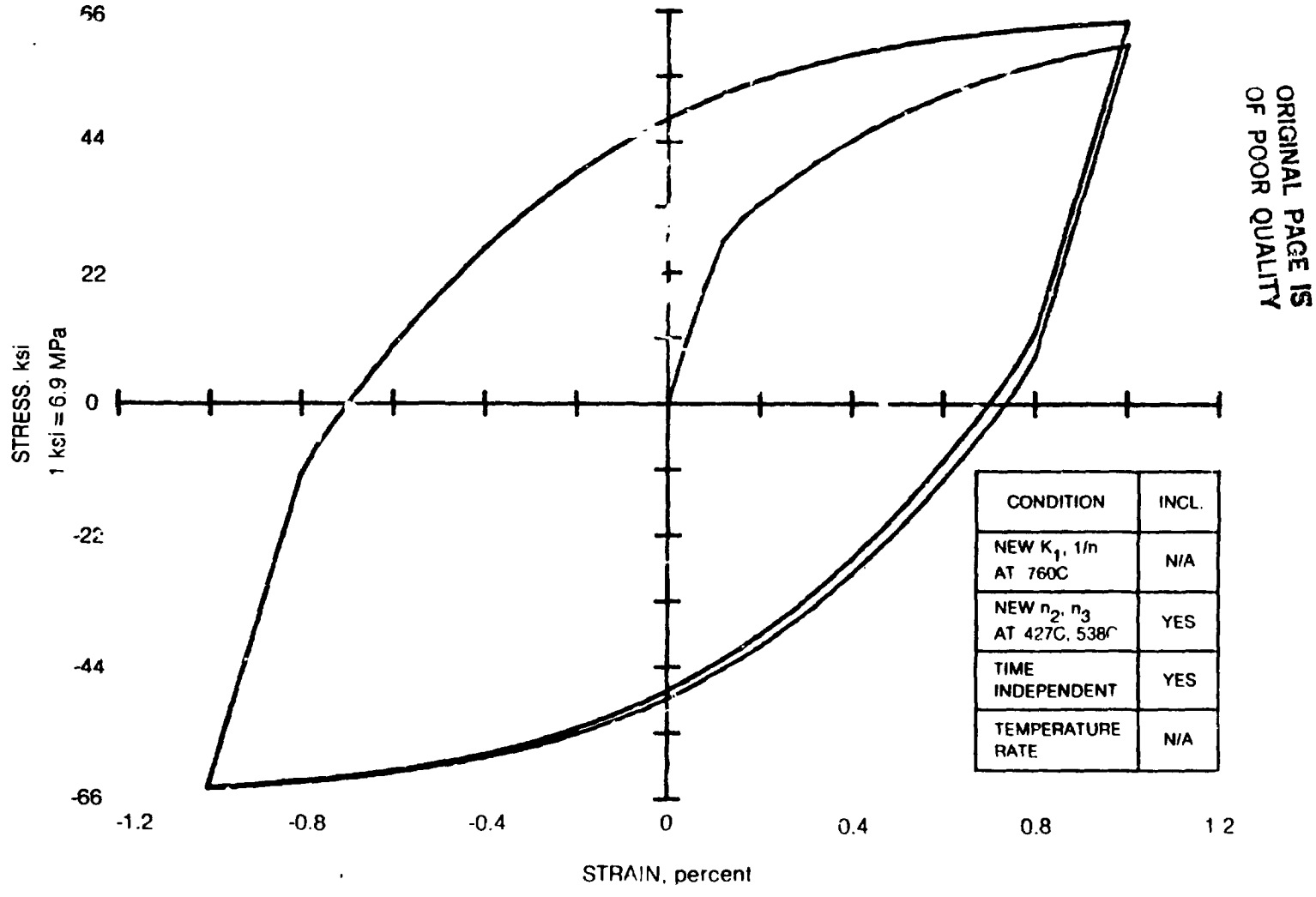

Figure 46. Modified Walker's Theory at 427 C and 0.02/sec Strain Rate

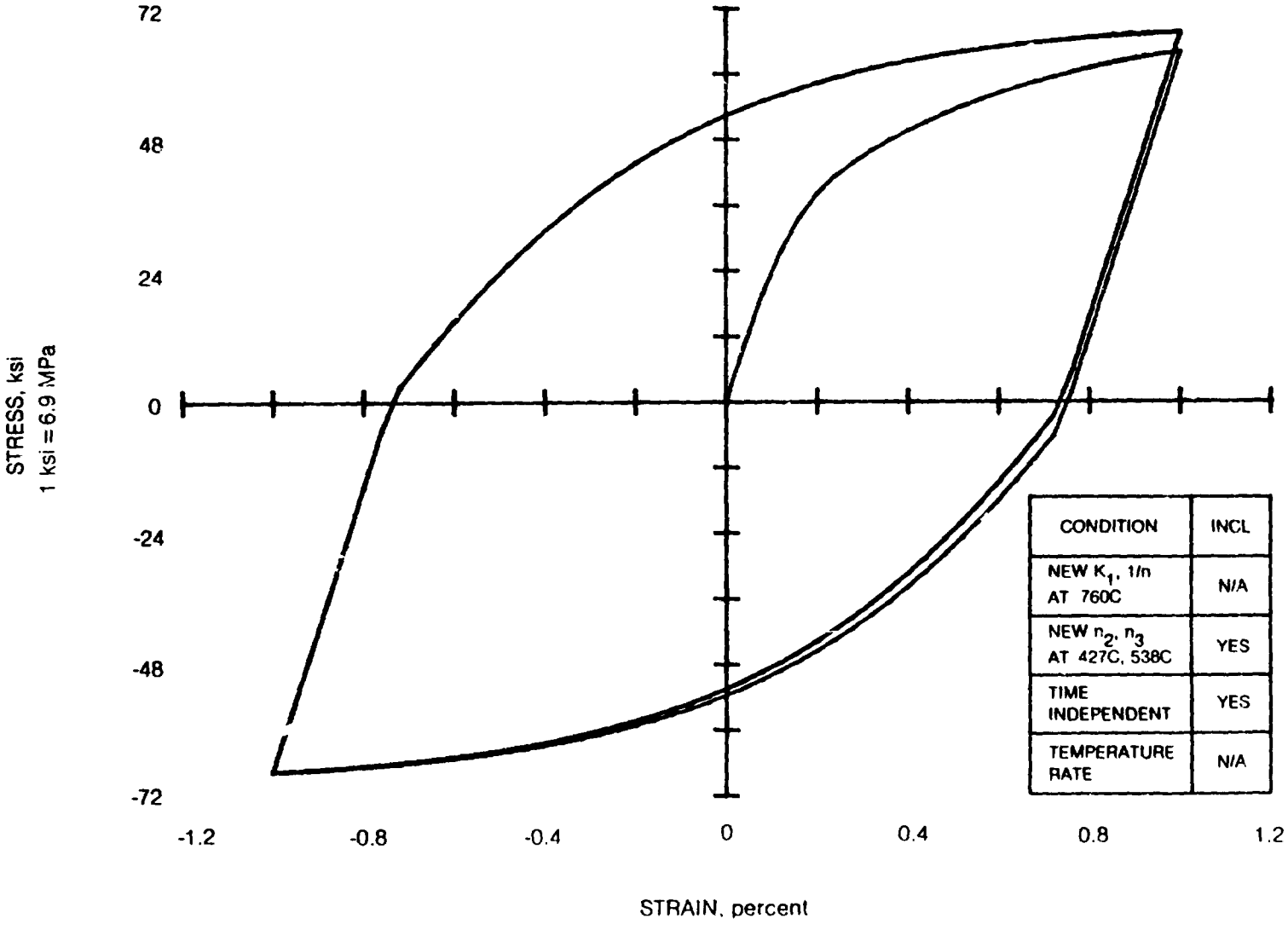

Figure 47. Modified Walker's Theory at 427 C and 0.000067/sec Strain Rate

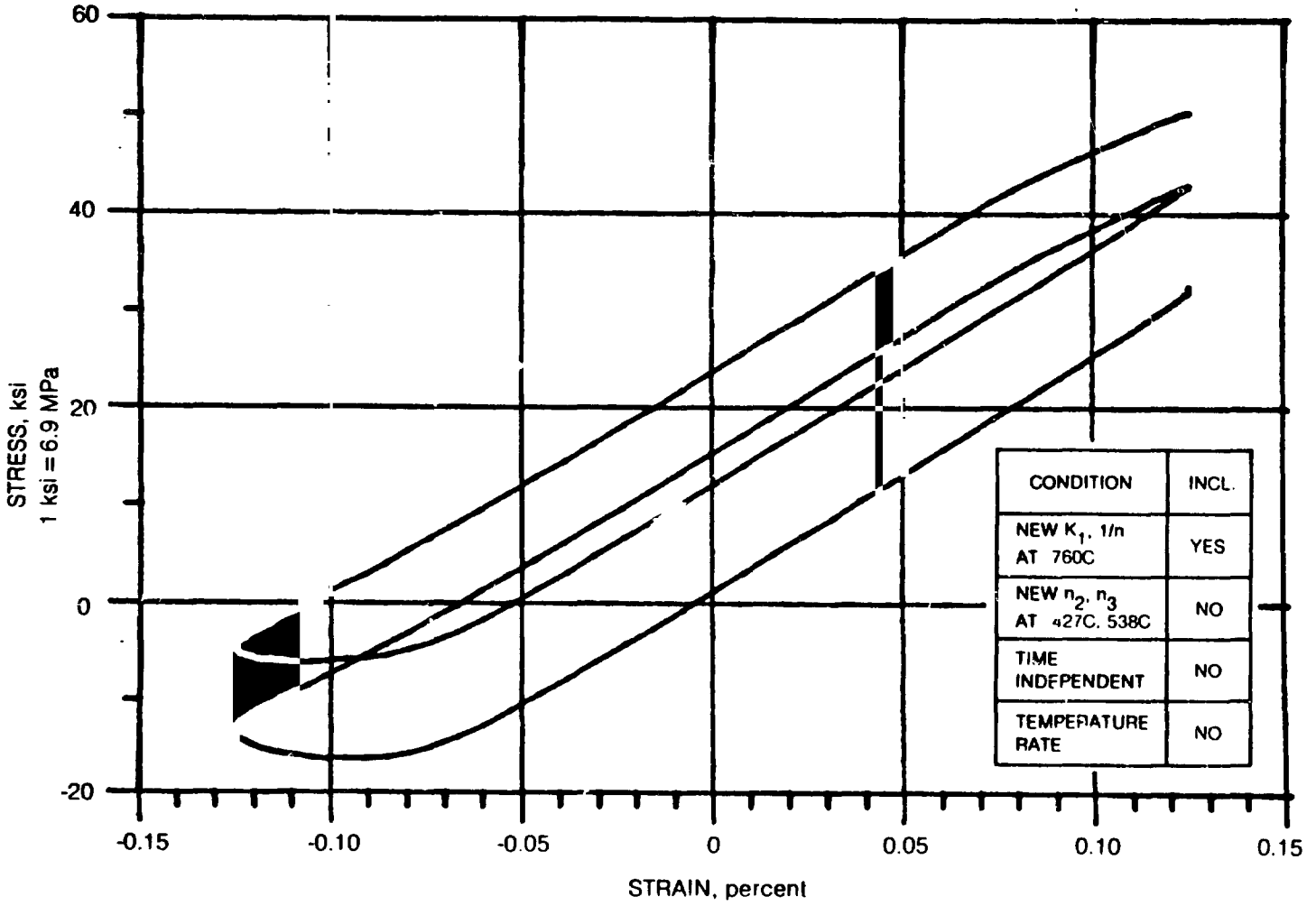

Figure 48. Hysteresis Loop for Closed Symmetric Cycle

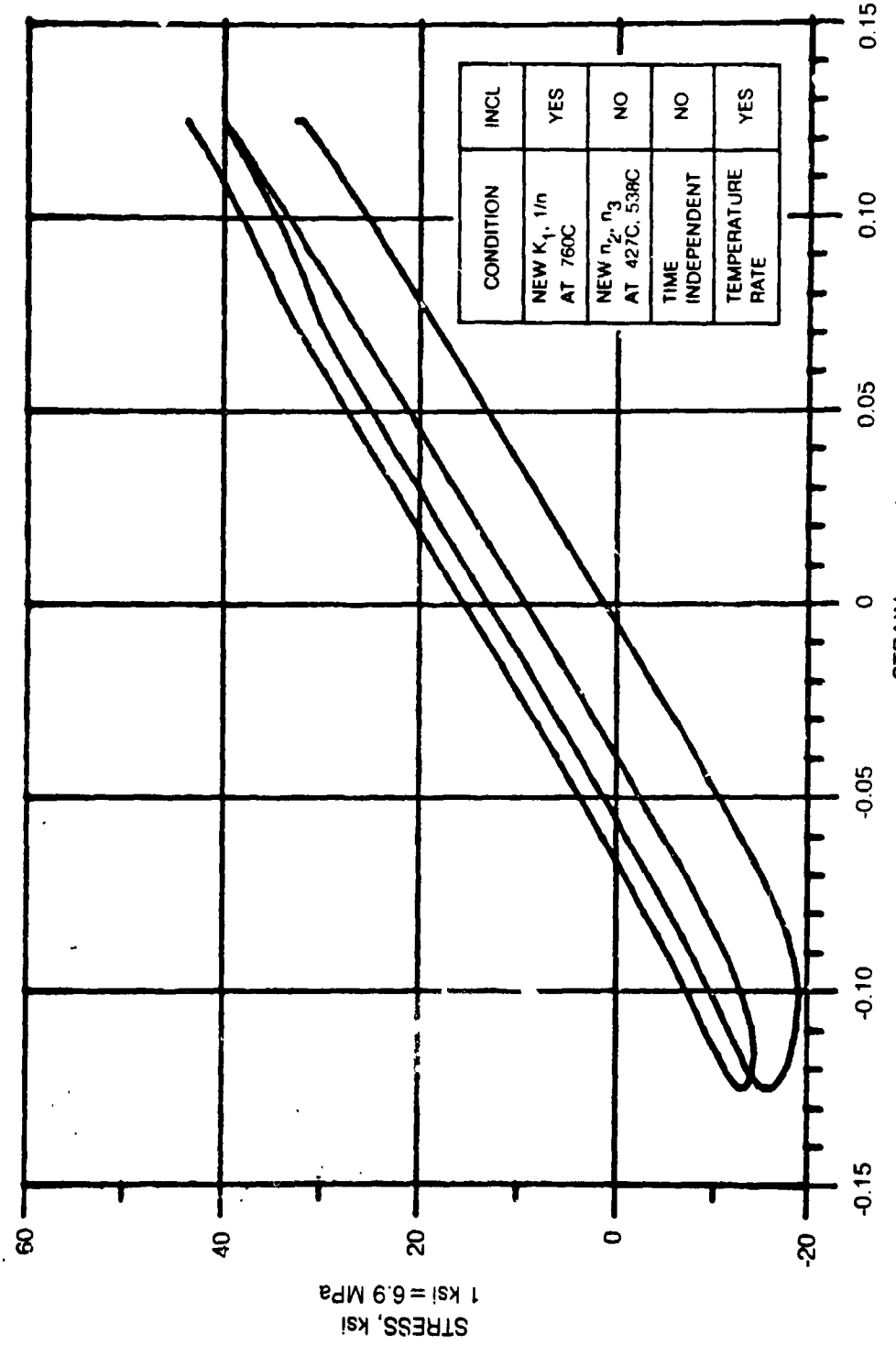

Figure 49. Hysteresis Loop for Closed Symmetric Cycle

82-8-58-10

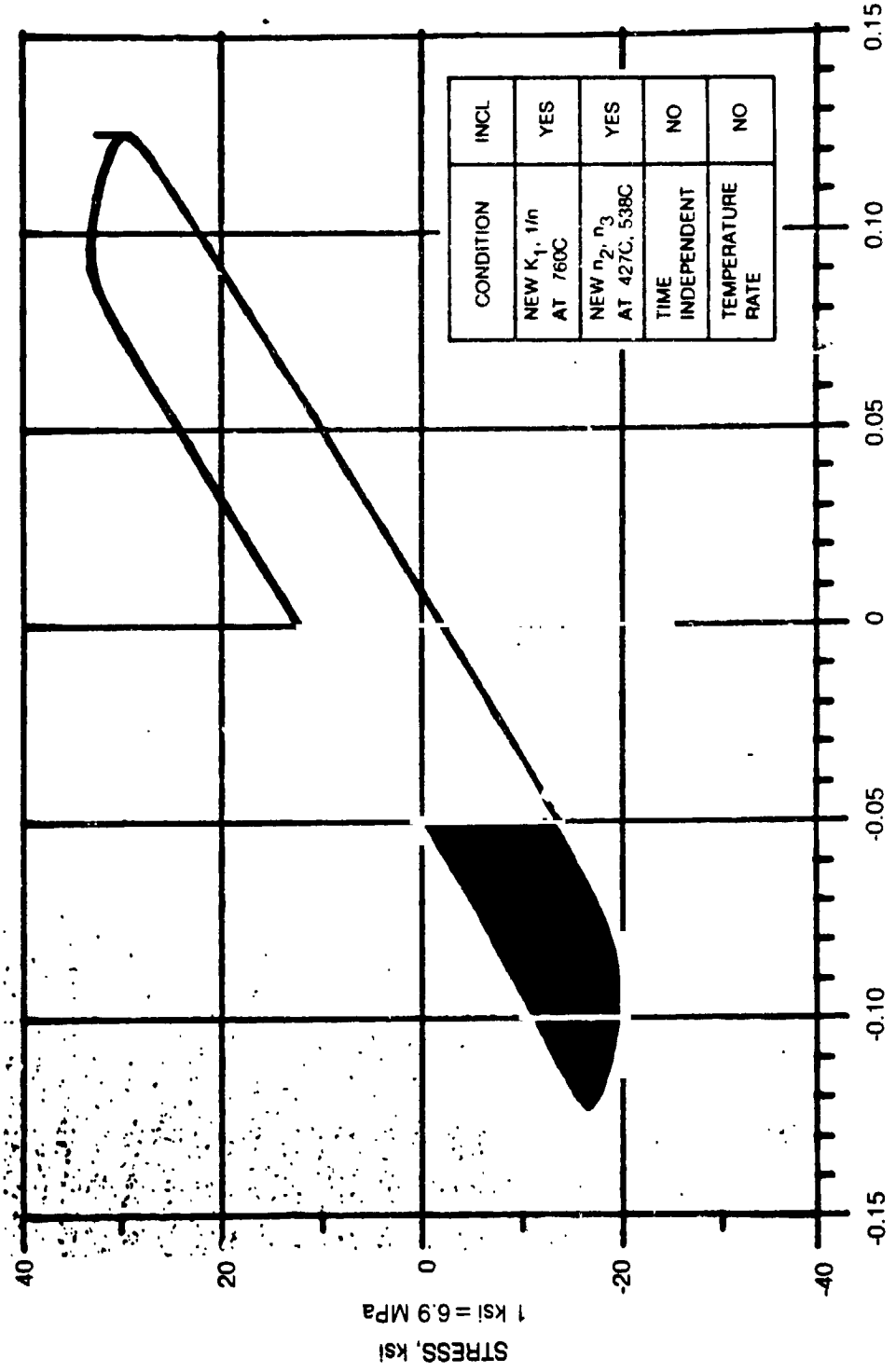

Figure 50. Hysteresis Loop for Closed Symmetric Cycle

82-8-58-11

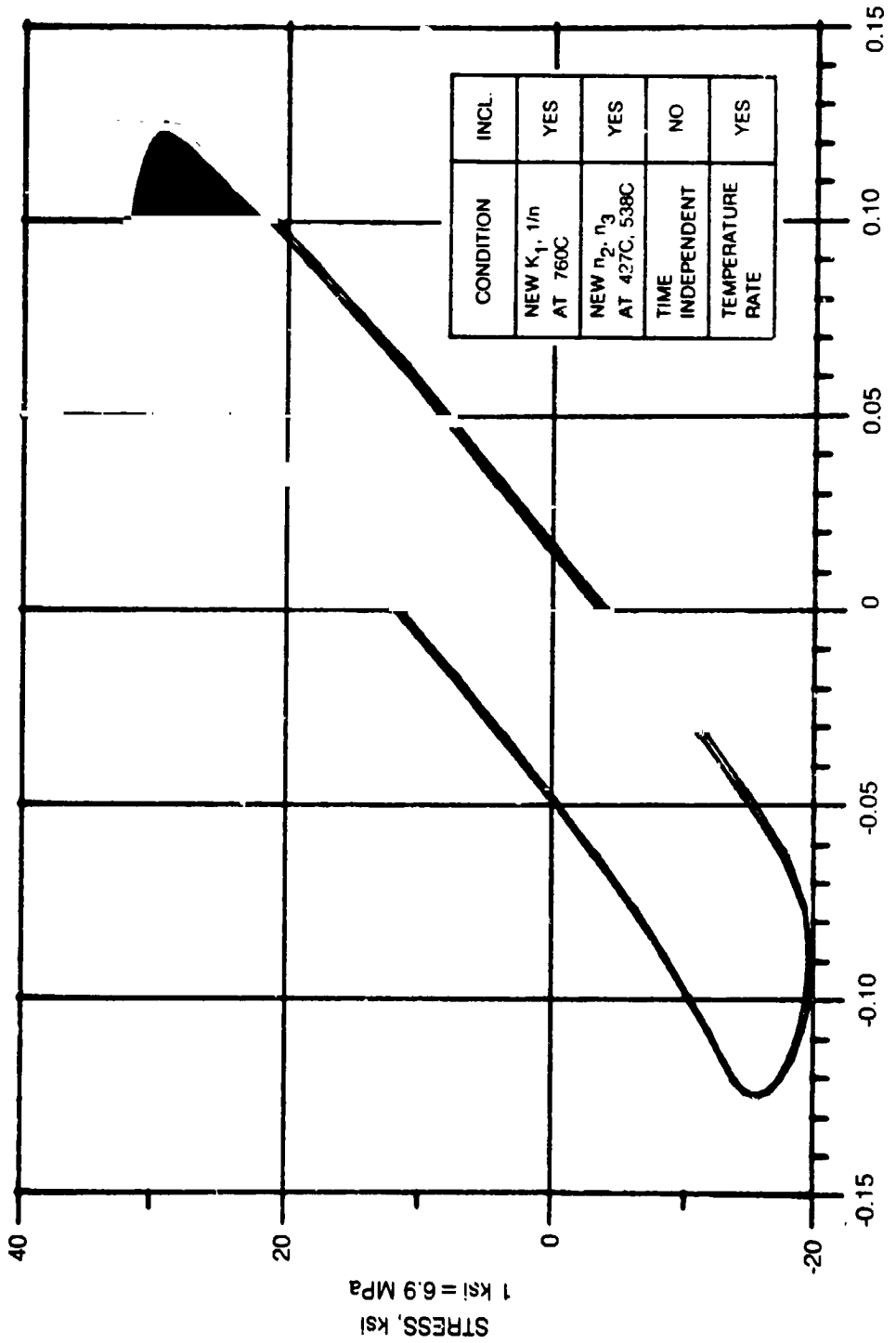

Figure 51. Hysteresis Loop for Closed Symmetric Cycle

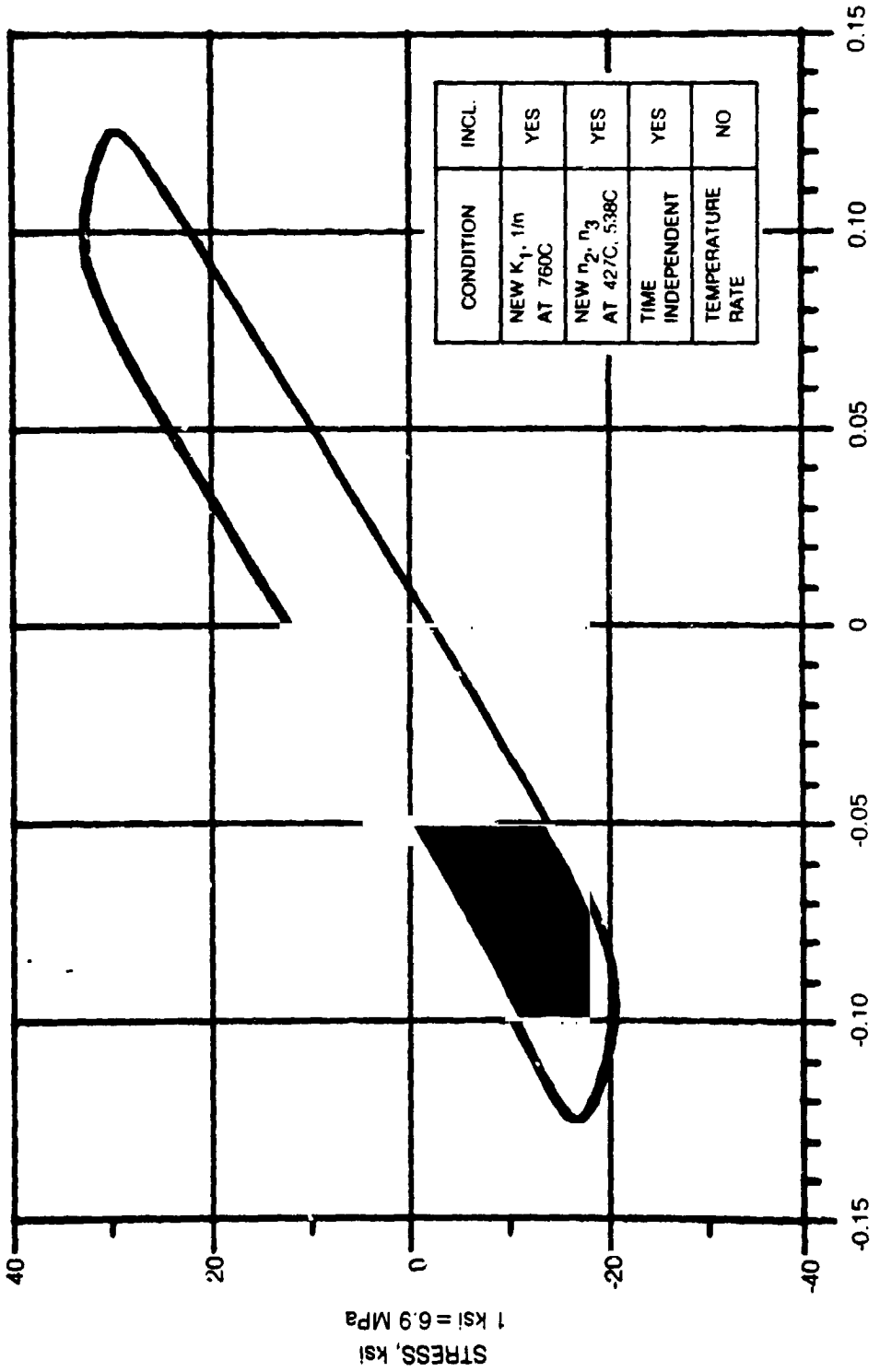

Figure 52. Hysteresis Loop for Close-to Symmetric Cycle

82-8-58-13

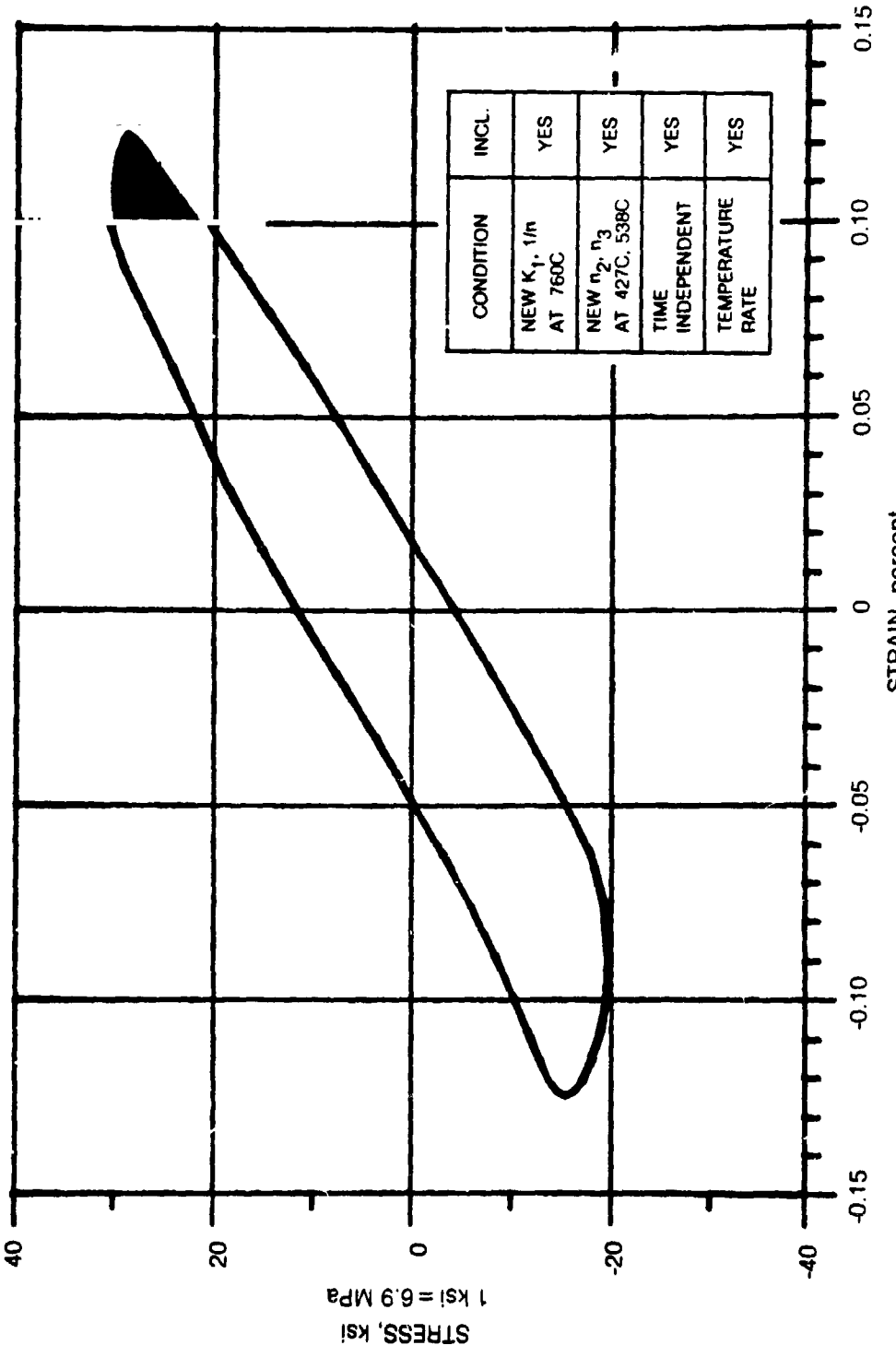

Figure 53. Hysteresis Loop for Closed Symmetric Cycle

82-8-58-14

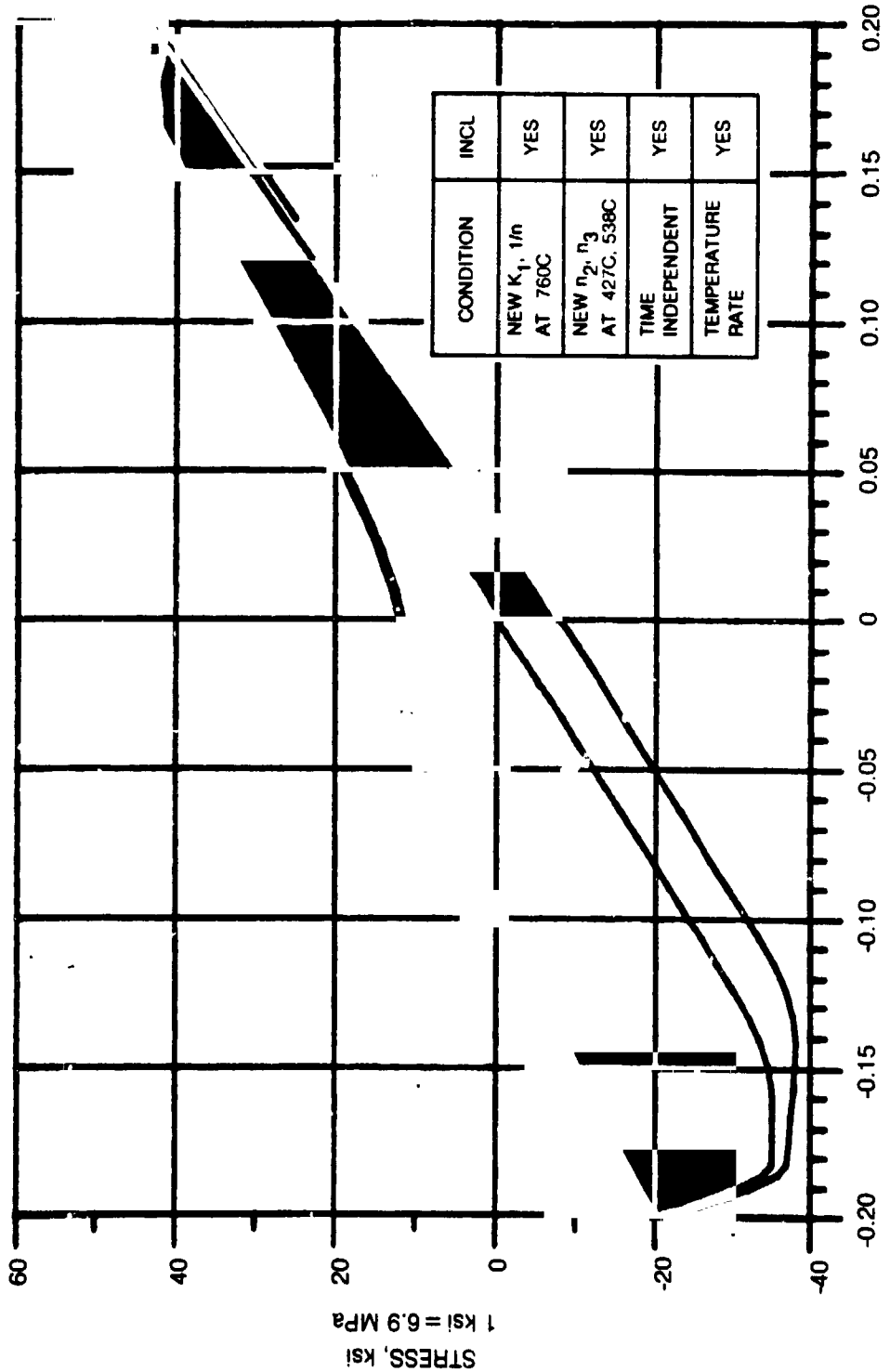

Figure 54. Hysteresis Loop for Open Symmetric Cycle

82-8-58-15

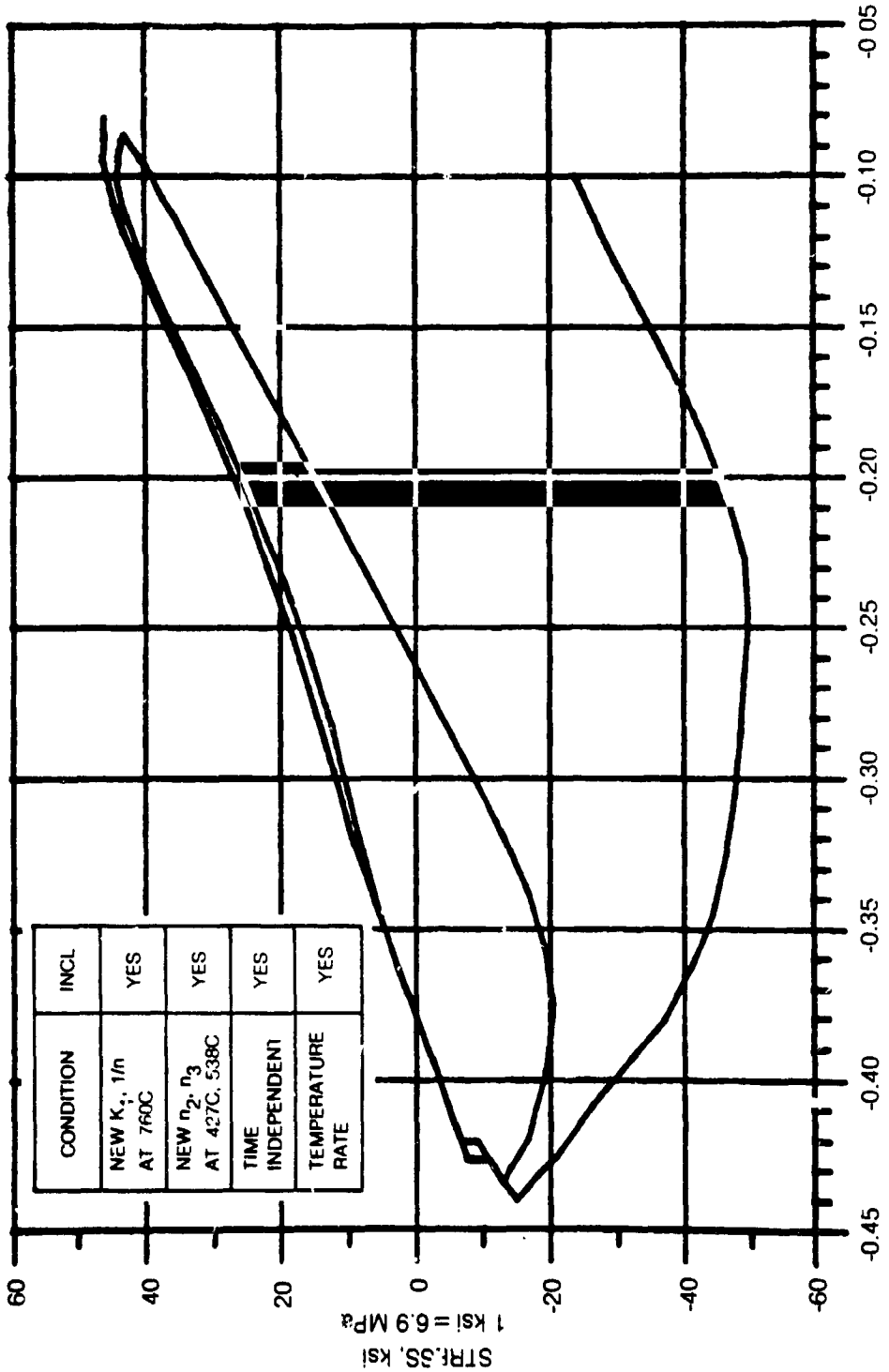

Figure 55. Hysteresis Loop for Open Nonsymmetric Cycle

82-8-58-16

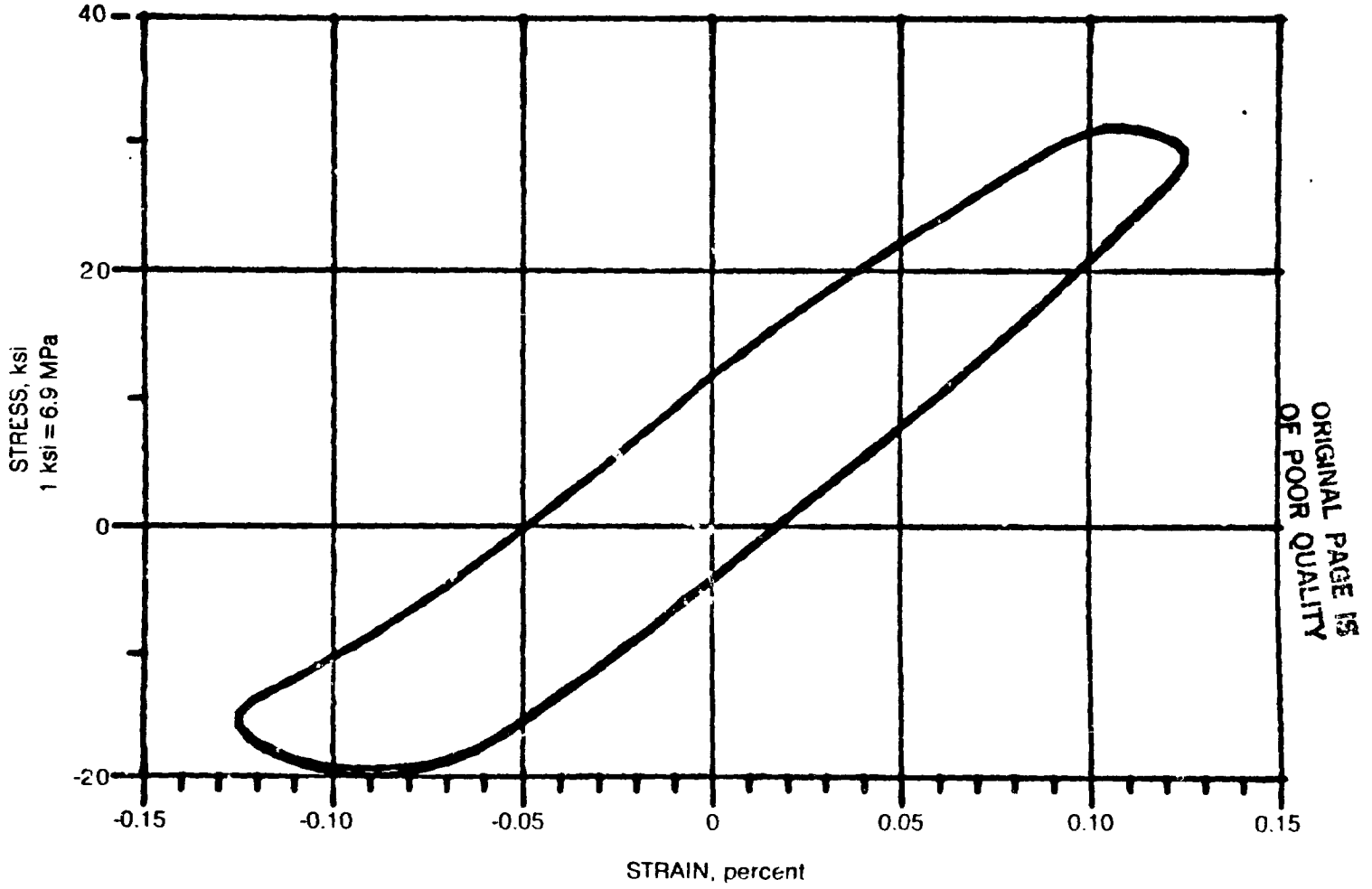

Figure 56. Predicted Stress/Strain Response of TMF Cycle No. 1 for σ_{∞} (649 C) Equal to 60 ksi

83-2-87-7

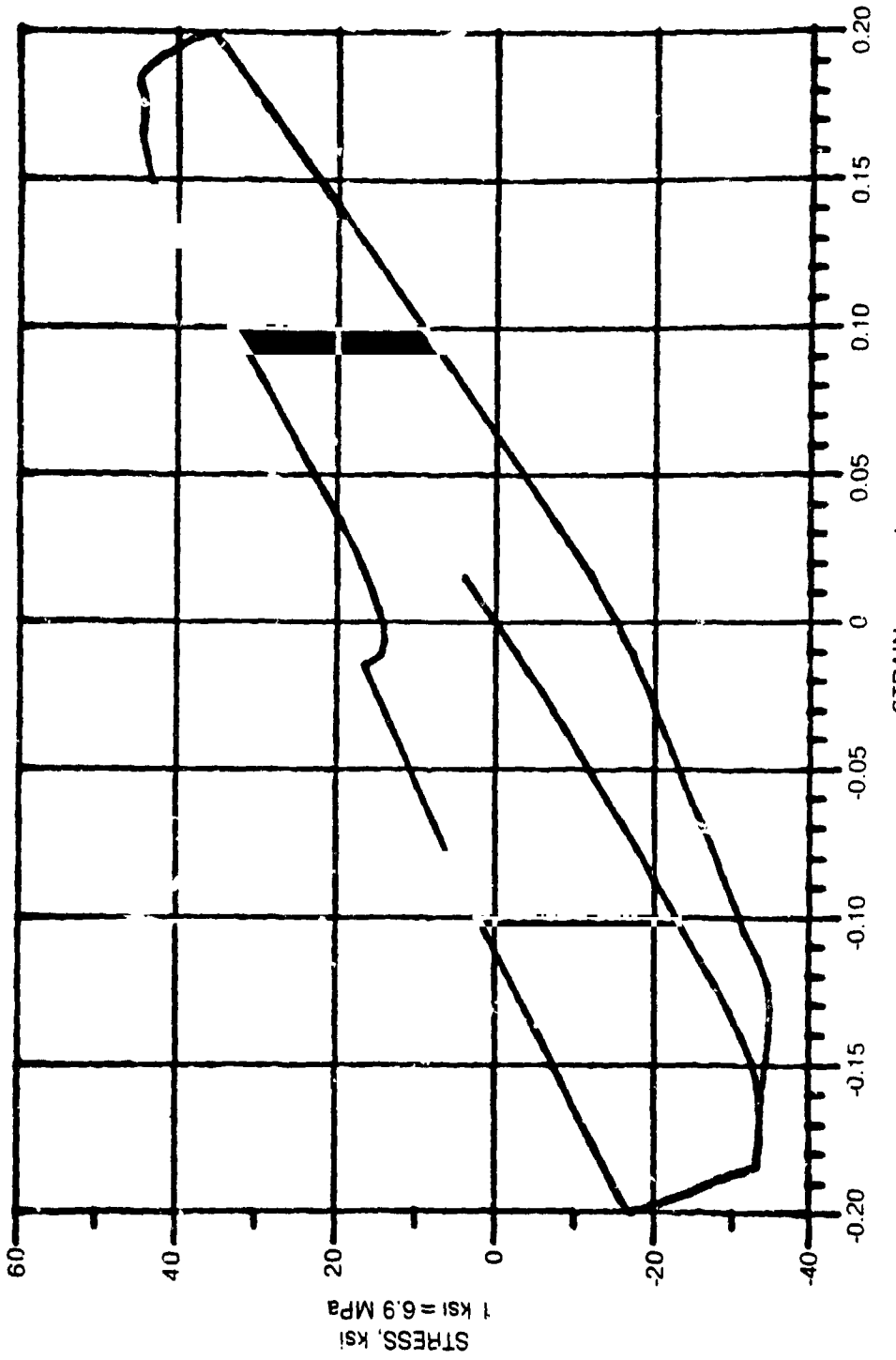

Figure 57. Predicted Stress-Strain Response of TMF Cycle No. 2 for σ_∞ (649 C) Equal to 60 ksi

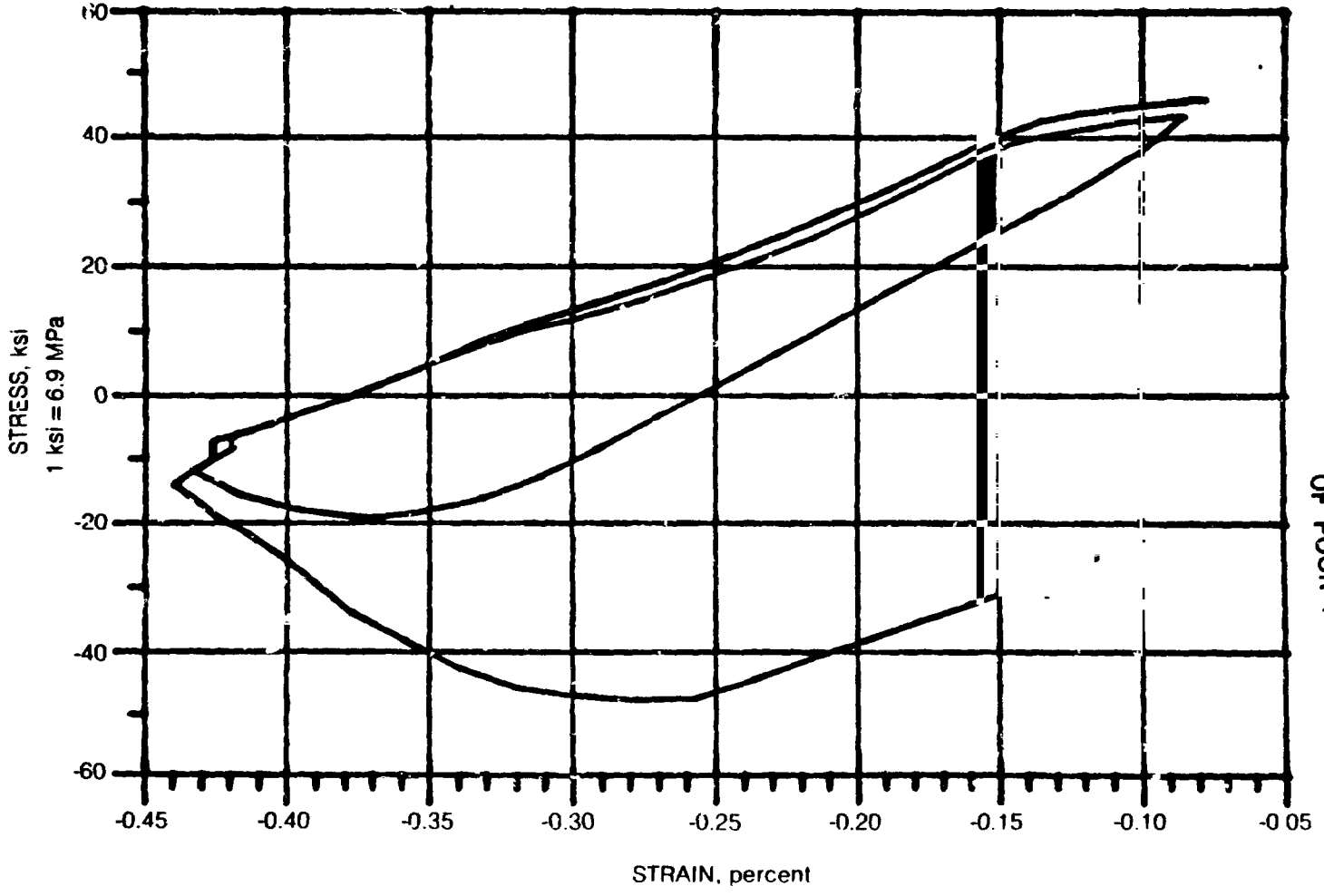

Figure 58. Predicted Stress-Strain Response of TMF Cycle No. 3 for σ_{∞} (649 C) Equal to 60 ksi

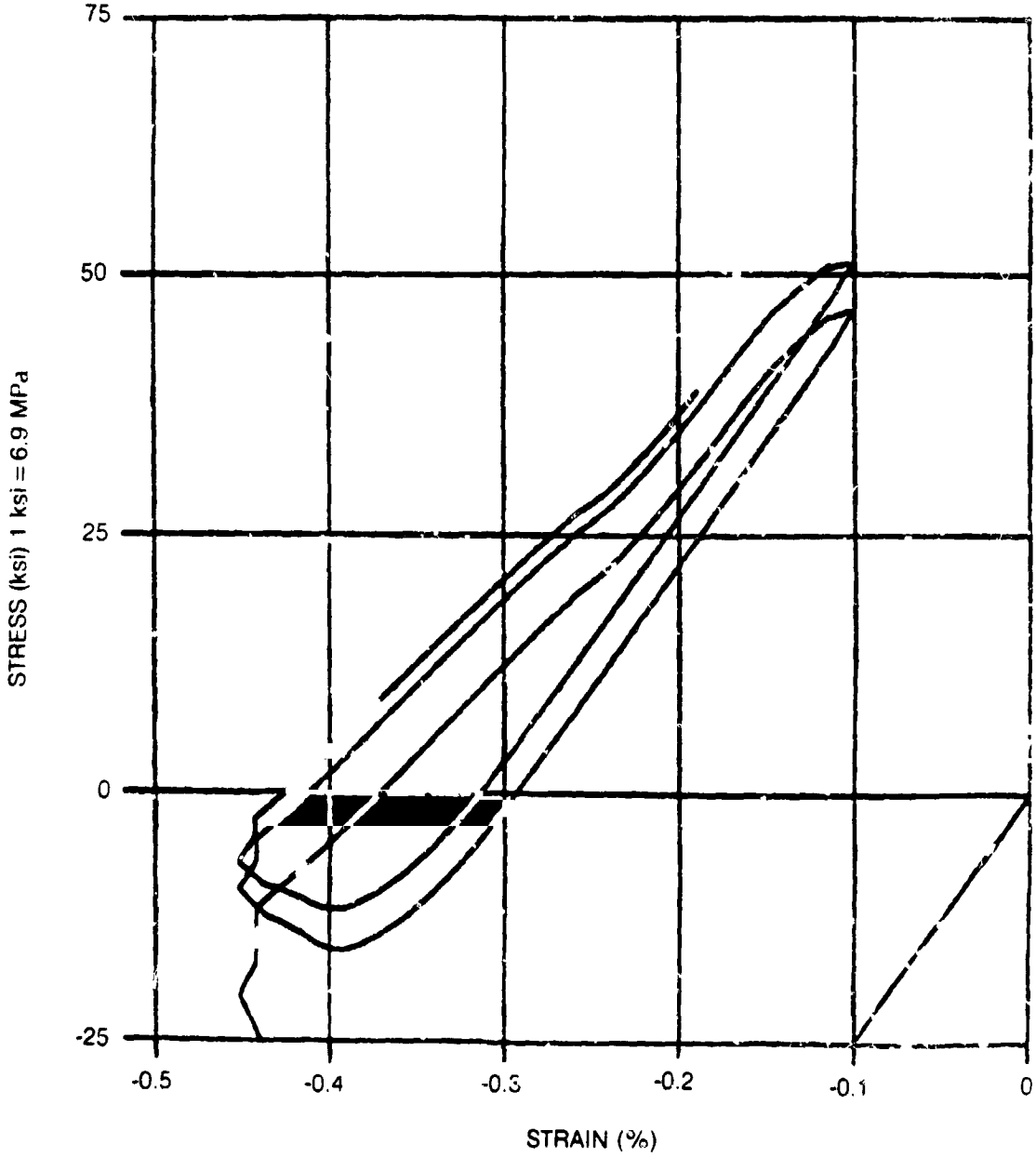

Figure 59. Thermomechanical Loop Predicted by Walker's Theory from Ref. 1

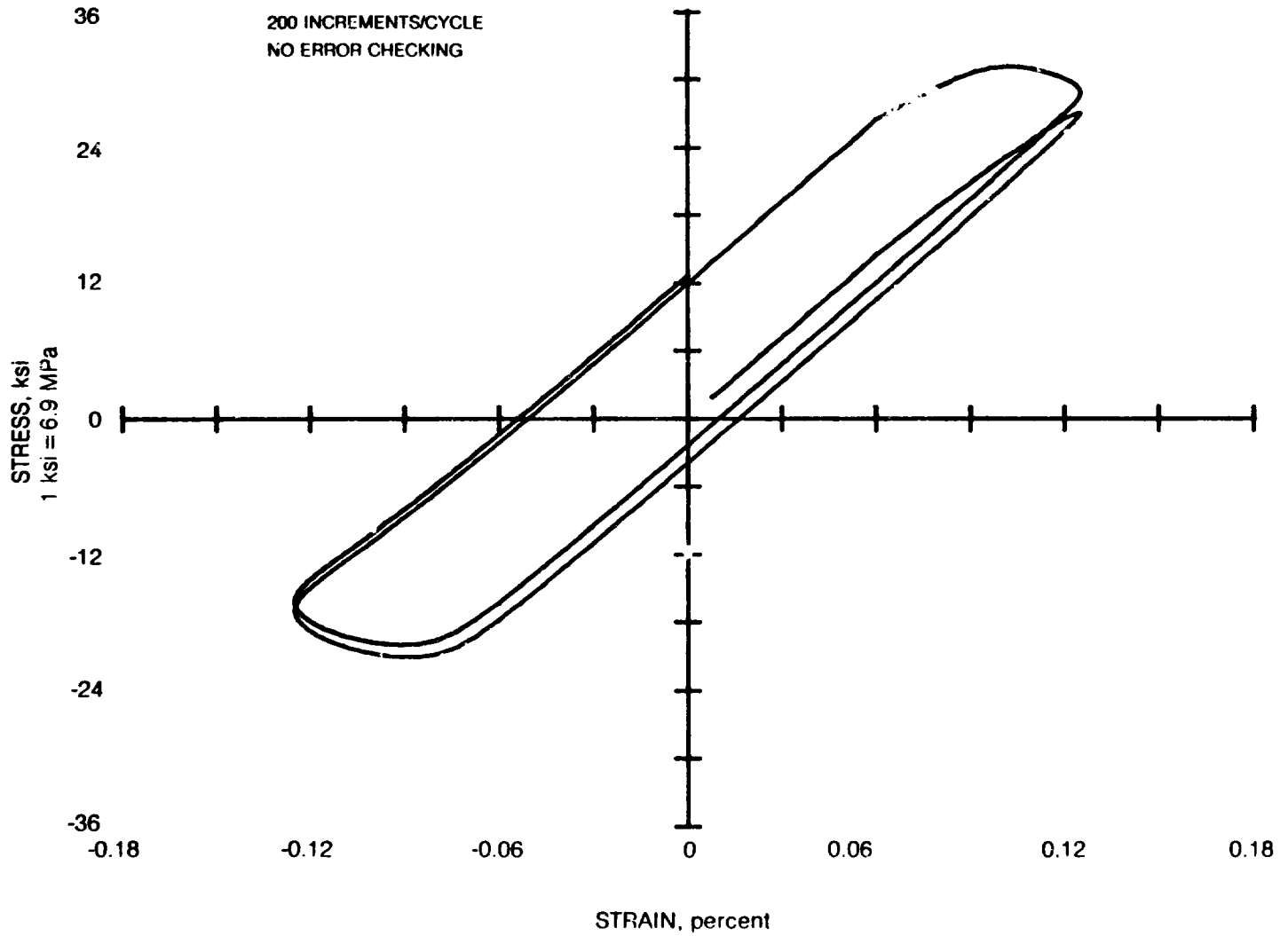

Figure 60. Forward Difference Integration

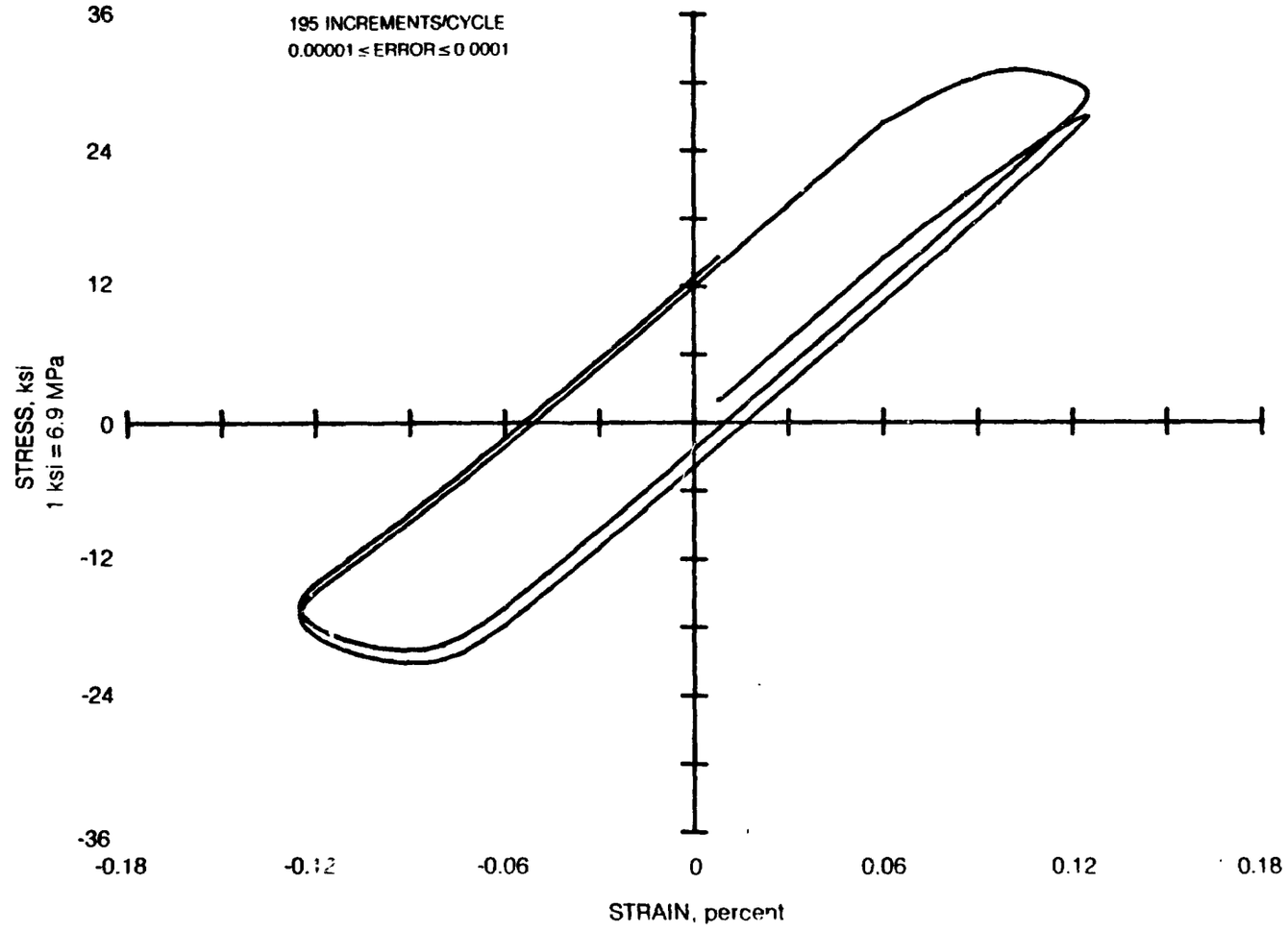

Figure 61. Forward Difference Integration

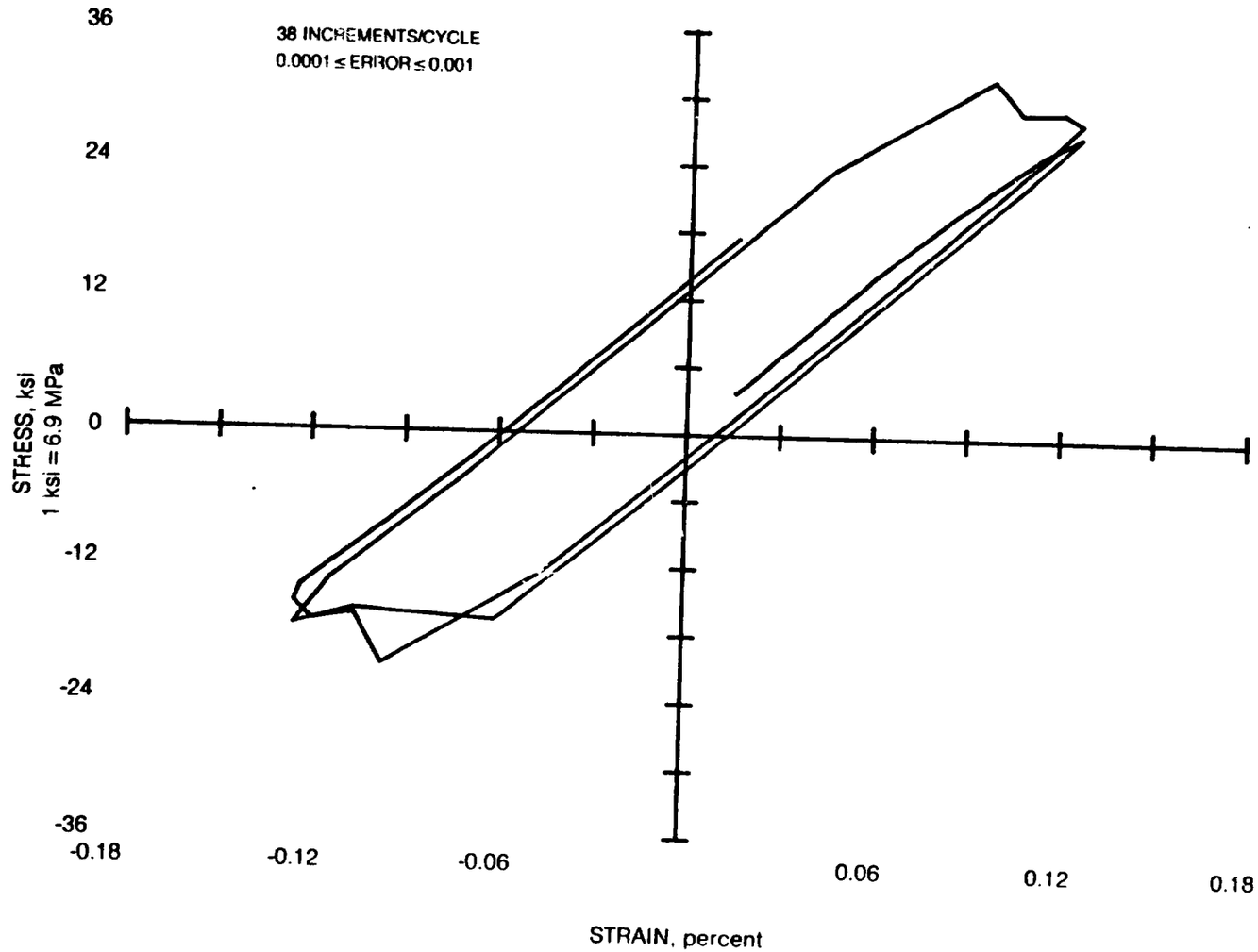

Figure 62. Forward Difference Integration

82-10-90-J

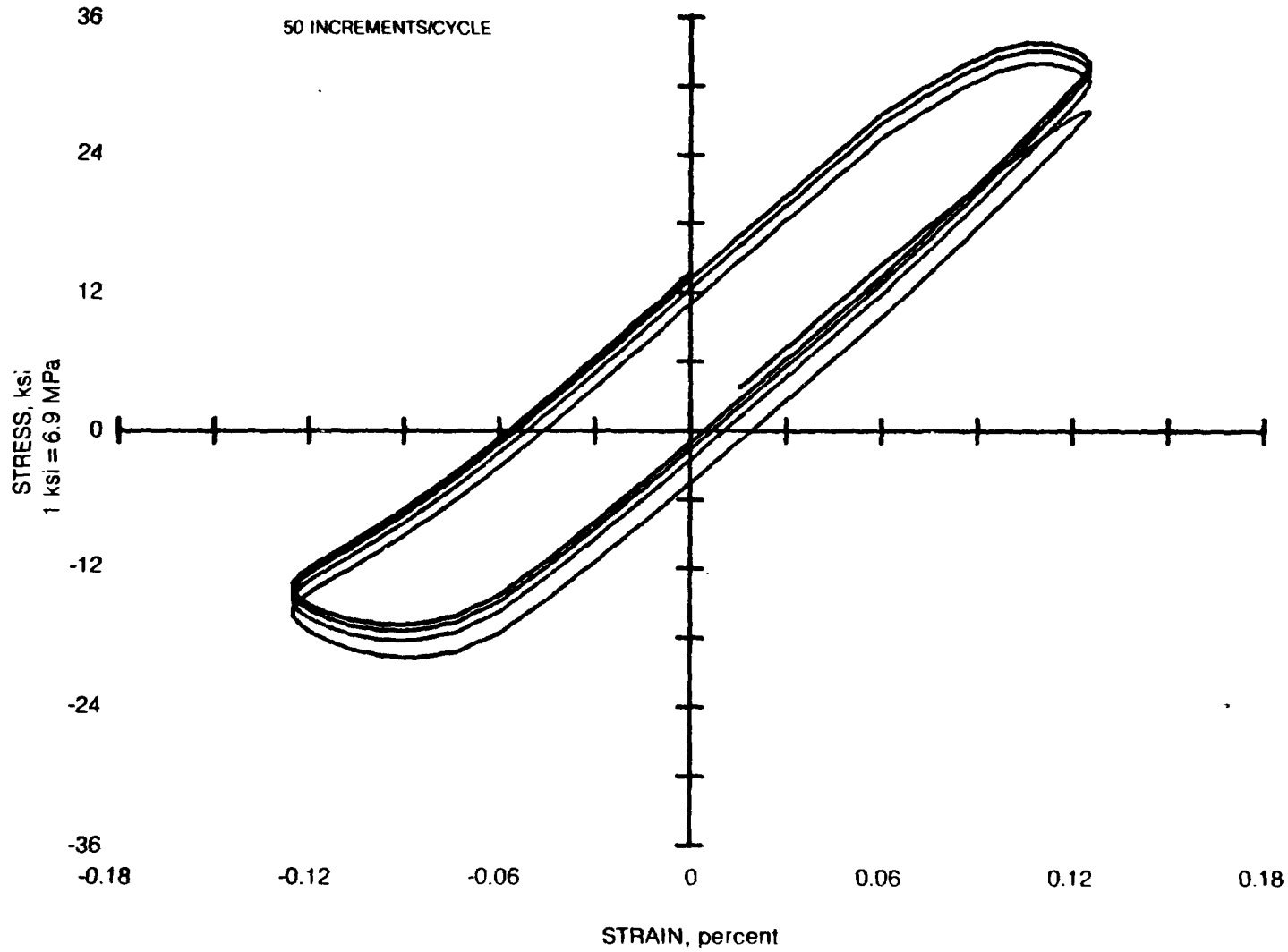

Figure 63. Backward Difference Integration

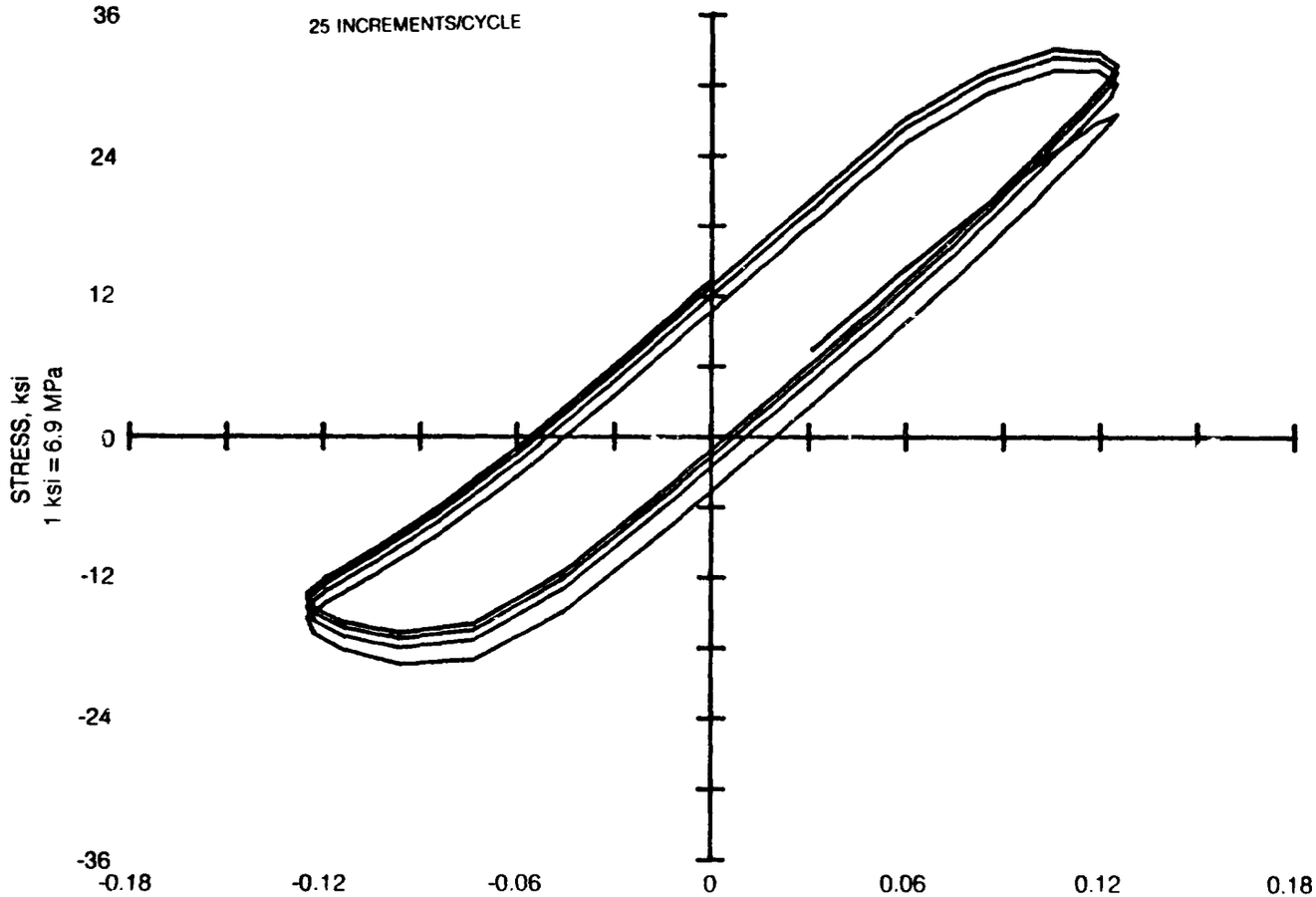

Figure 64. Backward Difference Integration

82-10-90-5

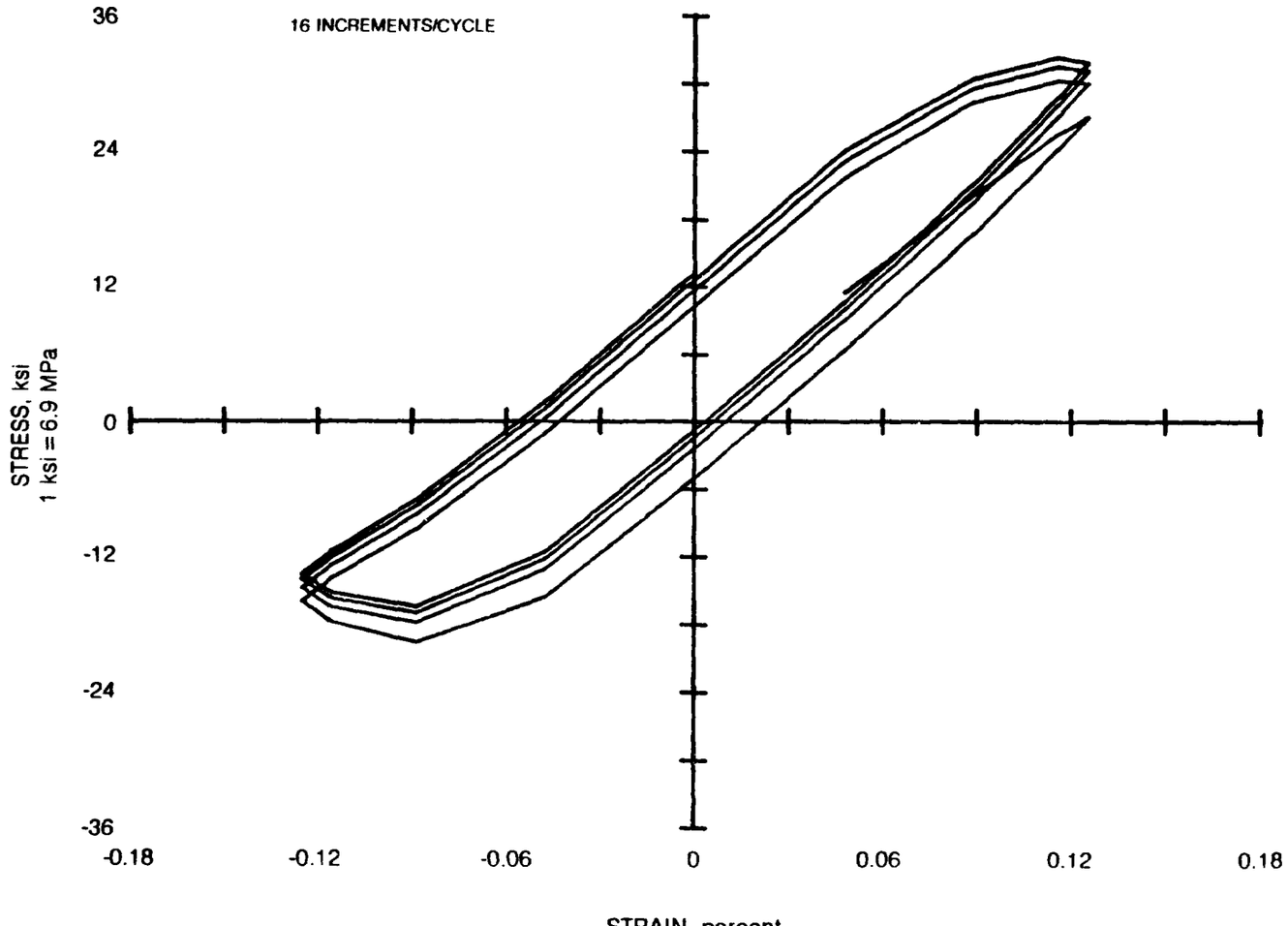

Figure 65. Backward Difference Integration

82-10-90-6

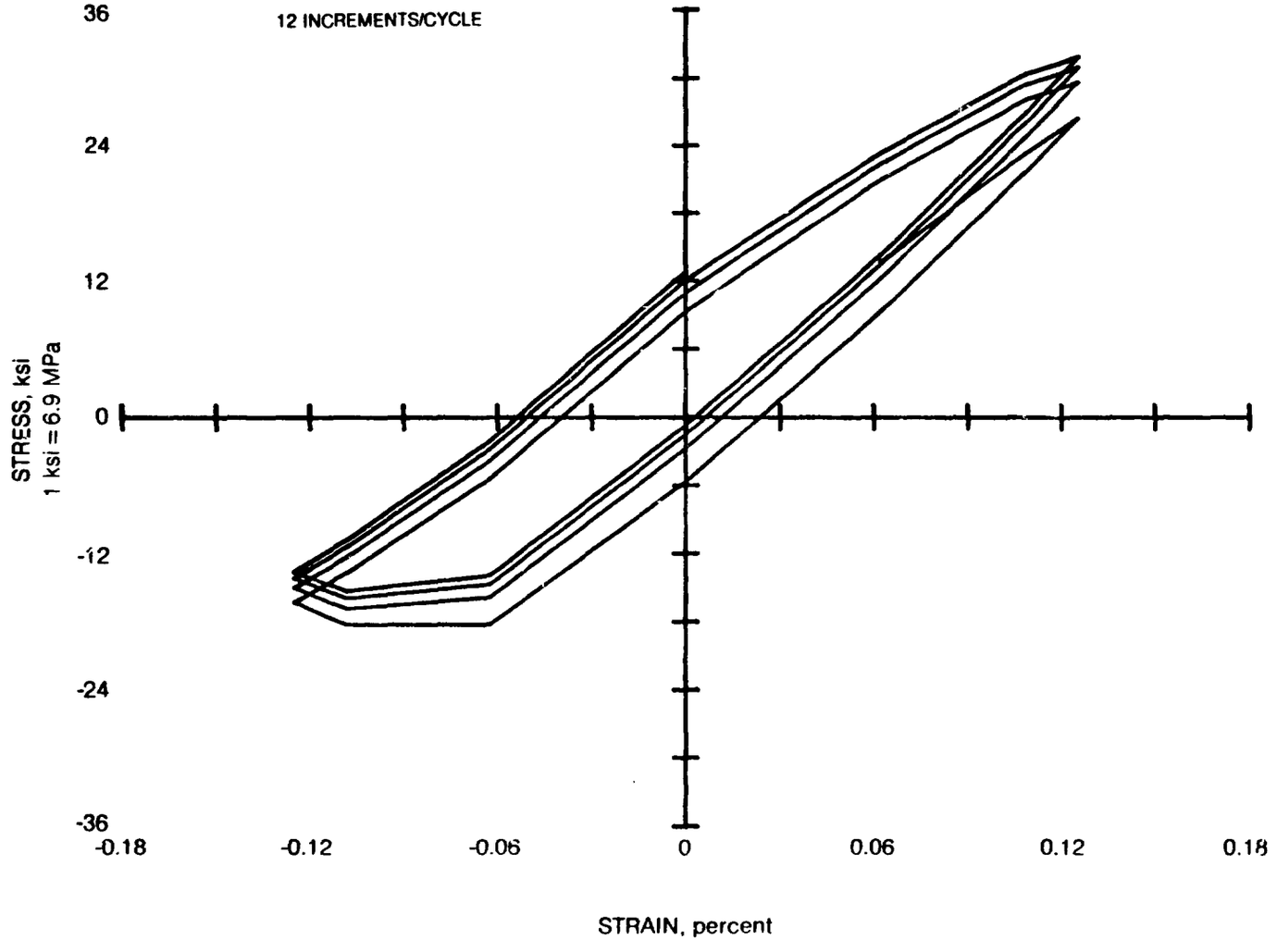

Figure 66. Backward Difference Integration

82-10-90-7

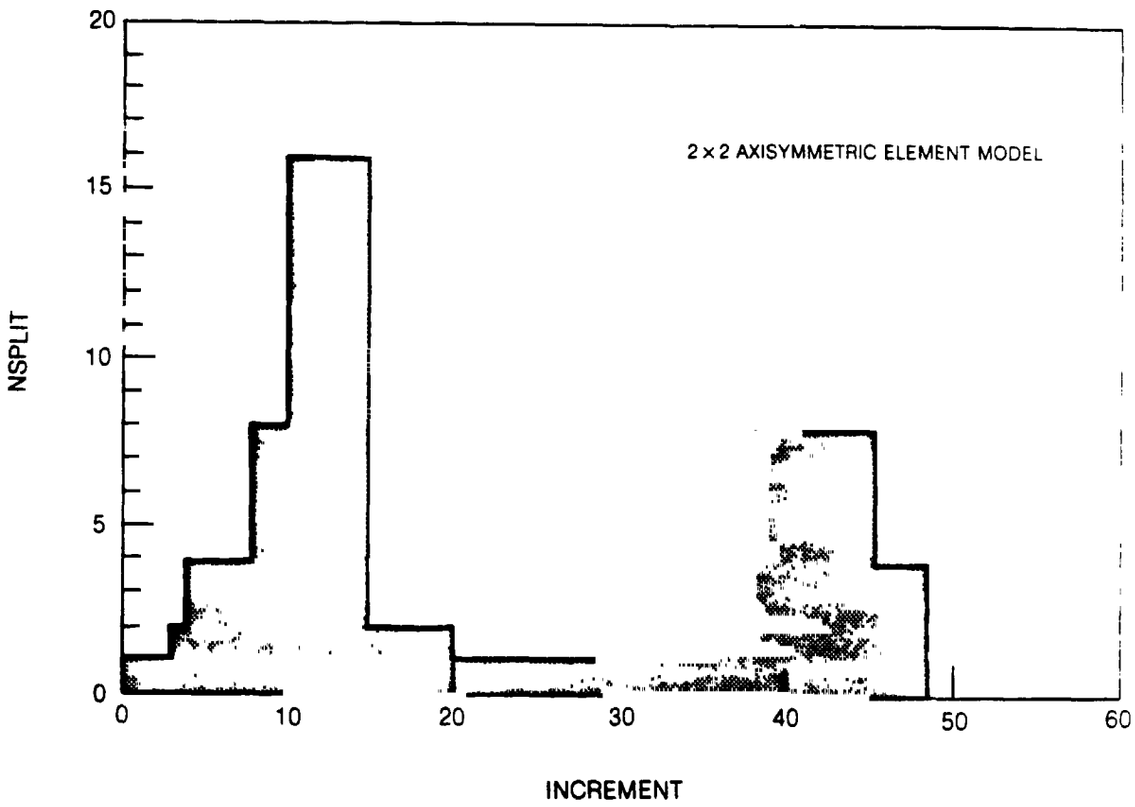

Figure 67. NSPLIT at End of Increment for Open Non-Symmetric TMF Cycle

APPENDIX 1

Constraints on Coefficient of Thermal Expansion
Using Tangent Moduli

For an elastic response

$$\dot{\sigma}_{ij} = 2\mu\dot{\epsilon}_{ij} + \lambda\dot{\epsilon}_{kk}\delta_{ij} - \alpha(3\lambda+2\mu)\dot{T}\delta_{ij} \tag{1.1}$$

But σ_{ij} is not history dependent, therefore,

$$\sigma_{ij} = F_{ij}(\underset{\sim}{\epsilon}, T) \tag{1.2}$$

and

$$\dot{\sigma}_{ij} = \frac{\partial F_{ij}}{\partial \epsilon_{\kappa\ell}}\dot{\epsilon}_{\kappa\ell} + \frac{\partial F_{ij}}{\partial T}\dot{T} \tag{1.3}$$

Comparing Eqs. (1.1) and (1.3)

$$\frac{\partial F_{ij}}{\partial \epsilon_{\kappa\ell}} = 2\mu\delta_{i\kappa}\delta_{j\ell} + \lambda\delta_{ij}\delta_{\kappa\ell} \tag{1.4}$$

and

$$\frac{\partial F_{ij}}{\partial T} = -\alpha(3\lambda+2\mu) \tag{1.5}$$

The mixed partial derivatives of Eqs. (1.4) and (1.5) must be equal or

$$\frac{\partial^2 F_{ij}}{\partial \epsilon_{k\ell}\partial T} = 2\frac{\partial \mu}{\partial T}\delta_{ik}\delta_{j\ell} + \frac{\partial \lambda}{\partial T}\delta_{ij}\delta_{k\ell} = -\frac{\partial\left[\alpha(3\lambda+2\mu)\right]}{\partial \epsilon_{k\ell}}\delta_{ij} \tag{1.6}$$

Contracting Eq. (1.6) on the indices i and j

$$\frac{1}{3}\frac{\partial K}{\partial T}\delta_{k\ell} + \frac{\partial(\alpha K)}{\partial \epsilon_{k\ell}} = 0 \tag{1.7}$$

where

$$K = \lambda + \frac{2}{3}\mu = \frac{E}{3(1-2\nu)} \tag{1.8}$$

If the material is linear elastic, the bulk modulus is not a function of strain and Eq. (1.7) becomes

$$\frac{\delta_{kl}}{3K}\frac{\partial K}{\partial T} + \frac{\partial \alpha}{\partial \epsilon_{kl}} = 0 \tag{1.9}$$

Multiplying Eq. (1.6) by the permeation tensor ϵ_{pij} results in

$$\frac{\partial \mu}{\partial T} Epmn = 0 \tag{1.10}$$

for all p, m, and n and therefore

$$\frac{\partial \mu}{\partial T} = 0 \tag{1.11}$$

APPENDIX 2

Constraints on Coefficient of Thermal Expansion for Mixed Formulation

For an elastic response

$$\sigma_{ij} = (\lambda + \frac{2}{3}\mu)\left\{\epsilon_{kk} - 3\int_0^t \alpha(\xi)\frac{\partial T}{\partial \xi}\,d\xi\right\}\delta_{ij} + 2\mu\epsilon_{ij} - \frac{2}{3}\delta_{ij}\mu\epsilon_{kk} \tag{2.1}$$

The integral in Eq. (2.1) can be written as

$$\int_0^t \alpha(\xi)\frac{\partial T}{\partial \xi}\,d\xi = \frac{1}{3}\epsilon_{kk} - \frac{\sigma_{kk}}{3(3\lambda+2\mu)} \tag{2.2}$$

Taking the derivative with respect of time of Eq. (2.1) and substituting Eq. (2.2)

$$\dot{\sigma}_{ij} = \left\{\lambda\delta_{ij}\delta_{k\ell} + 2\mu\delta_{ik}\delta_{j\ell} + 2\epsilon_{ij}\frac{\partial\mu}{\partial\epsilon_{k\ell}} - \frac{2}{3}\epsilon_{mm}\delta_{ij}\frac{\partial\mu}{\partial\epsilon_{k\ell}} + \frac{\sigma_{mm}\delta_{ij}}{3(3\lambda+2\mu)}\frac{\partial(3\lambda+2\mu)}{\partial\epsilon_{k\ell}}\right\}\dot{\epsilon}_{k\ell}$$

$$+\left\{2\frac{\partial\mu}{\partial\tau}\epsilon_{ij} - (3\lambda+2\mu)\alpha\delta_{ij} - \frac{2}{3}\frac{\partial\mu}{\partial T}\epsilon_{mm}\delta_{ij} + \frac{\sigma_{mm}\delta_{ij}}{3(3\lambda+2\mu)}\frac{\partial(3\lambda+2\mu)}{\partial T}\right\}\dot{T} \tag{2.3}$$

But σ_{ij} is not history dependent or

$$\sigma_{ij} = F_{ij}(\underset{\sim}{\epsilon}, T) \tag{2.4}$$

Taking the derivative with respect to time

$$\dot{\sigma}_{ij} = \frac{\partial F_{ij}}{\partial\epsilon_{k\ell}}\epsilon_{k\ell} + \frac{\partial F_{ij}}{\partial T}\dot{T} \tag{2.5}$$

Comparing Eqs. (2.3) and (2.5)

$$\frac{\partial F_{ij}}{\partial\epsilon_{k\ell}} = \lambda\delta_{ij}\delta_{k\ell} + 2\mu\delta_{ik}\delta_{j\ell} + 2\epsilon_{ij}\frac{\partial\mu}{\partial\epsilon_{k\ell}} - \frac{2}{3}\epsilon_{mm}\delta_{ij} + \frac{F_{mm}}{3(3\lambda+2\mu)}\frac{\partial(3\lambda+2\mu)}{\partial\epsilon_{k\ell}}\delta_{ij} \tag{2.6}$$

and

$$\frac{\partial F_{ij}}{\partial T} = 2\frac{\partial \mu}{\partial T}\epsilon_{ij} - (3\lambda+2\mu)\alpha\delta_{ij} - \frac{2}{3}\frac{\partial \mu}{\partial T}\epsilon_{mm}\delta_{ij} + \frac{F_{mm}}{3(3\lambda+2\mu)}\frac{\partial(3\lambda+2\mu)}{\partial T}\delta_{ij} \qquad (2.7)$$

Equations (2.6) and (2.7) can be contracted to yield

$$\frac{\partial F_{mm}}{\partial \epsilon_{kl}} = (3\lambda+2\mu)\delta_{kl} + \frac{F_{mm}}{3\lambda+2\mu}\frac{\partial(3\lambda+2\mu)}{\partial \epsilon_{kl}} \qquad (2.8)$$

and

$$\frac{\partial F_{mm}}{\partial T} = -3(3\lambda+2\mu)\alpha + \frac{F_{mm}}{3\lambda+2\mu}\frac{\partial(3\lambda+2\mu)}{\partial T} \qquad (2.9)$$

Setting the mixed partial derivatives of Eqs. (2.6) and (2.7) to be equal, and substituting Eqs. (2.8) and (2.9) results in

$$\frac{\partial \alpha}{\partial \epsilon_{kl}} = 0 \qquad (2.10)$$

Appendix 3. Walker's Theory (Differential Form)

$$\dot{c}_{ij} = \left(\sqrt{\frac{\frac{2}{3}\left(\frac{3}{2}s_{ij} - \Omega_{ij}\right)\left(\frac{3}{2}s_{ij} - \Omega_{ij}\right)}{K}} \right)^{n} \frac{\left(\frac{3}{2}s_{ij} - \Omega_{ij}\right)}{\sqrt{\frac{2}{3}\left(\frac{3}{2}s_{ij} - \Omega_{ij}\right)\left(\frac{3}{2}s_{ij} - \Omega_{ij}\right)}} \tag{3.1}$$

$$\dot{\Omega}_{ij} = (n_1 + n_2)\dot{c}_{ij} + c_{ij}\frac{\partial n_1}{\partial \Theta}\dot{\Theta} - (\Omega_{ij} - \overset{0}{\Omega}_{ij} - n_1 c_{ij})\left(\dot{G} - \frac{1}{n_2}\frac{\partial n_2}{\partial \Theta}\dot{\Theta}\right) + \overset{\circ}{\Omega}_{ij} \tag{3.2}$$

$$K = K_1 - K_2 e^{-n_7 R}, \tag{3.3}$$

$$\dot{c}_{ij} = (\delta_{ij}\lambda\dot{\epsilon}_{kk} + 2\mu\dot{\epsilon}_{ij} - \dot{\sigma}_{ij} - \delta_{ij}(3\lambda + 2\mu)\alpha\dot{\Theta})/2\mu \tag{3.4}$$

$$\dot{G} = (n_3 + n_4 e^{-n_5 R})\dot{R} + n_6\left(\frac{2}{3}\Omega_{ij}\Omega_{ij}\right)^{\frac{m-1}{2}}, \tag{3.5}$$

$$\dot{R} = \sqrt{\frac{2}{3}\dot{c}_{ij}\dot{c}_{ij}}, \tag{3.6}$$

$$\overset{\circ}{\Omega}_{ij} = 3\overset{\circ}{\Omega}\left[\frac{\dot{C}_{ik}C_{kj}}{C_{pq}C_{pq}} + \frac{C_{ik}\dot{C}_{kj}}{C_{pq}C_{pq}} - \left(\frac{2C_{ik}C_{kj}}{C_{pq}C_{pq}}\right)\left(\frac{C_{rs}\dot{C}_{rs}}{C_{uv}C_{uv}}\right)\right] + \left[3\frac{C_{ik}C_{kj}}{C_{pq}C_{pq}} - \delta_{ij}\right]\frac{\partial \overset{\circ}{\Omega}}{\partial \Theta} \tag{3.7}$$

$$s_{ij} = \sigma_{ij} - \frac{1}{3}\delta_{ij}\sigma_{kk}. \tag{3.8}$$

Material constants: $\lambda, \mu, \overset{0}{\Omega}, n, m, n_1, n_2, n_3, n_4, n_5, n_6, n_7, K_1, K_2$ depend on temperature, Θ

Appendix 4. Walker's Theory (Integral Form)

$$\sigma_{ij}(t) = \frac{2}{3}\Omega_{ij}(t) + \delta_{ij}\int_0^t \left(\lambda(\Theta(t)) + \frac{2}{3}\mu(\Theta(t))\right)\left(\frac{\partial \epsilon_{kk}}{\partial \xi} - 3\alpha(\Theta(\xi))\frac{\partial \Theta}{\partial \xi}\right) d\xi + \int_0^t e^{-\{o(t)-o(\xi)\}}\left(2\mu(\Theta(t))\frac{\partial \epsilon_{ij}}{\partial \xi} - \delta_{ij}\frac{2}{3}\mu(\Theta(t))\frac{\partial \epsilon_{kk}}{\partial \xi} - \frac{2}{3}\frac{\partial \Omega_{ij}}{\partial \xi}\right) d\xi, \quad (4.1)$$

$$\Omega_{ij}(t) = \overset{0}{\Omega}_{ij}(t) + n_1(\Theta(t))c_{ij}(t) + n_2(\Theta(t))\int_0^t e^{-\{G(t)-G(\xi)\}}\frac{\partial c_{ij}}{\partial \xi}\, d\xi, \quad (4.2)$$

$$K(t) = K_1(\Theta(t)) - K_2(\Theta(t))e^{-n_7(\Theta(t))R(t)}, \quad (4.3)$$

$$c_{ij}(t) = \int_0^t \left(\delta_{ij}\lambda(\Theta(t))\frac{\partial \epsilon_{kk}}{\partial \xi} + 2\mu(\Theta(t))\frac{\partial \epsilon_{ij}}{\partial \xi} - \frac{\partial \sigma_{ij}}{\partial \xi} - \delta_{ij}\alpha(\Theta(\xi))\left(3\lambda(\Theta(t)) + 2\mu(\Theta(t))\right)\frac{\partial \Theta}{\partial \xi}\right) d\xi/2\mu, \quad (4.4)$$

$$\overset{0}{\Omega}_{ij}(t) = -\delta_{ij}\overset{0}{\Omega}(\Theta(t)) + 3\overset{0}{\Omega}(\Theta(t))\frac{c_{ik}(t)c_{kj}(t)}{c_{pq}(t)c_{pq}(t)}, \quad (4.5)$$

$$O(t) = \int_0^t \frac{3\mu(\Theta(\xi))}{K(\xi)}\left(\frac{\partial R}{\partial \xi}\right)^{1-1/n(\Theta(\xi))} d\xi, \quad (4.6)$$

$$G(t) = \int_0^t \left\{\left(n_3(\Theta(\xi)) + n_4(\Theta(\xi))e^{-n_5(\Theta(\xi))R(\xi)}\right)\frac{\partial R}{\partial \xi} + n_6(\Theta(\xi))\left(\frac{2}{3}\Omega_{ij}(\xi)\Omega_{ij}(\xi)\right)^{\frac{m(\Theta(\xi))-1}{2}}\right\} d\xi, \quad (4.7)$$

$$R(t) = \int_0^t \sqrt{\frac{2}{3}\frac{\partial c_{ij}}{\partial \xi}\frac{\partial c_{ij}}{\partial \xi}}\, d\xi. \quad (4.8)$$

Material constants: $\lambda, \mu, \overset{0}{\Omega}, n, m, n_1, n_2, n_3, n_4, n_5, n_6, n_7, K_1, K_2$ depend on temperature

Appendix 5. Miller's Theory (Differential Form)

$$\dot{c}_{ij} = B\theta' \left\{ \sinh\left(\frac{\sqrt{\frac{2}{3}\left(\frac{3}{2}s_{ij}-\Omega_{ij}\right)\left(\frac{3}{2}s_{ij}-\Omega_{ij}\right)}}{K} \right)^{\frac{3}{2}} \right\}^{n} \frac{\left(\frac{3}{2}s_{ij}-\Omega_{ij}\right)}{\sqrt{\frac{2}{3}\left(\frac{3}{2}s_{ij}-\Omega_{ij}\right)\left(\frac{3}{2}s_{ij}-\Omega_{ij}\right)}} , \tag{5.1}$$

$$\dot{\Omega}_{ij} = H_1\dot{c}_{ij} - H_1 B\theta' \left\{ \sinh\left(A_1\sqrt{\frac{2}{3}\Omega_{ij}\Omega_{ij}} \right) \right\}^{n} \frac{\Omega_{ij}}{\sqrt{\frac{2}{3}\Omega_{ij}\Omega_{ij}}} \tag{5.2}$$

$$\dot{K} = H_2\dot{R}\left(C_2 + \sqrt{\frac{2}{3}\Omega_{ij}\Omega_{ij}} - \frac{A_2}{A_1}K^3 \right) - H_2 C_2 B\theta' \left\{ \sinh\left(A_2 K^3\right) \right\}^{n} , \tag{5.3}$$

$$\dot{c}_{ij} = \left(\delta_{ij}\lambda\dot{\epsilon}_{kk} + 2\mu\dot{\epsilon}_{ij} - \dot{\sigma}_{ij} - \delta_{ij}(3\lambda+2\mu)\alpha\dot{\Theta}\right)/2\mu \tag{5.4}$$

$$\dot{R} = \sqrt{\frac{2}{3}\dot{c}_{ij}\dot{c}_{ij}} , \tag{5.5}$$

$$s_{ij} = \sigma_{ij} - \frac{1}{3}\delta_{ij}\sigma_{kk} , \tag{5.6}$$

$$\theta' = \exp\left\{\frac{-Q^*}{kT}\right\} \text{ for } T \geq 0.6T_m , \tag{5.7}$$

$$\theta' = \exp\left\{\frac{-Q^*}{0.6kT}\ln\left(1 + \frac{0.6T_m}{T}\right)\right\} \text{ for } T < 0.6T_m \tag{5.8}$$

Material constants: $n, H_2, A_1, A_2, C_2, Q^*, k$ are independent of temperature.

Material constants: $\lambda, \mu, K_0, \theta'$ depend on temperature, where K_0 is the initial value of K, and T is the temperature in °K.

Apprendix 6. Miller's Theory (Integral Form)

$$\sigma_{ij}(t)=\frac{2}{3}\Omega_{ij}(t)+\delta_{ij}\int_0^t\left(\lambda(\Theta(\xi))+\frac{2}{3}\mu(\Theta(\xi))\right)\left(\frac{\partial\epsilon_{kk}}{\partial\xi}-3\alpha(\Theta,\epsilon)\frac{\partial\Theta}{\partial\xi}\right)d\xi+\int_0^t e^{-\{o(t)-o(\xi)\}}\left(2\mu(\Theta(\xi))\frac{\partial\epsilon_{ij}}{\partial\xi}-\delta_{ij}\frac{2}{3}\mu(\Theta(\xi))\frac{\partial\epsilon_{kk}}{\partial\xi}-\frac{2}{3}\frac{\partial\Omega_{ij}}{\partial\xi}\right)d\xi, \tag{6.1}$$

$$\Omega_{ij}(t)=H_1\int_0^t e^{-\{G(t)-G(\xi)\}}\frac{\partial c_{ij}}{\partial\xi}\,d\xi, \tag{6.2}$$

$$K(t)=K_0+H_2\int_0^t\left(C_2+\sqrt{\frac{2}{3}\Omega_{ij}(\xi)\Omega_{ij}(\xi)}-A_2K^3(\xi)/A_1\right)e^{-\{J(t)-J(\xi)\}}\frac{\partial R}{\partial\xi}\,d\xi, \tag{6.3}$$

$$c_{ij}(t)=\int_0^t\left(\delta_{ij}\lambda(\Theta(\xi))\frac{\partial\epsilon_{kk}}{\partial\xi}+2\mu(\Theta,\epsilon)\frac{\partial\epsilon_{ij}}{\partial\xi}-\frac{\partial\sigma_{ij}}{\partial\xi}-\delta_{ij}\alpha(\Theta,\epsilon)\left(3\lambda(\Theta(\xi))+2\mu(\Theta(\xi))\right)\frac{\partial\Theta}{\partial\xi}\right)d\xi, \tag{6.4}$$

$$O(t)=\int_0^t\frac{3\mu(\Theta(\xi))}{K(\xi)}\left\{\sinh^{-1}\left(\frac{1}{B\theta'(\Theta(\xi))}\frac{\partial R}{\partial\xi}\right)^{\frac{1}{n}}\right\}^{-\frac{2}{3}}\frac{\partial R}{\partial\xi}\,d\xi, \tag{6.5}$$

$$G(t)=H_1\int_0^t B\theta'(\Theta(\xi))\frac{\left\{\sinh\left(A_1\sqrt{\frac{2}{3}\Omega_{ij}(\xi)\Omega_{ij}(\xi)}\right)\right\}^n}{\sqrt{\frac{2}{3}\Omega_{ij}(\xi)\Omega_{ij}(\xi)}}\,d\xi, \tag{6.6}$$

$$J(t)=H_2C_2\int_0^t B\theta'(\Theta(\xi))\frac{\{\sinh(A_2K^3(\xi))\}^n}{K(\xi)-K_0}\,d\xi, \tag{6.7}$$

$$R(t)=\int_0^t\sqrt{\frac{2}{3}\frac{\partial c_{ij}}{\partial\xi}\frac{\partial c_{ij}}{\partial\xi}}\,d\xi \tag{6.8}$$

Appendix 7. Krieg, Swearengen and Rohde's Theory (Differential Form)

$$\dot{c}_{ij} = \left(\frac{\sqrt{\frac{2}{3}\left(\frac{3}{2}s_{ij}-\Omega_{ij}\right)\left(\frac{3}{2}s_{ij}-\Omega_{ij}\right)}}{K} \right)^{n} \frac{\left(\frac{3}{2}s_{ij}-\Omega_{ij}\right)}{\sqrt{\frac{2}{3}\left(\frac{3}{2}s_{ij}-\Omega_{ij}\right)\left(\frac{3}{2}s_{ij}-\Omega_{ij}\right)}} \tag{7.1}$$

$$\dot{\Omega}_{ij} = A_1 \dot{c}_{ij} - A_2 \Omega_{ij} \sqrt{\frac{2}{3}\Omega_{pq}\Omega_{pq}} \left(e^{A_3 \frac{2}{3}\Omega_{pq}\Omega_{pq}} - 1 \right), \tag{7.2}$$

$$\dot{K} = A_4 \dot{R} - A_5 (K - K_0)^n, \tag{7.3}$$

$$\dot{c}_{ij} = (\delta_{ij}\lambda\dot{\epsilon}_{kk} + 2\mu\dot{\epsilon}_{ij} - \dot{\sigma}_{ij} - \delta_{ij}(3\lambda+2\mu)\alpha\dot{\Theta})/2\mu, \tag{7.4}$$

$$\dot{R} = \sqrt{\frac{2}{3}\dot{c}_{ij}\dot{c}_{ij}}, \tag{7.5}$$

$$s_{ij} = \sigma_{ij} - \frac{1}{3}\delta_{ij}\sigma_{kk}. \tag{7.6}$$

Material constants. $\lambda, \mu, n, A_1, A_2, A_3, A_4, A_5, K_0$ depend on temperature, where K_0 is the initial value of K.

Appendix 8. Krieg, Swearengen and Rohde's Theory (Integral Form)

$$\sigma_{ij}(t)=\frac{2}{3}\,\Omega_{ij}(t)+\delta_{ij}\int_0^t\left(\lambda(\Theta(\xi))+\frac{2}{3}\mu\,(\Theta(\xi))\right)\left(\frac{\partial\epsilon_{kk}}{\partial\xi}-3\alpha(\Theta,\epsilon)\frac{\partial\Theta}{\partial\xi}\right)d\xi+\int_0^t-\left\{Q(t)-Q(\xi)\right\}\left(2\mu(\Theta(\xi))\frac{\partial\epsilon_{ij}}{\partial\xi}-\delta_{ij}\frac{2}{3}\mu(\Theta(\xi))\frac{\partial\epsilon_{kk}}{\partial\xi}-\frac{2}{3}\frac{\partial\Omega_{ij}}{\partial\xi}\right)d\xi, \tag{8.1}$$

$$\Omega_{ij}(t)=\int_0^t A_1(\Theta(\xi))e^{-\left\{G(t)-G(\xi)\right\}}\frac{\partial c_{ij}}{\partial\xi}\,d\xi, \tag{8.2}$$

$$K(t)=K_0(\Theta(t))+\int_0^t A_3(\Theta(\xi))\,e^{-\left\{J(t)-J(\xi)\right\}}\frac{\partial R}{\partial\xi}\,d\xi, \tag{8.3}$$

$$c_{ij}(t)=\int_0^t\left(\delta_{ij}\lambda(\Theta(\xi))\frac{\partial\epsilon_{kk}}{\partial\xi}+2\mu(\Theta(\xi))\frac{\partial\epsilon_{ij}}{\partial\xi}-\frac{\partial\sigma_{ij}}{\partial\xi}-\delta_{ij}\alpha(\Theta,\epsilon)\left(3\lambda(\Theta(\xi))+2\mu(\Theta(\xi))\right)\frac{\partial\Theta}{\partial\xi}\right)d\xi, \tag{8.4}$$

$$Q(t)=\int_0^t\frac{3\mu(\Theta(\xi))}{K(\xi)}\left(\frac{\partial R}{\partial\xi}\right)^{1-1/n(\Theta(\xi))}d\xi, \tag{8.5}$$

$$G(t)=\int_0^t A_2(\Theta(\xi))\sqrt{\frac{2}{3}\Omega_{ij}(\xi)\Omega_{ij}(\xi)}\left(e^{A_3(\Theta(\xi))\frac{2}{3}\Omega_{ij}(\xi)\Omega_{ij}(\xi)}-1\right)d\xi, \tag{8.6}$$

$$J(t)=\int_0^t A_4(\Theta(\xi))\left(K(\xi)-K_0(\Theta(\xi))\right)^{n(\Theta(\xi))-1}d\xi, \tag{8.7}$$

$$R(t)=\int_0^t\sqrt{\frac{2}{3}\frac{\partial c_{ij}}{\partial\xi}\frac{\partial c_{ij}}{\partial\xi}}\,d\xi. \tag{8.8}$$

Appendix 9. Modified Miller's Theory (Differential Form)

$$\dot{c}_{ij} = B\theta' \left\{ \sinh\left(\frac{\sqrt{\frac{2}{3}\left(\frac{3}{2}s_{ij}-\Omega_{ij}\right)\left(\frac{3}{2}s_{ij}-\Omega_{ij}\right)}}{K} \right)^{\frac{3}{2}} \right\}^{n} \frac{\left(\frac{3}{2}s_{ij}-\Omega_{ij}\right)}{\sqrt{\frac{2}{3}\left(\frac{3}{2}s_{ij}-\Omega_{ij}\right)\left(\frac{3}{2}s_{ij}-\Omega_{ij}\right)}} \quad , \tag{9.1}$$

$$\dot{\Omega}_{ij} = H_1\dot{c}_{ij} - H_1 B\theta' \left\{ \sinh\left(A_1\sqrt{\frac{2}{3}\Omega_{ij}\Omega_{ij}} \right) \right\}^{n} \frac{\Omega_{ij}}{\sqrt{\frac{2}{3}\Omega_{ij}\Omega_{ij}}} + \frac{\Omega_{ij}}{H_1}\frac{\partial H_1}{\partial \Theta}\dot{\Theta} \tag{9.2}$$

$$\dot{K} = H_2\dot{R}\left(C_2 + \sqrt{\frac{2}{3}\Omega_{ij}\Omega_{ij}} - \frac{A_2}{A_1}K^3 \right) - H_2 C_2 B\theta' \left\{ \sinh\left(A_2 K^3\right) \right\}^{n} \quad , \tag{9.3}$$

$$\dot{c}_{ij} = \left(\delta_{ij}\lambda\dot{\epsilon}_{kk} + 2\mu\dot{\epsilon}_{ij} - \dot{\sigma}_{ij} - \delta_{ij}(3\lambda+2\mu)\alpha\dot{\Theta}\right)/2\mu \tag{9.4}$$

$$\dot{R} = \sqrt{\frac{2}{3}\dot{c}_{ij}\dot{c}_{ij}} \quad , \tag{9.5}$$

$$s_{ij} = \sigma_{ij} - \frac{1}{3}\delta_{ij}\sigma_{kk} \quad , \tag{9.6}$$

$$\theta' = \exp\left\{ \frac{-Q^*}{kT} \right\} \text{ for } T \geq 0.6T_m \quad , \tag{9.7}$$

$$\theta' = \exp\left\{ \frac{-Q^*}{0.6kT} \ln\left(1 + \frac{0.6T_m}{T}\right) \right\} \text{ for } T < 0.6T_m \tag{9.8}$$

Material constants: n, H_2, A_1, A_2, C_2, Q^*, k are independent of temperature.

Material constants λ, μ, K_0, θ, H_1 depend on temperature, where K_0 is the initial value of K, and T is the temperature in °K.

Appendix 10. Modified Krieg, Swearengen and Rohde's Theory (Differential Form)

$$\dot{c}_{ij} = \left(\frac{\sqrt{\frac{2}{3}\left(\frac{3}{2}s_{ij}-\Omega_{ij}\right)\left(\frac{3}{2}s_{ij}-\Omega_{ij}\right)}}{K} \right)^{n} \frac{\left(\frac{3}{2}s_{ij}-\Omega_{ij}\right)}{\sqrt{\frac{2}{3}\left(\frac{3}{2}s_{ij}-\Omega_{ij}\right)\left(\frac{3}{2}s_{ij}-\Omega_{ij}\right)}} \tag{10.1}$$

$$\dot{\Omega}_{ij} = A_1 \dot{c}_{ij} - A_2 \Omega_{ij} \sqrt{\frac{2}{3}\Omega_{pq}\Omega_{pq}} \left(e^{A_3 \frac{2}{3}\Omega_{pq}\Omega_{pq}} - 1 \right) + \frac{\Omega_{ij}}{A} \frac{\partial A_1}{\partial \Theta} \dot{\Theta} \tag{10.2}$$

$$\dot{K} = A_4 \dot{R} - A_5 (K - K_0)^n , \tag{10.3}$$

$$\dot{c}_{ij} = (\delta_{ij} \lambda \dot{\epsilon}_{kk} + 2\mu \dot{\epsilon}_{ij} - \dot{\sigma}_{ij} - \delta_{ij}(3\lambda + 2\mu)\alpha\dot{\Theta})/2\mu , \tag{10.4}$$

$$\dot{R} = \sqrt{\frac{2}{3}\dot{c}_{ij}\dot{c}_{ij}} , \tag{10.5}$$

$$s_{ij} = \sigma_{ij} - \frac{1}{3}\delta_{ij}\sigma_{kk} \tag{10.6}$$

Material constants: $\lambda, \mu, n, A_1, A_2, A_3, A_4, A_5, K_0$ depend on temperature, where K_0 is the initial value of K.

Appendix 11. Updated Miller's Theory — Differential Form

$$\dot{C}^{c}_{ij} = B\theta\left\{\sinh\left(\frac{\sqrt{3J_2'}}{K}\right)^{3/2}\right\}^{n}\frac{\left(\frac{3}{2}S_{ij}-\Omega_{ij}\right)}{\sqrt{3J_2'}}$$

$$3J_2' = \frac{2}{3}\left(\frac{3}{2}S_{ij}-\Omega_{ij}\right)\left(\frac{3}{2}S_{ij}-\Omega_{ij}\right)$$

$$\dot{\Omega}_{ij} = H_1\dot{C}_{ij} - H_1\beta\theta'\left\{\sinh\left(A_1\sqrt{\frac{2}{3}\Omega_{kl}\Omega_{kl}}\right)\right\}^{n}\frac{\Omega_{ij}}{\sqrt{\frac{2}{3}\Omega_{kl}\Omega_{kl}}}$$

$$H_1 = H_1' e^{-H_3\left(\frac{2}{3}\Omega_{ij}\dot{C}_{ij}\right)/R}$$

$$K = \sqrt{F_1 + F_d(1+F_2)}$$

$$\dot{F}_d = H_2\dot{R}\left[C_2 + \sqrt{\frac{2}{3}\Omega_{ij}\Omega_{ij}} - \left(\frac{A_2}{A_1}\right)F_d^{3/2}\right]\mathrm{Min}\left(1, \frac{\theta''}{\theta'}\right) - H_2 C_2\beta\theta''\left[\sinh\left(A_2 F_d^{3/2}\right)\right]^{n}$$

$$F_1 = F_{1a} + F_{1b}\,\mathrm{Max}\left(0, \log_{10}\left(\frac{R}{\theta'}\right) - F_{1f}\right) + \sum_{i=2}^{3} F_{1c,i}\, e^{-\left[\frac{\log_{10}(R/\theta') - F_{1d,2}}{F_{1e,i}}\right]^2}$$

$$F_2 = \sum_{i=2}^{3} F_{2c,i}\, e^{-\left[\frac{\log_{10}(R/\theta') - F_{2d,i}}{F_{2e,i}}\right]^2}$$

$$R = \sqrt{\frac{2}{3}\dot{C}_{ij}\dot{C}_{ij}}$$

$$\theta' = \begin{cases} e^{-\frac{Q^*}{kT}\left[\ln\left(\frac{T_f}{T}\right)+1\right]} & T \le T_f \\ e^{-\frac{Q^*}{kT}} & T > T_f \end{cases}$$

$$Q\;\theta'' = X'' e^{-\frac{Q_T}{kT}},\quad X'' = e^{k_p X'},\quad Q_r = Q^*\left[1+(k_Q-1)X'\right]$$

$$X' = \begin{cases} (1-x)^2 & x \le 1 \\ 0 & x > 1 \end{cases}$$

Appendix 11. Updated Miller's Theory — Differential Form (Cont)

$$X = \sqrt{3J_2'} \Big/ \left[A^{2/3} F_d \sqrt{F_1 + F_d(1+F_2)} \right]$$

$$\dot{C}_{ij}^{P} = \frac{(1-k)(\frac{3}{2}S_{ij} - \Omega_{ij}) < \sigma_{ij} \dot{\epsilon}_{ij} >}{\sigma_\infty{}^2 - 3J_2'k}$$

$$\dot{C}_{ij} = \dot{C}_{ij}^{C} + \dot{C}_{ij}^{P}$$

$$C_{ij} = \epsilon_{ij} - \alpha \Theta \delta_{ij} - \frac{1}{E}\left[(1+\nu)\sigma_{ij} - \nu\sigma_{kk}\delta_{ij}\right]$$

CONSTANTS: $A_1, A_2, B, C_2, H_1', H_2, H_3, k, k_p, k_Q, n, Q^*, T_t, F_{1a}, F_{1b}, F_{1c,1}, F_{1d,1}, F_{1e,1}, F_{1c,2}$, $F_{1d,2}, F_{1e,2}, F_{1f}, F_{2c,1}, F_{2d,1}, F_{2e,1}, F_{2c,2}, F_{2d,2}, F_{2e,2}$

INITIAL CONDITIONS ON Ω_{ij} AND F_d

Appendix 12. Walker's Theory — One Dimensional Differential Form including Instantaneous Stress State Variable

$$\dot{\sigma} = \dot{\Xi} - E\left(\frac{|\sigma-\Omega|}{K}\right)^{n} \operatorname{sgn}(\sigma-\Omega)$$

$$\dot{\Omega} = (n_1+n_2)\dot{C} - (\Omega - \mathring{\Omega} - n_1 C)\dot{G} + \dot{\mathring{\Omega}}$$

$$\dot{\Xi} = \delta E \dot{\epsilon} + (1-\delta)\left\{(m_1+m_2)\dot{C} - (\Xi - \mathring{\Xi} - m_1 C)\dot{H} + \dot{\mathring{\Xi}}\right\}$$

$$\dot{C} = \dot{\epsilon} - \frac{\dot{\sigma}}{E} - \alpha\dot{\theta}$$

$$K = K_1 - K_2 e^{-n_7 R}$$

$$\dot{G} = (n_3 + n_4 e^{-n_5 R})\dot{R} + n_6 |\Omega|^{m-1}$$

$$\dot{H} = (m_3 + m_4) e^{-m_5 R})\dot{R} + m_6 |\Xi|^{p-1}$$

$$\dot{R} = \dot{C}$$

Material constants $E, K, n, \mathring{\Omega}, \mathring{\Xi}, \alpha, m_{1-6}, n_{1-6}, K_1, K_2, m, p$ depend on temperature.

Parameter δ is: 0 if instantaneous stress is inelastic
1 if instantaneous stress is elastic (previous formulation)

APPENDIX 13

Plastic Strain Rates in Classical Plasticity

Consider an elastic perfectly plastic material, the plastic strain rate, $\dot{c}_{ij}^{p}$, is given by the normal to the yield surface

$$f(\underline{\sigma}) = J_2 - \frac{1}{3}\sigma_y^2 = 0 \tag{13.1}$$

where $J_2 = \frac{1}{2} S_{ij} S_{ij}$ is the second invariant of the deviatoric stress tensor, S_{ij}, $S_{ij} = \sigma_{ij} - \frac{1}{2}\sigma_{kk}\delta_{ij}$, and σ_y is the uniaxial yield stress. Then

$$\dot{c}_{ij}^{p} = \dot{\lambda}\frac{\partial f}{\partial \sigma_{ij}} = \dot{\lambda} s_{ij} \tag{13.2}$$

where $\dot{\lambda}$ is a scalar that must be determined. The plastic work rate is

$$\dot{w}^p = \sigma_{ij}\dot{c}_{ij}^{p} = \dot{\lambda} s_{ij} s_{ij} = 2 J_2 \dot{\lambda} \tag{13.3}$$

and therefore

$$\dot{\lambda} = \frac{\dot{w}^p}{2J_2} = \frac{3\dot{w}^p}{2\sigma_y^2} \tag{13.4}$$

Substituting Eq. (13.4) into Eq. (13.2)

$$\dot{c}_{ij}^{p} = \frac{3\dot{w}^p s_{ij}}{2\sigma_y^2} \tag{13.5}$$

which is identical to the result presented in the text.

Appendix 4. Modified Walker's Theory Including Time Independent Response

$$\dot{C}_{ij}^{c} = \left(\frac{\sqrt{3J_2'}}{K}\right)^{n}\left(\frac{\frac{3}{2}s_{ij}-\Omega_{ij}}{\sqrt{3J_2'}}\right)$$

$$\dot{C}_{ij}^{p} = \frac{\left(\frac{3}{2}s_{ij}-\Omega_{ij}\right)(1-k)<\sigma_{ij}\dot{\epsilon}_{ij}>}{\sigma_{\infty}^{2}\left[1-k(3J_2'/\sigma_{\infty}^{2})\right]} \tag{14.1}$$

$$\dot{\Omega}_{ij} = (n_1+n_2)\dot{C}_{ij} + C_{ij}\frac{\partial n_1}{\partial \Theta}\dot{\Theta} - (\Omega_{ij}-\overset{o}{\Omega}_{ij}-n_1 C_{ij})\left(\dot{G}-\frac{1}{n_2}\frac{\partial n_2}{\partial \Theta}\dot{\Theta}\right) + \overset{\circ}{\Omega}_{ij} \tag{14.2}$$

$$K = K_1 - K_2 e^{-n_7 R} = \beta\sigma_{\infty} \tag{14.3}$$

$$\dot{C}_{ij} = \dot{C}_{ij}^{c} + \dot{C}_{ij}^{p} \tag{14.4}$$

$$C_{ij} = (\delta_{ij}\lambda\epsilon_{kk} + 2\mu\epsilon_{ij} - \sigma_{ij} - \delta_{ij}(3\lambda+2\mu)\alpha\Theta)/2\mu \tag{14.5}$$

$$\dot{G} = (n_3 + n_4 e^{-n_5 R})\dot{R} + n_6\left(\frac{2}{3}\Omega_{ij}\Omega_{ij}\right)^{\frac{m-1}{2}}, \tag{14.6}$$

$$\dot{R} = \sqrt{\frac{2}{3}\dot{C}_{ij}\dot{C}_{ij}}, \tag{14.7}$$

$$\overset{\circ}{\Omega}_{ij} = 3\overset{o}{\Omega}\left[\frac{\dot{C}_{ik}C_{kj}}{C_{pq}C_{pq}} + \frac{C_{ik}\dot{C}_{kj}}{C_{pq}C_{pq}} - \left(\frac{2C_{ik}C_{kj}}{C_{pq}C_{pq}}\right)\left(\frac{C_{rs}\dot{C}_{rs}}{C_{uv}C_{uv}}\right)\right] + \left[3\frac{C_{ik}C_{kj}}{C_{pq}C_{pq}} - \delta_{ij}\right]\frac{\partial\overset{o}{\Omega}}{\partial\Theta}\dot{\Theta} \tag{14.8}$$

$$s_{ij} = \sigma_{ij} - \frac{1}{3}\delta_{ij}\sigma_{kk}. \tag{14.9}$$

$$3J_2' = \frac{2}{3}\left(\frac{3}{2}s_{ij}-\Omega_{ij}\right)\left(\frac{3}{2}s_{ij}-\Omega_{ij}\right) \tag{14.10}$$

Material constants. $\lambda, \mu, \overset{o}{\Omega}, n, m, n_1, n_2, n_3, n_4, n_5, n_6, n_7, K_1, K_2, k, \sigma_{\infty}$ depend on temperature.

Appendix 15. Backward Difference Integration Algorithm

GIVEN: $\Delta\epsilon_{ij}$

GUESS: $\underset{K=0}{\overset{0}{\Delta C_{ij}}} = \Delta\epsilon_{ij} - 1/3\,\Delta\epsilon_{KK}\,\delta_{ij}$

CALCULATE IN ORDER:

$$\epsilon_{ij}^{K+1} = \epsilon_{ij}^{K} + \Delta\epsilon_{ij}$$

$$C_{ij}^{K+1} = C_{ij}^{K} + \Delta\epsilon_{ij}$$

$$\Delta R = \sqrt{\frac{2}{3}\,\Delta C^{K}_{ij}\,\Delta C_{ij}^{K}}$$

$$R^{K+1} = R^{K} + \Delta R$$

$$\sigma_{ij}^{K+1} = 2\mu(\epsilon_{ij}^{K+1} - C_{ij}^{K+1}) + \lambda\delta_{ij}\,\epsilon_{KK}^{K+1} - (3\lambda+2\mu)\delta_{ij}\,\alpha\,\Theta^{K+1}$$

$$\overset{0}{\Omega}_{ij}^{K+1} = \left[3\,\frac{C_{iK}^{K+1}\,C_{Kj}^{K+1}}{C_{pq}^{K+1}\,C_{pq}^{K+1}} - \delta_{ij}\right]$$

$$S_{ij}^{K+1} = \sigma_{ij}^{K+1} - 1/3\,\sigma_{KK}^{K+1}\,\delta_{ij}$$

$$K = K_1 - K_2\,e^{-n_7 R^{K+1}}$$

ITERATE TO FIND $\Delta G, \Omega_{ij}^{K+1}$:

GUESS: $\Delta G = (n_3 + n_4\,e^{-n_5 R^{K+1}})\,\Delta R + n_6\,(2/3\,\Omega_{ij}^{K}\,\Omega_{ij}^{K})^{\frac{m-1}{2}}\,\Delta t = \Delta G^{0}$

CALCULATE: $\Omega_{ij}^{K+1} = \overset{0}{\Omega}_{ij}^{K+1} + \left[\Omega_{ij}^{K} - \overset{0}{\Omega}_{ij}^{K} + (n_1+n_2)\,\Delta C_{ij} + C_{ij}^{K+1}\,\Delta n_1 + n_1 C_{ij}^{K+1}\left(\Delta G - \frac{\Delta n_2}{n_2}\right)\right] /$

$$\left[1 + \Delta G - \frac{\Delta n_2}{n_2}\right]$$

$$\frac{\partial \Omega_{ij}}{\partial \Delta G} = \frac{-(\Omega_{ij}^{K+1} - n_1 C_{ij}^{K+1})}{1 + \Delta G - \frac{\Delta n_2}{n_2}}$$

$$f(\Delta G) = \Delta G - (n_3 + n_4\,e^{-n_5 \Delta R})\,\Delta R + n_6 (\Omega_{ij}^{K+1}\,\Omega_{ij}^{K+1})^{\frac{m-1}{2}}\,\Delta t$$

$$f'(\Delta G) = 1 - n_6\left(\frac{m-1}{2}\right)\frac{\left(\frac{4}{3}\,\Omega_{ij}^{K+1}\,\frac{\partial \Omega_{ij}^{K+1}}{\partial \Delta G}\right)\Delta t}{\left(\frac{2}{3}\,\Omega_{ij}^{K+1}\,\Omega_{ij}^{K+1}\right)^{(3-m)/2}}$$

$$\Delta G^{N+1} = \Delta G^{N} - \frac{f(\Delta G)}{f'(\Delta G)}$$

CALCULATE UNTIL ΔG CONVERGES

Appendix 15. Backward Difference Integration Algorithm (Cont)

$$3J_2' = \frac{2}{3}\left(\frac{3}{2}S_{ij}^{K+1} - \Omega_{ij}^{K+1}\right)\left(\frac{3}{2}S_{ij}^{K+1} - \Omega_{ij}^{K+1}\right)$$

$$\Delta\tilde{C}ij = \left[\left(\frac{\sqrt{3J_2'}}{K}\right)^n \frac{1}{\sqrt{3J_2'}} + \frac{(1-k)<\sigma_{ij}^{K+1}\Delta\epsilon_{ij}>}{\sigma_\infty^2 - 3J_2'k}\right]\left(\frac{3}{2}S_{ij}^{K+1} - \Omega_{ij}^{K+1}\right)$$

$$E^K = \sqrt{(\Delta C_{ij}^K - \Delta\tilde{C}_{ij}^K)(\Delta C_{ij}^K - \Delta\tilde{C}_{ij}^K)}$$

IF $E^K <$ ERROR THE SOLUTION HAS CONVERGED, OTHERWISE CONTINUE

$$\Delta\theta_{ij} = (S_{ij}^{K+1} - S_{ij}^K)/2\mu$$

$$\Lambda^K = \sqrt{\Delta C_{ij}^K \Delta C_{ij}^K / \left[(\Delta\epsilon_{ij} - \Delta\theta_{ij}^K)(\Delta\epsilon_{ij} - \Delta\theta_{ij}^K)\right]}$$

IF $K = 0$ THEN SET $\Delta C_{ij}^1 = \Delta C_{ij}$, $K = 1$ AND BEGIN NEXT ITERATION

IF $K > 0$ CALCULATE

$$\Lambda^{K+1} = (\Lambda^{K-1}E^K - \Lambda^K E^{K-1})/(E^K - E^{K-1})$$

$$\Delta C_{ij}^{K+1} = \Lambda^{K+1}(\Delta\epsilon_{ij} - \Delta\theta_{ij})$$

$K = K+1$

BEGIN NEXT ITERATION

Appendix 16. Modified Walker's Theory — Integral Form

$$\sigma_{ij}(t) = \lambda(t)\,\epsilon_{KK}(t)\,\delta_{ij} + 2\mu(t)\int_0^t e^{-[\Lambda(t)-\Lambda(\xi)]}\left\{\dot{\epsilon}_{ij}(\xi) + \frac{\dot{\Lambda}(\xi)}{3}\left[\epsilon_{KK}(\xi)\,\delta_{ij} + \frac{\Omega_{ij}(\xi)}{\mu(\xi)}\right]\right\} d\xi$$

$$\dot{\Lambda}(t) = \left(\frac{\sqrt{3J_2'(t)}}{K(t)}\right)^n\left(\frac{3\mu(t)}{\sqrt{3J_2'(t)}}\right) + \frac{3\mu(t)[1-k(t)]<\sigma_{ij}(t)\dot{\epsilon}_{ij}(t)>}{\sigma_\infty{}^2(t) - 3J_2'(t)\,k(t)}$$

$$\Lambda(t) = \int_0^t \dot{\Lambda}(\xi)\,d\xi$$

$$\Omega_{ij}(t) = \overset{\circ}{\Omega}_{ij}(t) + n_1(t)\,C_{ij}(t) + n_2(t)\int_0^t e^{-[G(t)-G(\xi)]}\dot{C}_{ij}(\xi)\,d\xi$$

$$C_{ij}(t) = \left\{2\mu(t)\,\epsilon_{ij}(t) - \sigma_{ij}(t) + \lambda(t)\epsilon_{kk}(t)\delta_{ij} - [2\mu(t)+3\lambda(t)]\,\alpha(t)\,\Theta(t)\,\delta_{ij}\right\}/2\mu(t)$$

$$K(t) = K_1(t) - K_2(t)\,e^{-n_7(t)R(t)}$$

$$\overset{\circ}{\Omega}_{ij}(t) = \overset{\circ}{\Omega}(t)\left[\frac{3C_{ik}(t)C_{kj}(t)}{C_{pq}(t)C_{pq}(t)} - \delta_{ij}\right]$$

$$G(t) = \int_0^t \left\{\left[n_3(\xi) + n_4(\xi)\,e^{-n_5(\xi)R(\xi)}\right]\dot{R}(\xi) + n_6(\xi)\left[\frac{2}{3}\Omega_{ij}(\xi)\Omega_{ij}(\xi)\right]^{\frac{m(\xi)-1}{2}}\right\} d\xi$$

$$R(t) = \int_0^t \sqrt{\frac{2}{3}\,\dot{C}_{ij}(\xi)\dot{C}_{ij}(\xi)}\;d\xi$$

$$3J_2'(t) = \frac{2}{3}\left(\frac{3}{2}S_{ij}(t) - \Omega_{ij}(t)\right)\left(\frac{3}{2}S_{ij}(t) - \Omega_{ij}(t)\right)$$